



<https://theses.gla.ac.uk/>

Theses Digitisation:

<https://www.gla.ac.uk/myglasgow/research/enlighten/theses/digitisation/>

This is a digitised version of the original print thesis.

Copyright and moral rights for this work are retained by the author

A copy can be downloaded for personal non-commercial research or study, without prior permission or charge

This work cannot be reproduced or quoted extensively from without first obtaining permission in writing from the author

The content must not be changed in any way or sold commercially in any format or medium without the formal permission of the author

When referring to this work, full bibliographic details including the author, title, awarding institution and date of the thesis must be given

Enlighten: Theses

<https://theses.gla.ac.uk/>
research-enlighten@glasgow.ac.uk

**The Effects of Constraint On Three Dimensional
Elastic-Plastic Crack Tip Fields**

By

Ning Chen

**Thesis submitted to the Faculty of Engineering of
the University of Glasgow for the Degree of Master of Science**

January 1997

©Copyright 1997 Ning Chen

ProQuest Number: 10391402

All rights reserved

INFORMATION TO ALL USERS

The quality of this reproduction is dependent upon the quality of the copy submitted.

In the unlikely event that the author did not send a complete manuscript and there are missing pages, these will be noted. Also, if material had to be removed, a note will indicate the deletion.



ProQuest 10391402

Published by ProQuest LLC (2017). Copyright of the Dissertation is held by the Author.

All rights reserved.

This work is protected against unauthorized copying under Title 17, United States Code
Microform Edition © ProQuest LLC.

ProQuest LLC.
789 East Eisenhower Parkway
P.O. Box 1346
Ann Arbor, MI 48106 – 1346

Thesis 10954

Copy 2



Abstract

Detailed finite element analysis of the near tip region of a thin plate has revealed strong three-dimensional effects at the crack front. The field exhibits a gradual loss of plane strain conditions through the thickness which changes with increasing levels of deformation. A strain concentration is located at the intersection of free surface and crack plane. The distribution of J with a deformation levels coincides with the variation of the crack tip stress field. The effects of constraint were studied through modified boundary layer formulations using the first two terms of the William's expansion, K and T as boundary conditions. The results show that positive T stresses allow the strain close to the free surface to advance more than on the midplane. Negative T causes the strain to develop near the midplane more than close to the free surface. At large deformation levels, the crack tip deformation tends to a uniform plane stress field for both positive and negative T stresses. Numerical results show that the lateral contraction at the crack tip is approximately equal to the crack tip opening displacement in small scale yielding.

Acknowledgements

I wish to express my deep gratitude to my supervisor Professor J. Hancock for his valuable guidance, encouragement and inspiration conveyed to me during the course of my study.

I wish to thank all the members of Fracture Mechanics Group and others who gave me hands to lighten the burden of my research.

I am also indebted to my mother, and my wife, Peng Zhang, for their support, tolerance and sacrifice for my education. I feel ashamed for what I achieved hardly offsets the contribution they offered to me.

Contents

	Page
Abstract	I
Acknowledgements	II
1. Introduction	1
2. Linear Elastic Fracture Mechanics	1
2.1 Introduction	1
2.2 Two Dimensional Crack Tip Fields	3
2.2.1 Energetics of Crack Advance	3
2.2.2 Stress Intensity Factor	5
2.2.3 The Crack Tip Plastic Zone	7
2.2.4 The Thickness Effect	8
2.2.5 The Validity of LEFM	11
2.2.6 Williams Expansion	12
2.2.7 T- Stress	12
2.3 Three Dimensional Crack Tip Fields	14
2.3.1 Expression of Three Dimensional Field	14
2.3.2 Determination of Elastic T-stress in Three Dimensional Field	17
3. Elastic-Plastic Fracture Mechanics	20
3.1 Two Dimensional Crack Tip Fields	20
3.1.1 J-Integral	20
3.1.2 Dual Definition of the J-Integral	21
3.1.3 The HRR field	23

3.1.4	J Dominance	25
3.1.5	K-T and J-Q Theory	28
3.2	Three Dimensional Elastic-Plastic Crack Tip Fields	30
3.2.1	Three Dimensional Boundary Layer Formulation	34
3.2.2	J-Integral in Three Dimensional Stress Fields	36
3.2.3	J Dominance in Three Dimensional Stress Field	37
4.	Computational Model	39
4.1	Geometry and Computational Model	39
4.2	Computational Procedure	41
5.	Computational Results	41
5.1	Three Dimensional Boundary Layer Formulations	41
5.1.1	Small Scale Yielding for Non-hardening Material	41
5.1.2	Discussion	43
5.1.3	Moderate and Large Yielding for Non-hardening Material	46
5.1.4	Discussion	48
5.1.5	Stress Field for Strain Hardening Materials	49
5.1.6	Discussion	50
5.2	Three Dimensional Modified Boundary Layer Formulation	50
5.2.1	Stress and Strain field of Non-hardening Material	51
5.2.2	Discussion	52
6.	Conclusions	54
7.	References	55

1. Introduction

The fundamental problem of fracture mechanics is to transfer data from laboratory specimens to real structures. Test specimens are usually small and have a simple configuration. In contrast engineering components and structures are often large and have complicated geometries. The transfer of experimentally determined fracture toughness data to structures of different size and shape is far from being solved. The problem requires an understanding of the role of geometry, material properties, crack length, and loading on the crack tip stress field.

2. Linear Elastic Fracture Mechanics

2.1 Introduction

Linear elastic fracture mechanics (LEFM) deals with cracked materials when plastic deformation preceding crack advance is sufficiently small to regard plasticity as a minor, and negligible, perturbation of a largely elastic field.

A crack in a solid can be stressed in three different modes as illustrated in Figure 1. Mode I is called the opening mode. In this mode the body is subjected to a normal stress, and the displacements of the crack surface are symmetric about the crack plane. In-plane shear results in the mode II or the edge sliding mode. The displacements are anti-symmetric about the crack plane. The shearing mode or mode III is caused by out-plane shear such that the displacements are in the plane of the crack and parallel to the leading edge of crack. Mode I is usually the most important in engineering practice.

Plane stress and plane strain are fundamental concepts in continuum mechanics. Plane stress state is a simplification of the three dimensional stress field of a thin plate, in which one normal stress vanishes, while the other stresses may vary in the plane. Plane stress occurs in a thin plate loaded by forces parallel to the plane of the plate and distributed uniformly over the thickness. The out of plane stress components are zero on both faces of plate and it may assumed that they are zero within the plate (see Figure 2). Plane stress implies that all the stress components in the thickness z direction are zero and the non-zero components are contained in the x-y plane.

$$\sigma_{zz} = \tau_{xz} = \tau_{yz} = 0 \quad \text{and}$$

$$\frac{\partial \sigma_{zz}}{\partial z} = \frac{\partial \tau_{xz}}{\partial z} = \frac{\partial \tau_{yz}}{\partial z} = 0 \quad (1)$$

The term plane strain is used to denote a condition in which all the displacements in a body occur parallel to a given plane. The displacement in one direction is zero which means the strain in the thickness direction is prevented by a physical restraint. In the interior of thick plate at the points far from the boundary the state of stress can be viewed as plane strain. Plane strain is defined as,

$$e_{zz} = \gamma_{zx} = \gamma_{zy} = 0 \quad \text{and}$$

$$\frac{\partial e_{zz}}{\partial z} = \frac{\partial \gamma_{zx}}{\partial z} = \frac{\partial \gamma_{zy}}{\partial z} = 0 \quad (2)$$

Under linear elastic isotropic conditions, the stress-strain relation gives the condition

$$\sigma_{zz} = \nu (\sigma_{xx} + \sigma_{yy}) \quad (3)$$

As an example, long cylindrical thick tubes with internal pressure are often analysed as a plane strain problem since the displacement in the tube axis z is zero for most parts of plate thickness (see Figure 3).

2.2 Two Dimensional Crack Tip Fields

2.2.1 Energetics of Crack Advance

Griffith (1921) investigated an infinite cracked panel of a perfectly brittle material, like glass, with a central crack of length $2a$. The plate is loaded under fixed grip conditions. Crack extension requires energy, which may be supplied from the work done by applied external load or from the strain energy stored in the structure. Griffith defined the energy balance for crack growth as,

$$dU / da = dW / da \quad (4)$$

where U is the elastic energy and W is the energy absorbed in crack growth, a is the crack length. When energy released by extending the crack is more than the energy required to form new surface, the crack will propagate. Denoting the potential energy supply per unit of crack area extension by G , the strain energy release rate is:

$$G = -d\Pi / da = -d(F-U) / da = dW/da \quad (5)$$

where Π is potential energy, F is the work performed by the external load and U is the elastic energy contained in the plate. W is the energy for crack formation. The critical condition may be defined by

$$G = -d(F-U) / da = G_c \quad (6)$$

G_c is defined as the critical energy consumed during crack extension. In Griffith's model, F is zero since the remote displacement is fixed. $U = \pi\sigma^2 4a^2 t / 4Et = \pi\sigma^2 a^2 / E$.

$$G = dU / da = 2\pi\sigma^2 a / E \quad (7)$$

In a brittle material the energy of crack advance is taken to equal to the surface energy to form the new free surface, i.e.

$$W = 4a\gamma \quad \text{and} \quad dW/da = 4\gamma = G_c \quad (8)$$

Here γ is the surface energy per unit area. Equating the energy release rate to the work done in cracking fresh surface Griffith proposed:

$$\begin{aligned} \pi\sigma^2 a / E' &= 2\gamma \quad \text{and} \\ \sigma_c &= (2\gamma E' / a \pi)^{1/2} \end{aligned} \quad (9)$$

where $E' = E$ in plane stress and $E / (1-\nu^2)$ in plane strain.

Irwin (1960) and Orowan (1948) noted that the energy needed for crack extension in a metal is much larger than the energy to create the new free surfaces. In metals plastic deformation occurs in front of the crack. During crack advance extra energy is consumed in the formation of the plastic zone at the tip of crack. If the plastic energy R per unit area is seen as a material constant,

$$G_c = dW / da = d(\gamma + R) / da \quad (10)$$

G_c is still a constant. As R is much larger than γ the equation (9) becomes:

$$\pi\sigma^2 a / E = R \quad (11)$$

Orowan (1948) provided an important modification to Griffith's theory which extends the theory from ideal brittle materials to real elastic-plastic materials.

2.2.2 Stress Intensity Factor

Using Westergaard's (1939) complex stress function, Irwin (1952) demonstrated that the elastic stress field near the crack tip in a infinite plate with crack length $2a$ under extension could be described for Mode I in the form :

$$\begin{aligned} \sigma_{xx} &= K_I (2\pi r)^{-1/2} \cos \theta / 2 [1 - \sin \theta / 2 \sin 3\theta / 2] \\ \sigma_{yy} &= K_I (2\pi r)^{-1/2} \cos \theta / 2 [1 + \sin \theta / 2 \sin 3\theta / 2] \\ \sigma_{xy} &= K_I (2\pi r)^{-1/2} \cos \theta / 2 \sin \theta / 2 \cos 3\theta / 2 \\ \sigma_{zz} &= \nu (\sigma_{11} + \sigma_{22}) \quad \text{Plane strain} \\ \sigma_{zz} &= 0 \quad \text{Plane stress} \end{aligned} \quad (12)$$

where r, θ are cylindrical co-ordinates centred at the crack tip. The analysis indicates that the stress and deformation field near the crack tip can be uniquely characterised by a single parameter called the stress intensity factor, K . The stress intensity factor can be regarded as a measurement of the strength of the crack tip singularity. At large distances from the crack tip the stress σ_{22} approaches zero in equation (12), but should approaches external loading stress σ . The stress field of the plate consists of two parts, the crack tip stress field and the far field. As the stress intensity factor K characterises the strength of crack tip stress field, critical values of K can be used to measure crack advance. Under strictly defined conditions the fracture criterion in mode I is:

$$K_I = K_{Ic} \quad (13)$$

In order to relate K to the strain energy released rate, Irwin (1952) considered a small crack extension in the crack plane and calculated the energy release rate by the displacement of the crack surface normal to the crack plane. It was found that

$$K^2 = E'G \quad (14)$$

Where $E' = E$ for plane stress and $E' = E/(1-\nu^2)$ for plane strain. The critical value of K corresponding to G_c is denoted K_{Ic} . K_{Ic} is a material constant which quantifies the ability to resist fracture. The stress field for a central crack in an infinite plate can be expressed in the form:

$$\sigma_{ij} = \frac{\sigma \sqrt{\pi a}}{\sqrt{2\pi r}} f_{ij}(\theta) + \dots + O(r) \quad (15)$$

In the case of a finite geometry,

$$\sigma_{ij} = \frac{Y\sigma \sqrt{\pi a}}{\sqrt{2\pi r}} f_{ij}(\theta) + \dots \quad (16)$$

Where Y is a non-dimensional function of geometry. When $\theta = 0$, $f(\theta) = 1$, $K_I = Y\sigma (a\pi)^{1/2}$

$$K_I = \lim_{r \rightarrow 0} \sigma_{ij} \sqrt{2\pi r} \quad (17)$$

K_I is thus proportional to the applied load and the square root of a characteristic dimension such as the crack length a and is a function of the geometry of the

cracked structure. Various methods have been used to determine K and important results are tabulated by Rooke & Cartwright (1976).

2.2.3 The Crack Tip Plastic Zone

To determine the size and shape of the crack tip plastic zone, either the Tresca criterion or the Von Mises criterion can be applied. The Tresca yield criterion predicts that yielding occurs when the maximum shear stress τ_{\max} exceeds the yield stress in shear. The Von Mises criterion, can be written in terms of principal stresses, $\sigma_1, \sigma_2, \sigma_3$, and the uniaxial yield stress σ_0 :

$$(\sigma_1 - \sigma_2)^2 + (\sigma_2 - \sigma_3)^2 + (\sigma_3 - \sigma_1)^2 = 2 \sigma_0^2$$

That is

$$\{1/2 [(\sigma_1 - \sigma_2)^2 + (\sigma_2 - \sigma_3)^2 + (\sigma_3 - \sigma_1)^2]\}^{1/2} = \sigma_e = \sigma_0 \quad (18)$$

σ_e is the effective stress. The crack tip stress field can be expressed in terms of the principal stresses, $\sigma_1, \sigma_2, \sigma_3$:

$$\begin{aligned} \sigma_1 &= K_I (2\pi r)^{-1/2} \cos \theta / 2 (1 + \sin \theta / 2) \\ \sigma_2 &= K_I (2\pi r)^{-1/2} \cos \theta / 2 (1 - \sin \theta / 2) \\ \sigma_3 &= 2\nu K_I (2\pi r)^{-1/2} \cos \theta / 2 && \text{for plane strain} \\ \sigma_3 &= 0 && \text{for plane stress} \end{aligned} \quad (19)$$

Substitution of eqs (19) into (18) provides a simple estimate of the extent of the plastic zone as a function of θ :

$$r_p(\theta) = (K^2 / 4\pi\sigma_0^2) [3/2 \sin^2 \theta + (1-2\nu)^2 (1 + \cos \theta)] \quad \text{for plane strain}$$

$$r_p(\theta) = (K^2 / 4\pi\sigma_0^2)[1 + 3/2\sin^2\theta + \cos\theta] \quad \text{for plane stress} \quad (20)$$

Directly ahead of the crack ($\theta = 0$ and $\nu = 1/3$), the difference between the radius of the plane stress and plane strain plastic zone is a factor of 9. The Tresca criterion gives the shape of the plastic zone as :

$$r_p(\theta) = (K^2 / 2\pi\sigma_0^2)[\cos^2(\frac{\theta}{2})(1 + \sin\frac{\theta}{2})]^2 \quad \text{for plane stress}$$

$$r_p(\theta) = (K^2 / 2\pi\sigma_0^2)[\cos^2(\frac{\theta}{2})(1 - 2\nu + \sin\frac{\theta}{2})]^2 \quad \text{for plane strain} \quad (21)$$

The shape of the Von Mises and Tresca plastic zones are shown in Figure 4.

In deriving the plastic zone boundaries the stresses are limited to the yield stress and some extra load has to be carried by the material outside the boundary. A more accurate approximation to the plastic zone can be obtained by correcting the plastic zone for this stress redistribution. More accurate analyses of plastic zone were contributed by Tuba (1976) using relaxation methods. His results are shown in Figure 5.

The plane strain plastic zone is smaller than the plane stress plastic zone. This results from the fact that effective yield stress in plane strain is larger than in plane stress. In plane stress the maximum stress is limited to the yield stress in the plastic zone. In plane strain the maximum principal stress can be as high as three times the uniaxial yield stress.

2.2.4 The Effect of Thickness

The thickness of a plate affects the state of stress at the crack tip. Although there may be a state of plane strain in the interior of a plate, there must always be a

state close to plane stress at the surface. The surface stress state is not exactly plane stress, since plane stress formally requires that,

$$\sigma_{zz} = \frac{\partial \sigma_{zx}}{\partial z} = \frac{\partial \sigma_{zy}}{\partial z} = 0 \quad (22)$$

and the stress gradient conditions are not generally met at the surface. The stress σ_{zz} does however gradually increase from zero at the free surface to the plane strain value near the mid plane. Correspondingly, the size of plastic zone gradually decreases from the plane stress size near the free surface to the plane strain size in the interior of plate. Large displacements in the plastic zone require the movement of material from elsewhere. Thus when the plastic zone is large compared to the thickness, yielding can take place freely in the thickness direction by lateral contraction, and plane stress conditions apply over most of the plastic zone. However when the plastic zone is small compared to the thickness, deformation in the thickness direction is contained by the surrounding elastic material and yielding can not occur freely in the thickness direction.

Plastic deformation can be viewed as slip caused by shear stresses. The plane on which the maximum shear stress is located and the magnitude of maximum shear stress differ in plane stress and plane strain. The two cases are plotted in Figure 6. Slip on a plane through the x axis and at 45° degrees to the surface is an out of plane shear deformation which occurs in plane stress (Figure 6a). In contrast plane strain slip occurs on the plane through z axis and at 45° from x-z plane as illustrated as Figure 6b.

As the ratio of plastic zone size to the thickness determines the state of stress, plane strain conditions are maintained when the plate thickness is larger than the plastic zone size. The ASTM standard test method for plane-strain fracture toughness K of metallic materials (E399-83) requires the specimen dimensions to meet the following requirements:

$$a, b, B \geq 2.5 (K_{Ic} / \sigma_0)^2 \quad (23)$$

a is the length of crack, b is the width of the ligament and B is the thickness. K_{Ic} is the fracture toughness. σ_0 is yield stress. Within these conditions all the specimen dimensions are more than 25 times the radius of the plane strain plastic zone.

The experimental dependence of fracture toughness K_{Ic} on thickness is illustrated in Figure 7 (Kaufman, 1970) which shows that K_{Ic} is a thickness dependent property. K_{Ic} decreases with increasing thickness and reaches a constant value as plane strain conditions are approached.

Figure 8 (Broek, 1986) shows schematically the dependence of fracture toughness on thickness which indicates that beyond a certain thickness B_s a state of plane strain prevails and the toughness reaches the plane strain value K_{Ic} . There is a thickness B_0 ($B_0 < B_s$) at where the fracture toughness $K_{Ic, max}$ reaches its highest level. The value is usually considered to be the real plane stress fracture toughness. Between B_0 and B_s there is a transition region. There is uncertainty about the toughness at thicknesses less than B_0 , where necking may precede fracture.

Anderson (1969) has analysed the effects of thickness on the toughness and demonstrated that between B_0 and B_s the data can reasonably be approximated in a linear manner. The thickness of B_s is specified by $B_s = 2.5K_{Ic}^2 / \sigma_0^2$ and B_0 by $B_0 = K_{Ic}^2 / 3\pi\sigma_0^2$. Anderson and Dodds (1991) proposed a less restrictive size requirement for cleavage fracture toughness measurement in term of the J-integral given by,

$$a, b, B \geq \frac{200J_e}{\sigma_0} \approx \frac{400K^2(1-\nu^2)}{E(\sigma_0 + \sigma_{uts})} \quad (24)$$

They performed finite element analyses to calculate the ratio of J-integral in a finite size specimen to the J-integral under small scale yielding which can produce the equivalent stresses ahead of both crack front, and thereby equivalent conditions for

cleavage fracture. The proposed size requirement specifies the deformation at which the ratio deviates from unity for deeply cracked bending specimens. Koppenhoefer and Dodds (1994) compared this criterion with five sets of experimental data (Jones and Brown et al,1970).

An alternative account of the role of thickness effects follows from the work of Sih and Hartranft (1973), who pointed out that the energy released per unit length crack front length is a function of the thickness. If a large part of the thickness is under plane stress the average stress intensity factor is lower than the nominal stress intensity factor.

The usual method of determining K is a global method which assumes that the toughness is a constant through the plate thickness. The method of determining K in the three point bending is usually based on two dimensional analyses which result in expressions of the form:

$$K = \frac{PS}{BW^{3/2}} f(a/w) \quad (25)$$

P is the applied load. S is the distance between the two support points. B is the thickness. W is the width of specimen and a the length of crack. The stress intensity factor is related linearly to the load on the boundary of specimen. The calculation of fracture toughness K_c does not consider plastic deformation which is an inherent limitation of LEFM.

2.2.5 The Validity of LEFM

The application of LEFM requires that the material exhibits linear elastic behaviour and that any plastic deformation preceding the crack extension is contained within a surrounding elastic zone. This ensures that the crack tip stress field is dominated by the

stress intensity factor K . To maintain K dominance it is necessary that the plastic zone is located within a zone of K dominance. These conditions are expressed formally by codified requirements (23). The criteria are based on the requirement that the characteristic size of the plate must be larger than the 30 times of the size of plastic zone in order to maintain valid LEFM.

2.2.6 Williams Expansion

Williams (1957) investigated the linear elastic problem of a two dimensional infinite plate with central crack. The stress field was expressed as an asymptotic expansion:

$$\sigma_{ij}(r,\theta) = A_{ij}(\theta) r^{-1/2} + B_{ij}(\theta) + c_{ij}(\theta) r^{1/2} + \dots \quad (26)$$

r, θ are polar co-ordinates centred at the crack tip. σ_{ij} are the cartesian components of the stress tensor. The first term in the expansion of crack tip stress field can be written in term of the stress intensity factor K_I . The second term in the expansion has been denoted T by Rice (1974). The T stress is independent of the distance and can be regarded as a uniaxial tensile or compressive stress parallel to the crack flanks. Neglecting terms which disappear at the crack tip ($r=0$), the field can be expressed in the form:

$$\sigma_{ij} = K_I / (2\pi r)^{1/2} f_{ij}(\theta) + T\delta_{ij} \quad (27)$$

2.2.7 T-Stress

Elastic fracture mechanics usually assumes that fracture process occurs close to the crack tip where stresses are dominated by K , which is the leading term in the Williams expansion. The stress field in the neighbourhood of the crack tip is then of most concern. Because of the inverse square root singularity at crack tip stress field, the

T-stress is small relative to the singular field and is usually neglected. The values of T-stress of a wide range of geometries have been tabulated by Sham (1991).

Deeply cracked geometries in both tension and bending exhibit a positive T-stress.

In geometries with shallow cracks, the T-stress is negative. Levers and Radon (1983) introduced a biaxiality parameter β . This enables the T-stresses to be expressed either in terms of a stress concentration factor T / σ or as a biaxiality parameter β in the form :

$$\beta = T (\pi a)^{1/2} / K \quad (28)$$

Carlsson and Larsson (1973) demonstrated that the second term in the Williams expansion has a significant effect on the shape and size of the plastic zone developed at the crack tip. A compressive T-stress both enlarged the maximum radius of the plastic zone and caused the plastic lobes to swing forward. A tensile T-stress decreased the size of plastic zone and caused it to rotate backwards. To determine the role of constraint on the stress field, Bilby et al (1986) introduced T as a constraint parameter in addition to K .

Betegón and Hancock (1991) modelled the plane-strain elastic-plastic crack tip fields with modified boundary layer formulations based on first two terms, K and T , of the Williams expansion. Boundary layer formulations were originally introduced by Rice and Tracey (1973) to analyse the crack tip deformation in the small scale yielding. The displacement or tractions of the K field are applied on the outer boundary of a region around the crack tip. The addition of the non-singular T-stress to the K field as the boundary condition gives the modified boundary layer formulation. The results indicated that the geometries characterised by zero and positive T stress can be characterised by J , while geometries with a negative T-stress require a two parameter characterisation. These observation means that the stress field is characterised by two terms J and T . The T-stress is a constraint parameter which depends on load and geometry.

Du and Hancock (1991) studied the effects of the T-stress on the small scale

yielding crack tip stress field for a non-hardening material in plane strain conditions using modified boundary layer formulations. The mesh of the model consisted of 12 rings of 12 second order elements. The boundary conditions applied to the outer edge of the mesh corresponded to the displacements of the mode I linear stress field and the displacements caused by the T-stresses. The stresses surrounding the crack tip were represented by Prandtl slip line field when $T \geq 0.44\sigma_0$. The validity of slip line field as a representation of the limiting stress state at the crack tip in small-scale yielding ($T \geq 0$) is consistent with the non-linear HRR field. The stress field ahead of the crack was reduced by a compressive T-stress. Compressive T-stresses resulted in reduction of hydrostatic components at all angles within the plastic zone. Tensile T-stress that is greater than $0.44\sigma_0$ induced plasticity on the flank of crack and gave rise to region of constant stress state between 150 and 180 degrees. However for a zero and negative T-stress, an elastic region was encountered in the crack flanks.

2.3 Three Dimensional Elastic Crack Tip Fields

The three dimensional problem studied is a thin plate with a through crack subjected to mode I loading. Plane stress is a two dimensional concept which is applied to a three dimensional model with the condition that the out of plane stress components σ_{33} , τ_{23} , τ_{13} are zero and the in plane stress component σ_{11} , σ_{22} , and τ_{12} are independent of position through the thickness. Within the context of a three dimensional formulation, these assumptions are strictly consistent only if the direct stresses σ_{11} , σ_{22} are a linear function of the in-plane co-ordinates x and y.

2.3.1 Expression of Three Dimensional Fields

As the mathematical difficulties posed by three dimensional elastic problems are greater than those associated with planar problems, there is still no complete solution

to the full three dimensional problem. Nevertheless, numerical studies have been conducted and progress has been made. These studies can be sorted into two categories, mathematical analyses and finite element analyses.

The problem of a three dimensional stress distribution in a plate with an orthogonal through crack was first investigated by Hartranft and Sih (1970) using a variational method. In their study they assumed that the local stress field interior to the plate is in a state of plane strain. The results show that the stress state depends on the plate thickness to crack length ratio and a dimensionless parameter characterising the stress distribution through the thickness. An approximate three dimensional stress field distribution formulation was put forward.

Sih and Hartranft (1973) pointed out that the strain energy release per unit length, G , is a function of thickness. The strain energy release rate was shown to decrease with increasing plate thickness

Folias (1975) addressed the problem by the means of the so-called 'symbolic method'. The analysis showed that in the interior of plate only the σ_{11} , σ_{22} , σ_{33} and τ_{12} components are singular, while in the vicinity of the corner all the stresses exhibit a singularity of order $(1/2+2\nu)$. As the thickness $\rightarrow \infty$, the plane strain solution was recovered and as $\nu \rightarrow 0$ the plane stress solution was recovered.

Levy, Marcal and Rice (1971) presented finite element analyses of the three dimensional stress fields of a thin plate which showed that the three dimensional near tip stress field coincides with the plane stress solution at a distance of twice the thickness from the crack tip along mid plane of a thin plate. Though detailed results were not given, their work was one of the first finite element analysis to present quantitative results of the three dimensional field near a crack tip.

Crush (1971) used a direct potential method to study the problem. Numerical results indicated the stresses are lower than those obtained from stress intensity factor, while σ_{33} was a function of thickness. It was found that plane strain is induced close to the crack front and the existence of a corner singularity was demonstrated.

A three dimensional finite element analysis of a through cracked elastic plate was

presented by Burton et al (1984). They found a decay in the energy release rate through the plate thickness and indicated that the drop in energy release rates as the free surface is approached is probably not significant from a fracture toughness testing point of view.

An approximate analytical solution which employed a boundary layer approach was given by Yang and Freund (1985). Their results showed finite lateral contraction at the crack tip in contrast to the plane stress results. The crack tip stress field merged smoothly with the plane stress solution at the distance from the tip of one-half to three quarters of the plate thickness.

Nakamura and Parks (1988) used a three dimensional boundary layer formulation of a thin elastic plate. The results revealed strong three dimensional effects within a radial distance of about one and half thickness from the crack tip. The transition between the three dimensional - two dimensional field occurred at the distance of approximately 1.5 times the thickness. On the mid-plane of plate the crack tip field converged to that given by the local plane strain stress intensity factor solution within a radial distance from the tip less than 0.5 % of the plate thickness. Nakamura and Parks also indicated that the amplitude of the corner singularity field could be described by a corner stress intensity factor. The asymptotic behaviour of stress near the intersection of free surface and crack plane was expressed by Benthem (1975,1977) in the form,

$$\sigma_{ij} \propto \rho^\lambda g_{ij}(\lambda, \theta, \Phi) \quad \rho/t \rightarrow 0 \quad (29)$$

Here λ is the singularity exponent which depends on Poisson's ratio, the leading root lay in the range $-0.5 \leq \lambda \leq -0.333$ for $0 \leq \nu \leq 1/2$. g_{ij} is a dimensionless function. Spherical co-ordinates at the vertex are defined as:

$$\rho = (r^2 + z^2)^{1/2} \quad (30)$$

$z = t/2 - x_3$, t is the thickness of the plate. x_3 is distance to the free surface into the

plate. $\phi = \tan^{-1} (r/z)$. Let the local stress intensity factor along the crack front be defined as,

$$K^{local} (z) = \lim \sigma_{22} (2\pi r)^{1/2} \quad (31)$$

With the aid of equation (26), Benthem argued that for small values of z

$$K^{local} (z) = B z^{\lambda+1/2} \quad (32)$$

B is a constant which represents the intensity of the corner singularity field. B is the amplitude of the corner stress intensity factor. Using equation (28) the corner stress field can therefore be expressed as,

$$\sigma_{ij} = B / (2\pi)^{1/2} \rho^{\lambda} g_{ij} (\lambda, \theta, \Phi) \quad (33)$$

The work of Nakamura and Parks (1988) demonstrates that there is a full three dimensional near tip stress field within a radial distance of about one and half plate thickness from the crack tip while at greater distances the three dimensional stress field coincides with two dimensional plane stress field.

2.3.2 Determination of Elastic T-Stress in Three Dimensional Fields

The studies of Larsson and Carlsson, 1973; Cardew et al., 1984; Sham, 1991, have shown that the T-stress depends strongly on the loading as well as the crack length and overall geometry. In two dimensional problems, the T-stress is independent of material elastic properties such as Young's modulus or Poisson's ratio and plate thickness.

Nakamura and Parks (1992) introduced a general computationally effective method for calculating T stress distribution along a three dimensional crack front from finite element solutions based on a method originally implemented by Kfourri (1986).

The method is based on an auxiliary solution corresponding to a plane strain line load with magnitude f located along the crack front segment. The stress field in the crack tip front is given by,

$$\begin{aligned}\sigma_{11} &= \frac{f}{\pi r} \cos^3 \theta, & \sigma_{22} &= \frac{f}{\pi r} \cos \theta \sin^2 \frac{\theta}{2}, & \sigma_{33} &= \frac{f}{\pi r} \nu \cos \theta \\ \sigma_{12} &= \frac{f}{\pi r} \cos^2 \theta \sin \theta, & \sigma_{13} &= \sigma_{23} = 0\end{aligned}\quad (34)$$

The leading terms in a series expansion of the three dimensional mode I crack tip stress field are supposed to be expressed by the two dimensional plane strain mode I crack tip stress field:

$$\begin{aligned}\sigma_{11} &= \frac{K_I}{\sqrt{2\pi r}} \cos \frac{\theta}{2} \left(1 - \sin \frac{\theta}{2} \sin \frac{3\theta}{2}\right) + T \\ \sigma_{22} &= \frac{K_I}{\sqrt{2\pi r}} \cos \frac{\theta}{2} \left(1 + \sin \frac{\theta}{2} \sin \frac{3\theta}{2}\right) \\ \sigma_{33} &= \frac{K_I}{\sqrt{2\pi r}} 2\nu \cos \frac{\theta}{2} + T_{33} \\ \sigma_{12} &= \frac{K_I}{\sqrt{2\pi r}} \cos \frac{\theta}{2} \sin \frac{\theta}{2} \cos \frac{3\theta}{2} \\ \sigma_{13} &= \sigma_{23} = 0\end{aligned}\quad (35)$$

Where the term T ($= -T_{11}$) and T_{33} are the amplitudes of the second order terms. For the purposes of analysis a reference stress σ^* can be conveniently defined by $\sigma^* = \epsilon_{33} E$, where ϵ_{33} is strain in thickness direction. The stress component in thickness direction T_{33} is then decomposed into the form :

$$T_{33} = \sigma^* + \nu T \quad (36)$$

The crack tip stress fields consist of the superposition of the mode I crack tip stress field and the field due to the line-load. An energy conservation integral at the crack front location s , $I(s)$, allows the interaction integral to be written using the relation $\epsilon_{33} = \sigma^*/E$,

$$I(s) = \frac{f}{E} [T(s)(1-\nu^2) - \nu\sigma^*(s)] \quad (37) \quad \text{or}$$

$$T(s) = \frac{E}{f(1-\nu^2)} [I(s) + \nu\epsilon_{33}(s)] \quad (38)$$

In the integral, the leading term K in the crack tip field cancels out exactly and only the non-singular term $T(s)$ contributes to $I(s)$. Here $T(s)$ is the T-stress at the location s of the crack front, and ν is Poisson's ratio. f is the line load with unit magnitude. E is Young's modulus. $I(s)$ is the energy conservation integral which can be evaluated numerically by domain integral methods (Li, et al., 1985; Shih, et al., 1980). Equation (38) is used to evaluate the T-stress in three dimensional stress fields. The T-stress is a function of the elastic constants, E and ν . The T-stress as shown in Fig.9 from the analysis of Nakamura and Parks (1992) increases essentially uniformly across the crack front with increasing Poisson's ratio, but the through thickness variation remains small except in the region near the free-surface.

As the plate thickness increases, the T-stress decreases and approaches the two-dimensional plane strain solution. T is however strongly dependent on the thickness of thin plates due to the role of the out of plane strain ϵ_{33} as shown in equation (38).

In three-dimensional stress fields the T stress has characteristics that do not exist in two dimensional stress field. An important characteristic is that the plate exhibits an inherent positive biaxiality parameter displayed in Fig. 10 (Nakamura & Parks, 1992).

3. Elastic-Plastic Fracture Mechanics

3.1 Two Dimensional Crack Tip Fields

3.1.1 J-integral

Eshelby (1956) has defined some contour integrals based on energy conservation which are path independent. A two dimensional form of one of these integrals can be written as:

$$J = \int_{\Gamma} (w \, dy - t \, \partial u / \partial x \, ds) \quad (39)$$

with $w = w(x,y) = \int \sigma_{ij} \, d\varepsilon_{ij}$

Here Γ is a closed counter clockwise contour in a stressed body. t is the tension vector perpendicular to the closed contour in the outside direction, $t = \sigma_{ij} n_j$, u is the displacement in the x direction and ds is an element of contour length. w is the strain energy per unit volume. J is equal to zero along any closed contour in a stressed body.

Cherepanov (1967) and Rice (1968) independently applied this J-integral to crack problems. The closed contour Γ begins at the lower surface of crack and ends at the upper surface of crack. Rice (1968) demonstrated that the integral is path-independent with the following argument. Consider the closed contour ABCDEF around the crack tip in Figure 11a. Since $T_1 = 0$ and $dy = 0$ along the CD and AF, the integral is zero, if the contribution of ABC is equal to the contribution of DEF, but in opposite sign. This means that the integral will have a same value along the contour Γ_1 as that along the contour Γ_2 (see Figure 11b)

In the linear elastic plane strain stress field, the J-integral can be expressed in the form:

$$J = K_I^2 / E' \quad (40)$$

Where $E' = E$ for plane stress and $E' = E / (1 - \nu^2)$ for plane strain. This equation defines the important relationship between J and K within the context of LEFM.

3.1.2 Dual Definition of J-integral

Rice (1968) has shown that the J-integral, defined as a contour integral around crack tip, is also the variation of potential energy for a virtual crack advance da which provides an alternative definition of J , in terms of the potential energy release rate.

$$J = -d\Pi / da B = d(F-U) / da B \quad (41)$$

where Π is potential energy. B is thickness of the plate. F is work performed by the external force and U is the elastic energy. Since $F = U + W$, for a plate of unit thickness the condition for crack growth is,

$$d(F-U)/da = dW/da \quad (42)$$

Where W is the energy for crack formation. The potential energy release rate

$$J = d(F-U)/da = dW/da \quad (43)$$

The equation $J = d(F-U) / da$ relates J to the external force and displacement of the loading point, and is the basis of the experimental determination of J . The equation $J = dW/da$ states that J is also equal to dissipation energy release rate for virtual crack extension which allow J to be determined by numerical methods. The definition of J as a potential energy release rate allows it to be calculated from the externally applied forces

and displacement. The definition of contour integral of crack tip stress field allows J to characterise the stress field, while equation (43) establishes the relationship between these two definitions.

The strain energy density of linear elastic body has the form:

$$\begin{aligned} w &= 1/2 \sigma_{ij} \epsilon_{ij} \\ &= 1 + \frac{\nu}{2E} [(1-\nu)(\sigma_{11}^2 + \sigma_{22}^2) - 2\nu\sigma_{11}\sigma_{22} + 2\sigma_{12}^2] \end{aligned} \quad (44)$$

Substituting the stress components of the mode I crack tip stress field :

$$W = \frac{K_I^2(1+\nu)}{2\pi r E} [\cos^2(\theta/2)(1-2\nu) + \sin^2 \theta/2] \quad (45)$$

Insert $J E = K^2$ into (45)

$$\begin{aligned} W &= \frac{J(1+\nu)}{2\pi r(1-\nu^2)} [(1-2\nu) \cos^2 \theta/2 + \sin^2 \theta/2] \\ &= \frac{J}{2\pi r(1-\nu)} [\cos^2 \theta/2 (1-2\nu) + \sin^2 \theta/2] \end{aligned} \quad (46)$$

If J is path independent in the crack tip stress field, the strain energy density is necessarily singular, with a strength r^{-1} .

In the elastic-plastic stress field, Hutchinson (1968), Rice and Rosengren (1968) derived the stress and strain crack tip field in term of the J-integral for the non-linear elastic material expressed by a Ramberg-Osgood relation. The strain energy density of the HRR field is :

$$W = W(\epsilon) = \int \sigma_{ij} d\epsilon \quad (47)$$

So that the dimension of W is $\sum_{i=1}^2 \sum_{j=1}^2 \sigma_{ij} \epsilon_{ij}$, substituting the components of the HRR

stress and strain fields into the equation gives:

$$\begin{aligned}
 \sum_{i=1}^2 \sum_{j=1}^2 \sigma_{ij} \varepsilon_{ij} &= \sum \sum \sigma_0 (EJ / \alpha \sigma_0^2 I_n r)^{1/1+n} \tilde{\sigma}_{ij}(n, \theta) * \alpha \varepsilon_0 (EJ / \alpha \sigma_0^2 I_n r)^{n/1+n} \tilde{\varepsilon}_{ij}(n, \theta) \\
 &= \sum \sum (J / I_n r) \tilde{\sigma}_{ij}(n, \theta) * \tilde{\varepsilon}_{ij}(n, \theta) \\
 &= J / I_n r \sum \sum \tilde{\sigma}_{ij}(n, \theta) * \tilde{\varepsilon}_{ij}(n, \theta) \quad (48)
 \end{aligned}$$

$$W \cong J / I_n r \sum \sum \tilde{\sigma}_{ij}(n, \theta) * \tilde{\varepsilon}_{ij}(n, \theta) \quad (49)$$

From (46) and (49), the J- integral is a quantity directly related to the magnitude of strain energy density of both linear and non-linear elastic crack tip stress fields.

3.1.3 The HRR field

Hutchinson (1968), and Rice and Rosengren (1968) independently investigated elastic plastic crack tip stress and strain fields with the aid of a path-independent energy line integral for a two dimensional deformation field of power law hardening material under mode I loading. The uniaxial stress strain curve was modelled by the Ramberg-Osgood relation,

$$\varepsilon = \alpha \left(\frac{\sigma}{\sigma_0} \right)^{n-1} \frac{\sigma}{E} \quad (50)$$

where α is material constant and n is hardening exponent. The asymptotic crack tip fields were described using a stress function technique to give the nature of the dominant singularity:

$$\begin{aligned}
 \sigma_{ij} &= \sigma_0 (E J / \alpha \sigma_0^2 I_n r)^{1/1+n} \tilde{\sigma}_{ij}(n, \theta) \\
 \varepsilon_{ij} &= \alpha \varepsilon_0 (E J / \alpha \sigma_0^2 I_n r)^{n/1+n} \tilde{\varepsilon}_{ij}(n, \theta) \quad (51)
 \end{aligned}$$

The J-integral controls the amplitude of the stress field, in which $\tilde{\sigma}_{ij}(n, \theta)$ and $\tilde{\varepsilon}_{ij}(n, \theta)$ are angular functions. E is Young's modulus. r is the radial distance. I_n is

a tabulated dimensionless constant which depends on strain hardening exponent and the angle θ .

Other parameters are defined by a power law idealisation of the flow behaviour (Eqn.51). The expression provides insight into the crack tip stress field of non-linear elastic materials. The elastic-plastic stress and strain fields are known as the HRR fields or the HRR singularity.

Hutchinson (1968) employed deformation plasticity and a stress function method to analyse the stress and strain field in plane strain and plane stress conditions. Equilibrium was ensured for all stresses derived from a stress function. A higher order differential equation was solved by numerical methods to yield the stress components in the form:

$$\sigma_{ij}(r,\theta) = K r^{-1/1+n} \tilde{\sigma}_{ij}(\theta) \quad (52)$$

where K is a constant and $\tilde{\sigma}_{ij}(\theta)$ is function of its argument. Utilising the property of path independence of the J-integral, two paths were selected. One was taken entirely in the elastic region for which the results of J-integral had been obtained. Another path was chosen such that it lies within the zone dominated by the full plastic singularity. The integral must be equal to the value obtained from former, allowing the amplitude, K , to be obtained and thus fully defining the field.

Rice and Rosengren (1968) also used the method, but selected a different stress function. The crack tip singularity was verified by a simple method. For a circular path of radius r enclosing the crack tip J can be expressed,

$$J = \int_r (w \cos\theta \, r d\theta - T_i \partial u_i / \partial x_i \, r d\theta) \quad \text{or}$$

$$J / r = \int_r (w \cos\theta \, d\theta - T_i \partial u_i / \partial x_i \, d\theta) \quad (53)$$

As J is path-independent, the integrand which is product of stress and a strain-like component ensures path-independence,

$$w \sim \sigma_{ij} \varepsilon_{ij} \rightarrow f(\theta) \quad \text{as } r \rightarrow 0 \quad (54)$$

For power law hardening materials fulfilling this equation, this implies that

$$\begin{aligned} \sigma_{ij} &= K r^{-1/(1+n)} \tilde{\sigma}_{ij}(\theta) \\ \varepsilon_{ij} &= \alpha \varepsilon_0 K^n r^{-1/(1+n)} \tilde{\sigma}_{ij}(\theta) \end{aligned} \quad (55)$$

As deformation plasticity was used in the analysis, the elastic plastic stress field must meet the conditions of small scale yielding and proportional loading. This requires that the crack tip process zone, where non-proportional loading, large strain and other phenomena associated with fracture occurs, are encompassed and controlled by the J -dominated region.

3.1.4 J Dominance

The asymptotic crack tip solution for power law hardening materials, developed independently by Hutchinson (1968), Rice and Rosengren (1968), is known as the HRR field. J based fracture mechanics requires that the fracture process zone is encompassed by a zone which is independent of specimen geometry and defined by the HRR field. This defines the conditions for valid single parameter fracture mechanics. The J -integral, like the stress intensity factor K in the linear elastic stress field, characterises the strength of the HRR field. The elastic-plastic crack tip stress field is characterised by the J -integral. J -dominance defines the conditions under which the crack tip stress field can be expressed uniquely by the HRR field.

McClintock (1971) observed that in the limit of non-hardening behaviour and in the fully plastic state there is no unique stress and strain field in the crack tip region. Rather these fields are dependent on the crack geometry and loading. The slip-line field

solution for the CBB (cracked bend bar), CCP (central cracked panel) are radically different. As an illustration, the plane strain slip line field of a centre cracked panel loaded in tension is shown in Figure 12a. In contrast, the deeply cracked bend bar shown by Figure 12b exhibits a fully constrained flow field in which plasticity is confined to the ligament.

Numerical and experimental work has been conducted to confirm the relevance of the HRR solution and the J-dominance of real specimens. McMeeking and Parks (1979) used plane strain finite element analysis to study the deeply cracked bend bar (CBB) and centre cracked panel (CCP) for low hardening and non hardening materials. Deformation was followed from small scale yield into full plasticity. The criterion used to judge the degree of dominance was the extent to which stress and deformation field corresponded to the large geometry change field calculated under small yielding conditions.

Shih and German (1981) also used the finite element method to analyse the stress field of CBB, CCP and single edge cracked panel (SECP) specimen for contained and large plasticity. Small geometry change stress fields were compared with the HRR field to determine the region of agreement. Under large scale yielding condition, J-dominance is dependent on specimen type and hardening properties. The conditions to ensure J-dominance criterion for low hardening rates were suggested to be:

$$\begin{aligned}
 C &> \mu J / \sigma_0 \\
 \mu &> 200 && \text{centre deep cracked tensile panel} \\
 \mu &> 25\sim 50 && \text{edge cracked bending bar}
 \end{aligned}
 \tag{56}$$

Here C is the uncracked ligament, σ_0 is the uniaxial yield stress and μ is a geometry and loading dependent coefficient. For high hardening rates the size requirement may be reduced somewhat.

Al-Ani and Hancock (1991) examined the transition from deeply cracked to shallow cracked behaviour in edge cracked bend and tension bars. In weakly strain hardening

materials the J-dominance of short cracks in tension and bending specimen was lost. When a/W was less than 0.3 in bending or 0.55 in tension, plasticity develops initially to the cracked face. In this case the crack length becomes the controlling dimension, and J-dominance is lost before:

$$a > 200 \ J/\sigma_0 \quad (57)$$

Under large scale yielding conditions, non proportional loading occurs outside the intense strain region near crack tip and the crack tip is no longer uniquely characterised by the J-integral (Anderson, 1989). Though the J-integral can be successfully used in deeply cracked specimens loaded predominantly in bending. For the CCP and DECP (double edge cracked panel) geometry, fracture toughness becomes geometry dependent (O'Dowd, 1995). The J-dominant crack tip field is only limited to high constraint crack geometries. J-dominance will be lost for low constraint so that the critical value of J-integral is not a material constant but a specimen dependent parameter.

The derivation of the J-integral and the HRR field is based on deformation plasticity theory which is only valid as long as each point of material experiences proportional loading. The main application of the J-integral is to stationary crack tip stress fields.

The assumption of non-linear elastic stress-strain behaviour of material does not reflect the strong deformation in the region near the crack tip. However, the J-integral can still be used to characterise the crack tip field if the high strain zone is surrounded by the HRR field. In large scale yielding, plastic deformation occurs outside the crack tip zone and depends on the geometry and loading of the specimen. The nature of the crack tip singularity is affected by the nature of the macroscopic flow field. Under these conditions, the crack tip stress field is no longer dominated by J.

3.1.5 K-T and J-Q theory

Linear elastic fracture mechanics (LEFM) is based on the assumption that the near crack tip stress and deformation field is characterised by a single parameter, the stress intensity factor K_I . In LEFM, it is understood that the crack tip plastic zone is very much smaller than the specimen dimensions and is surrounded by an elastic zone characterised by K . The stress field can be characterised by the first singular term of the Williams (1957) expansion. However, Larsson and Carlsson (1973) showed that two dimensional plane strain crack tip stress fields are geometry and loading dependent, and argued that these effects arise from second term in the Williams (1957) expansion, the T-stress, on the crack tip elastic stress field. T is a function of geometry and loading. The shape and size of the plastic zone in modified boundary layer formulation (MBLF) solutions were much closer to those of corresponding specimens. Rice (1974) noted the T-stress does not affect the J- integral. This suggested that the single parameter K is not sufficient to characterise the near tip fields in some specimens. Bilby et al (1986) showed that two parameters (K and T) remote loading characterises the near tip elastic plastic field better than K alone.

In a recent study, Betegón and Hancock (1991), using the MBLF approach, compared the stress profile on small geometry change solution with small scale yielding solution in an actual specimen closely matched that of the MBLF solution with the same biaxiality parameter β as the actual specimen.

An approach developed by Bilby (1986), Betegón and Hancock (1991), Al-Ani and Hancock (1991), and Du and Hancock (1991) is based on the introduction of T as a constraint parameter. The linear elastic stress field is thus characterised by two parameters. The stress intensity factor quantifies the applied loading, while T-stress quantifies crack tip constraint. This two parameter fracture mechanics is called K-T theory.

Elastic plastic fracture mechanics is based on the concept of J-dominance. Whereby

the near tip stress and strain states are set by the single parameter. There is now general agreement that the applicability of the J approach is limited to high constraint geometries. For power law hardening materials, the elastic plastic stress field can be expressed by HRR field. Apart from the deeply cracked bend bar, the crack tip fields deviate very quickly from HRR singularity. If the crack tip stresses influence the fracture toughness, a fracture criterion based on J alone would be expected to be very conservative.

Asymptotic expansions of crack tip fields for Ramberg-Osgood materials have been sought by Xia, Wang and Shih (1992) and Chao, Yang and Sutton (1993). The expansions have been expressed by the Chao, Yang and Sutton (1993) in the form :

$$\frac{\sigma_{ij}}{\sigma_0} = \left(\frac{J}{\alpha \varepsilon_0 \sigma_0 I_n L} \right)^{1/n+1} \left\{ \left(\frac{r}{L} \right)^{-1/1+n} \tilde{\sigma}_{ij}^1(\theta) + A_2 \left(\frac{r}{L} \right)^{s1} \tilde{\sigma}_{ij}^2(\theta) + A_2^2 \left(\frac{r}{L} \right)^{s2} \tilde{\sigma}_{ij}^3(\theta) \right\} \quad (58)$$

The first term is the HRR field. The exponents of the second and third order terms are again functions of n. The amplitude A_2 is not determined by the asymptotic analysis and can only be obtained by the numerical analysis.

O'Dowd and Shih (1991,1992) have shown that a two parameter description, using J and a constraint parameter Q, fully characterises the near tip stress and strain state in a range of cracked geometries. The stress field is thus expressed in the form:

$$\frac{\sigma_{ij}}{\sigma_0} = \left(J / \alpha \sigma_0 \varepsilon_0 I_n r \right)^{1/1+n} \tilde{\sigma}_{ij}(n, \theta) + Q \left(\frac{r}{J} \right)^t \tilde{\sigma}_{ij}(n, \theta) \quad (59)$$

It is argued that the exponent t can be nearly zero which lead Q to be a distance independent second order term. The form of elastic-plastic crack tip stress field becomes:

$$\sigma_{ij} = (\sigma_{ij})_{ref} + Q \delta_{ij} \quad \text{for } r > J/\sigma_0 \quad |\theta| \leq \pi/2 \quad (60)$$

The parameter Q is determined from a finite element analysis and is the difference between the actual stress and reference field stress. It was shown that Q is a measure of hydrostatic stress. Xia, Wang and Shih (1992) have shown that Q represents the effect of the four higher order terms in the elastic-plastic field. Two fields have been considered as the reference field, the HRR singular field $(\sigma_{ij})_{HRR}$ and $(\sigma_{ij})_{ssy}$ which is the solution to the small scale yielding problem derived from the elastic K field. The first term of this expression is a high triaxiality reference field and the second term is a hydrostatic term which is independent of distance and angle. The form provides an approximate, but robust description of the near tip field over physically significant distance. Introduction of Q which depending on the load and geometry as the second term into single parameter fracture mechanics have been called J - Q theory.

3.2 Three Dimensional Elastic-Plastic Crack Tip Fields

Brocks and Olschewski (1986) were among the first to study the crack tip stresses under elastic-plastic conditions using three dimensional models for different specimens. The specimens included compact tension specimens of different size, a pressurised cylinder with a semi-elliptical inner surface flaw in the axial direction and a plate under pure bending with a semi-elliptical surface crack. The results showed that in large scale yielding conditions, the energy release rate J of the three dimensional model dominates the local stress and strain field in a confined area ahead of the crack front independent of the specimen size. The relationship between CTOD and J was confirmed to be of the same form as the two dimensional problem:

$$\delta_t = d_n J / \sigma_0 \quad (61)$$

Here d_n is a constant depending on the material strain hardening rate. δ_t is crack tip opening displacement in the mid-plane.

Narasimhan et al (1988) analysed a plane sided single edge bending panel having $W/B=8$ with a refined model and demonstrated the maintenance of high stress levels on the mid-plane.

Nakamura and Parks (1990) investigated a three dimensional crack front field in a thin plate. The existence and size of local J-dominated field were determined from a comparison of the near tip stress field with the plane strain HRR solution using a dominance parameter, ρ , which was expressed in the form,

$$\rho = \frac{\| \sigma_{ij} - \sigma_{ij}^{HRR(PL, strain)} \|}{\sigma_{ij}^{HRR(PL, strain)}} \quad (62)$$

The HRR field was only found at low load levels. The loss of HRR dominance occurred at a loading, $J^{tip}/\sigma_0 \varepsilon_0 t = 2$, the loss of dominance in the plane $z/t = 0.3$ occurred at a loading level of $J^{tip}/\sigma_0 \varepsilon_0 t = 1$. On the mid-plane, the distance of the J-dominance region $R(3\delta)$ is $0.0011 t$.

Faleskog (1994) performed fracture tests on a large surface cracked ductile plate and on small compact tension specimens. Constraint parameters h and Q were evaluated by detailed three dimensional finite element computations. h is a parameter in a damage integral suggested by Anderson (1993) which has the form,

$$\Phi = \int_0^{\varepsilon^p} \exp\left(\frac{3h}{2}\right) d\varepsilon^{-p} \quad (63)$$

Where h is equal to σ_m/σ_e , $\sigma_m = \sigma_{kk}/3$, σ_e is von Mises effective stress, ε^p is effective plastic strain. In a three dimensional form, if the HRR field has been chosen as the reference field, the h can be written as :

$$h = \frac{(\sigma_{kk})_{ref}}{(\sigma_e)_{ref}} + \frac{Q\sigma_0}{(\sigma_e)_{ref}} \quad (64)$$

and

$$Q = Q_m = \frac{\sigma_{kk} - (\sigma_{kk})_{ref}}{3\sigma_y} \quad (65)$$

There is a strong physical coupling between the parameter h and the ductile crack growth process. Two local positions along the crack front were chosen. The J values as a function of the amount of crack growth for these two positions showed the local constraint influenced the crack growth resistance curve markedly. The initiation of ductile crack growth along a three dimensional crack front appears to be independent of the degree of local constraint.

More recently Navalainen and Dodds (1995) studied the crack front field for SE(B) and C(T) specimens with very detailed three dimensional non-linear analyses. The J - Q methodology and the constraint scaling model for cleavage fracture toughness proposed previously by Dodds and Anderson (1991) were applied to determine the crack tip constraint. The constraint scaling model was coupled to the J_c with a near tip fracture criterion applicable to transgranular cleavage.

The material volume V on which the normalised principal stress σ_1/σ_0 exceeds a critical value was used as local failure criterion. Attainment of equal stressed volume ahead of the crack front in different specimens implied the same probability for fracture. The volume of material along the crack front over which the principal stress σ_1/σ_0 exceeds critical value is given by:

$$V = \int_{-B/2}^{B/2} A(s, \sigma_c) ds \quad (66)$$

Walloon (1993) employed extreme value statistics to derive a correction for fracture toughness data in specimen with different thicknesses $B(1)$ and $B(2)$:

$$K_{IC(2)} = K_{min} + (K_{IC(1)} - K_{min}) \sqrt[4]{B(1)/B(2)} \quad (67)$$

where the K_{min} denoted the threshold toughness of the material. Rewriting above equation in the term of J yields,

$$J_{c(2)} = J_{c(1)} \sqrt{B(1) / B(2)} \quad (68)$$

where the J equivalent of K_{min} was neglected as a small term. Dodds (1993) gave a model of two dimensional toughness scaling which had the form:

$$J_{FB} / J_0 = \sqrt{A_0(\sigma_c) / A_{FB}(\sigma_c)} \quad (69)$$

where A_0 denoted the enclosed area within the principal stress contour for an applied $J=J_0$ in the SSY boundary layer formulation, A_{FB} denoted the enclosed area for the same contour in a fracture specimen loaded to $J = J_{FB}$. J_{FB} is taken on the measured values at fracture, J_c . With computing J_0 from a two dimensional constraint scaling model with $A_{FB} = A_{max}$, replacing $J_{c(1)}$ in Eqn.(68) with the J_0 and the actual specimen thickness appearing in Eqn (68) with the effective thickness, $B_{eff} = V/A_{max}$, which quantifies the actual portion of specimen thickness over which crack front stresses reach the level of fracture, a measured toughness value, J_c , is then constraint and thickness corrected to the SSY condition using the modified form :

$$\overline{J_0} = J_0(J_c) \sqrt{B_{eff} / B} \quad (70)$$

Equation (70) is a three dimensional form of the toughness scaling model which reflects both the statistical effects of volume sampling due to the thickness difference and constraint loss on crack front stress field due to large scale yielding.

3.2.1 Three Dimensional Boundary Layer Formulations

The boundary layer formulation is a technique to model two and three dimensional crack tip stress fields. In general the stress or displacement distribution of the mode I K field are applied as the boundary conditions. In the three dimensional model, the displacements (u,v) derived from the two dimensional plane stress field are used to model the three dimensional boundary conditions of a thin plate containing a mode I crack.

$$\begin{aligned}
 u &= \frac{K_I}{2G} \sqrt{r/2\pi} \cos(\theta/2) (\kappa - 1 + 2 \sin^2 \theta/2) \\
 v &= \frac{K_I}{2G} \sqrt{r/2\pi} \sin(\theta/2) (\kappa + 1 - 2 \cos^2 \theta/2) \\
 G &= E / 2(1+\nu) \\
 \kappa &= 3 - \nu / 1 + \nu
 \end{aligned} \tag{71}$$

Plane stress is a two dimensional simplified form of the three dimensional stress field of a thin plate whose thickness is small compared with all the in plane dimensions. This means the stress field does not change through the thickness and in particular the out of plane σ_{33} is assumed to be zero. It is apparent that some degree of approximation is involved in applying the displacement derived from the two dimensional plane stress field to a three dimensional thin plate model.

Nakamura and Parks (1988) used the elasticity theory of Timoshenko and Goodier (1970) to obtain an approximate three dimensional crack tip field for a thin plate:

$$\begin{aligned}
 \sigma_{\theta\theta} &= \frac{K_I^{far}}{\sqrt{2\pi r}} \frac{1}{4} \left\{ \left[\frac{3 - 3\nu}{1 + \nu} \left(\frac{z}{r}\right)^2 \right] \cos \theta/2 + \cos 3\theta/2 \right\} \\
 \sigma_{\theta z} &= \frac{K_I^{far}}{\sqrt{2\pi r}} \frac{1}{4} \left\{ \left[\frac{1 - 3\nu}{1 + \nu} \left(\frac{z}{r}\right)^2 \right] \sin \theta/2 + \sin 3\theta/2 \right\}
 \end{aligned}$$

$$\sigma_r = \frac{K^{\text{far}}}{\sqrt{2\pi r}} \frac{1}{4} \left\{ \left[\frac{5}{1+\nu} + \frac{3\nu}{r} \left(\frac{z}{r}\right)^2 \right] \cos \theta/2 - \cos 3\theta/2 \right\} \quad (72)$$

Where K^{far} is the stress intensity factor of the plane stress field. Numerical results showed that this field accurately represents the complete field in the region $r/t \geq 1$. And at a distance $r = 5t$, the tractions obtained from (71) were in good agreement with the results from (70).

The stress distribution along a crack front of a three dimensional elastic thin plate has also been studied by Hartranft and Sih (1970). The three dimensional elastic stress field was expressed in the form:

$$\sigma_{11} = \frac{k_1(z)}{\sqrt{2r}} [\cos(\theta/2) - 1/2 \sin \theta \sin 3\theta/2] + o(1)$$

$$\sigma_{22} = \frac{k_1(z)}{\sqrt{2r}} [\cos(\theta/2) + 1/2 \sin \theta \sin 3\theta/2] + o(1)$$

$$\sigma_{12} = \frac{k_1(z)}{\sqrt{2r}} [1/2 \sin \theta \sin 3\theta/2] + o(1)$$

$$\sigma_{33} = \frac{k_1(z)^*}{\sqrt{2r}} [2\nu \cos 3\theta/2] + o(1)$$

$$\sigma_{13} = \sigma_{23} = o(1) \quad \text{as } r \rightarrow 0 \quad (73)$$

In equation (73), the stress intensity factors $k_1(z)$ and $k_1(z)^*$ vary along the z direction and are functions of ν , t/a and z . The stress intensity factor increases in magnitude very sharply near a free surface and remains constant far from the free surface in small scale yielding. The value of $k_1(z)$ is nearly a constant in most parts of the plate. Comparing (73) with the stress formulation of the two dimensional mode I stress field (74),

$$\sigma_{22} = \frac{k_I}{\sqrt{2\pi r}} [\cos\theta/2 + \sin\theta/2 \sin(3\theta/2)\cos\theta/2] + 0(1)$$

$$\sigma_{11} = \frac{k_I}{\sqrt{2\pi r}} [\cos\theta/2 - \sin\theta/2 \sin(3\theta/2)\cos\theta/2] + 0(1)$$

$$\sigma_{12} = \frac{k_I}{\sqrt{2\pi r}} \cos\theta/2 \sin\theta/2 \cos(3\theta/2) + 0(1) \quad (74)$$

The main difference between Eqn.(74) and Eqn.(73) is that the stress intensity factor k_I is constant through thickness rather than variable. Any error is focused near the free surface, since in most parts of plate $k_I(z)$ is largely independent of (z) (Hartranft and Sih, 1970). Thus two dimensional elastic crack tip stress field formulations of mode I in a thin plate are acceptable remote boundary conditions for the three dimensional near tip stress field of an elastic thin plate.

3.2.2 J-integral in Three Dimensional Stress Fields

In two dimensional stress fields the J-integral generalises a surface integral which provides a global energy release rate. For a three dimensional configuration, we can appeal to the same energetic argument $J da = -d\Pi$ for a pointwise definition of energy release rate along the crack tip. Let $da(s)$ denote the crack advance at the points in the direction normal to the crack front and in the crack plane. Let ds denote an elemental length along the crack front. Then $J(s)$ is defined by the relation.

$$\int_{\Gamma} J(s) da(s) ds = -d\Pi \quad (75)$$

$J(s)$ can also be defined by the equation ,

$$J(s) = \lim_{\Gamma \rightarrow 0} \mu(s) \int_{\Gamma} (w n_k - \sigma_{ij} n_j \partial u_i / \partial x_k) d\Gamma \quad (76)$$

Here $J(s)$ is a pointwise value along a three-dimensional crack front, s represents

the location of the crack tip on crack front, w is strain energy density, σ_{ij} and u_i are the components of the stress and displacement tensors, n_j are components of a unit vector normal to Γ and to the crack front tangent vector s . Γ is a contour at s surrounding the crack front lying in the plane perpendicular to crack front. The unit vector $\mu(s)$ denotes the local direction of crack advance. This integral defines a local energy release rate along any crack front in three dimensional space. The J -integral as a path independent integrand like that in two dimensions does not exist in three dimensional stress fields. However the accurate calculation of quantities of near tip fields is not easy. The J -integral of three-dimensional crack body is now usually determined by the domain integral (Li, Shih, and Needleman, 1985). In the present analysis the domain integral method provided by ABAQUS (1995) is employed.

3.2.3 J Dominance of a Three Dimensional Thin Cracked Plate

Nakamura and Parks (1992) have used a three dimensional boundary layer formulation method to investigate J -dominance under elastic-plastic conditions. Two different boundary layer formulations were applied. The displacement formulation of a mode I plane stress K field was applied under small scale yielding conditions as well as the displacement field of the plane stress HRR field solution for fully plastic conditions. The analysis showed that when a plane stress small scale yielding condition exists in the far field, strong three dimensional effects were observed within a radial distance of half thickness from the crack front. The in-plane stresses of the three dimensional field merged with the dominant K solution at a radial distance of 1.5 times of the plate thickness. The distance, denoted by R^k , which increased with increasing load, may be expressed by,

$$R^k = 1.5 t + \beta J^{far} / \sigma_0 \varepsilon_0 \quad (77)$$

Here β is constant which is approximately equal to 0.1 on the basis that the variation of the computed stresses from the K solution is less than 10%. As a dominant K field in two dimensional plate exists within a radial distance from the tip of 10% of the smallest characteristic length, b , the geometric requirement for the small scale yielding condition of the three dimensional thin plate can be written in the form:

$$b \geq 15 t + J^{\text{far}} / \sigma_0 \varepsilon_0 \quad (78)$$

At higher loading levels, a plane stress HRR field was assumed to exist within the plate. A local plane strain HRR field was confined to the crack front while the in plane stresses coincided with the plane stress HRR solution at the radial distance of 1.5 times the thickness. Taking into account the finite deformation zone, D , whose size (McMeeking and Parks, 1979) is given approximately by:

$$D \cong 0.006 J^{\text{local}} / \sigma_0 \varepsilon_0 \quad (79)$$

J-dominance demands that the radius of the zone in which the plane strain HRR dominates must exceed D . The mid-plane normalised radius, R^{HRR} can be approximated based on the local stress being within 80% of the corresponding plane strain HRR value, in term of normalised far-field load as,

$$\frac{R^{\text{HRR}}}{J^{\text{local}} / \sigma_0 \varepsilon_0} \cong 0.026 - 0.002 J^{\text{far}} / \sigma_0 \varepsilon_0 t \quad (80)$$

If the criterion of dominance for plane strain HRR dominance is that $R^{\text{HRR}} > D$, Equations (78) and (79) require,

$$J^{\text{far}} / \sigma_0 \varepsilon_0 t \leq 10 \quad (81)$$

It would seem that no dominant local plane strain condition can exist in a thin plate at higher levels of loading.

4. Computational Model

The three dimensional problem studied is a thin plate with a through crack subjected to mode I loading. The distribution of the components of the three dimensional crack tip stress field is investigated. The purpose of this study is to assess the effects of free surface on stress field and to set up a numerical relation between J and the quantities of stress field, and in particular identify the role of the T stress on the plane strain- plane stress transition.

4.1 Geometry and Computational Model

A cracked geometry similar to that used by Nakamura (1988) has been adopted to study the three-dimensional stress field near a through crack front in a thin plate. The region around the crack tip of the thin plate has been represented by a circular disk which contains a radial crack, as illustrated in Figure 13. The straight crack front is located at the centre of the disk along the z axis ($x = y = \text{zero}$). The radius of disk was sufficiently large compared with the thickness to contain the three-dimensional field within the outer boundary. The maximum radius of the disk was about one thousand times the thickness ($R_{\text{max}}/t \cong 1000$). On the outer ring of the circular disk displacement boundary conditions derived from the mode I plane stress field were applied.

For the finite element analysis only a quarter of the disk needs to be modelled (see fig. 14) since the problem has symmetry with respect to the mid-plane, the crack, and the ligament plane. The finite element mesh was constructed with 8-noded hexahedron elements. The element size gradually increased with radial distance from the crack tip. The angular span of each element was constant 15° throughout the

mesh. The same planar mesh was repeated along the x_3 direction from the symmetry plane (mid-plane) to the free surface. To accommodate the strong variation of the field quantities along thickness, the thickness of the element layer was gradually reduced toward the free surface. The behaviour of the material can be represented by a power law idealisation. In uniaxial deformation, the stress-strain relation can be written:

$$\begin{aligned} \varepsilon &= \alpha (\sigma / \sigma_0)^{n-1} \sigma / E & \sigma &\geq \sigma_0 \\ \varepsilon &= \sigma / E & \sigma &\leq \sigma_0 \end{aligned} \quad (82)$$

The stress σ_0 is a reference value, usually taken to be the 0.2 percent offset of yield strength. α is a material constant. For deformation plasticity theory the power law flow behaviour can be generalised as:

$$\varepsilon_{ij} = 3/2 \alpha (\sigma_e / \sigma_0)^{n-1} S_{ij} / E \quad (83)$$

where S_{ij} is the deviatoric stress and σ_e is the effective stress. In the model the modulus E was $2.0E11$. The yield stress σ_0 $2.0E07$, Poisson's ratio ν 0.3 and the material constant α was $3/7$. Calculation were performed for three values of the hardening exponent n , 13 and 6 .

In the present work two finite element models were set up. The first mesh models the whole of disk with the displacement of mode I plane stress field applied on the outer boundary. The second model is a substructure which has the same thickness and similar element arrangement. (Figure 15 shows the mesh of substructure). The radius of the second mesh is half first one and the mesh is finer at the tip. The substructure mesh is used to obtain the accurate solution near the crack tip and in the intersection of crack front and free surface. The boundary condition of the finer mesh were obtained by interpolating the displacements of the coarser mesh to the nodal position on the outer perimeter of the inner mesh.

4.2 Computational Procedure

All the finite element analysis results were obtained using the finite element code ABAQUS (1995). The three dimensional finite element mesh was built up using the package PATRAN (1991). In the present analyses, two finite element meshes were employed. The coarser mesh has a total of about 12,000 elements. The finer mesh has about 8000 elements. The loading was applied by increasing the stress intensity factor K . Three different levels of deformation were achieved corresponding to small scale, moderate and large scale yielding. The largest level was reached at $R_y / t \approx 100$. Numerical values of the stresses were obtained at the centre of each element. The computing time for each non-linear calculation was 16 hours. The calculation was carried out on a SUN 4/80 (SPARC station 10).

5. Computational Results.

5.1 Three Dimensional Boundary Layer Formulation Model

5.1.1 Small Scale Yielding for Non-hardening Materials

In small scale yielding, the radius of plastic zone R_y is defined to be less than the thickness of the plate. The opening stress σ_{22} directly ahead of crack ($\theta = 0$) is plotted as a function of radial distance in Figure 16. σ_{22} is normalised by the yield stress σ_0 . While the radial distance is normalised by the thickness of plate t . The mid plane is denoted $z / t = 0$ and the free surface, $z / t = 1$. Figure 16 shows that the opening stress σ_{22} changes slowly along the thickness throughout most of the thickness, but in the region close to the free surface the stress drops sharply. Figure 16(a) shows the variation of the stress σ_{11} near crack tip through the plate thickness. Both σ_{22} and σ_{11} decrease markedly near the free surface.

The out of plane stress σ_{33} normalised by σ_0 is shown in Figure 16(c). The maximum value appears at the crack tip on the mid-plane and decreases slowly in both x and z directions. σ_{33} declines sharply near the free surface.

Figure 17(a) shows the distribution of $\sigma_{33} / (\sigma_{11} + \sigma_{22})$. In plane strain conditions $\sigma_{33} / (\sigma_{11} + \sigma_{22})$ is equal to Poisson's ratio ν and is zero in plane stress. The term $\sigma_{33} / (\sigma_{11} + \sigma_{22})$ can be denoted a 'lateral coefficient' since its values characterise the role of out of plane constraint. In the zone near the crack tip the coefficient is greater than 0.4 which shows a strong constraint effect. The values near mid-plane are larger than the values near free surface.

The stress field demonstrates the results that all the stresses gradually decline from plane strain at the mid-plane to the surface. The distributions of the stresses σ_{11} , σ_{22} and σ_{33} through the plate thickness on the crack front in the elastic case are shown in Figures 31, 32 and 33, respectively. The x direction in the graph is indicated by 1 and z direction is indicated by 3.

Figure 17(c) shows the distribution of the elastic strain energy density W_e along the crack front. The elastic strain energy density is a singular quantity which also shows the same characteristic decline along the crack front, dropping sharply near the surface zone.

Figure 17(b) is a plot of the distribution of the out of plane strain ϵ_{33} . This strain component increases from the mid-plane to surface and where it reaches a high level. The main characteristic of the strain field is a strain concentration zone located at the intersection of the crack plane and free surface. It is the strain concentration which causes the thickness reduction and lateral contraction of the free surface. The local thinning caused by the thickness reduction is an important feature of the field.

The J- integral or local strain energy release rate along the crack front has been obtained using the domain integral method in ABAQUS (1993). The variation of J along the crack front is shown in the Figure 18. In this figure, J is a function of location on the crack front for various levels of loading. Each curve is made up of two parts. One

part has a small slope and another has high slope. The high slope is located in a zone near the free surface where the strain energy density drops sharply and the size of this zone expands with the increasing load. The distribution of J coincides with the distribution of elastic strain energy density along the crack front.

5.1.2 Discussion

The stress distribution in a thin plate with a through crack in small scale yielding exhibits a highly triaxial stress field near the crack tip which is surrounded by the dominant plane stress field. The transition from the plane stress state to the triaxial field occurs at a distance of about three thicknesses from the crack tip. The transition from plane stress to the plane strain crack tip is gradual.

In the interior of specimen the stresses within the plastic zone near the crack tip are highly elevated above the yield stress leading to a strongly triaxial stress field. The emergence of a near tip plane strain crack tip stress field is one of the essential characteristics of the plane stress field of a thin plate.

The three dimensional crack tip stress field in small scale yielding shows a variation from plane strain conditions in the mid-plane zone to a low triaxiality stress state near the free surface. The plane strain condition ($\epsilon_{33}=0$) is gradually lost along the crack front since the degree of out-plane constraint is reduced as the free surface is approached. The chief features of the free surface region are low stresses (σ_{11} , σ_{22} and σ_{33}) and a low energy density which are neither characteristic of plane stress, nor of plane strain, but a characteristic of the full three dimensional stress field.

In small scale yielding, the local strain energy release rate, J , along the crack front has a similar distribution to both the stress distribution, and the elastic strain energy density. As J is a quantity related to the strain energy density of crack tip field, the region in which J is weakly dependent on z is also necessarily the region in which the stresses are weakly dependent on z .

In the two dimensional elastic stress field the stress intensity factor K is used to characterise the crack tip stress field. Its relationship with J is expressed in the familiar formulation $K^2 = J E'$. In the case of a thin plate field, a plane strain stress intensity factor K_I^{local} at each section through the thickness can be obtained using the equation:

$$K_I^{local} = \sqrt{J^{local} E / (1 - \nu^2)} \quad (84)$$

where J^{local} is the pointwise strain energy release rate along the thickness calculated numerically.

The three dimensional elastic crack tip stress field of each section along the thickness can be approximated using a two dimensional mode I crack tip stress field. In general, the elastic crack tip stress field through the thickness can be expressed by,

$$\sigma_{ij} = \frac{Y K_I^{local}}{(2\pi r)^n} f_{ij}(\theta) \quad (85)$$

Here Y is a modifying coefficient and n is exponent which is a function of loading and thickness z . In the interior of plate (plane strain state) $n=1/2$, but in the region near the free surface n will be bigger than $1/2$.

The stresses resulting from calculations using K_{local} are in an agreement with the finite element results. Figure 19 (a, b, c, d) shows the distribution of σ_{22} obtained from the numerical calculation at different section ahead of the crack and through the thickness of the plate compared with σ_{22} determined from the local K . Figure 20 (a, b, c, d) shows a comparison of σ_{11} from these two methods. These results illustrate that stress components of the three dimensional field can be calculated through a local pointwise J in small yielding conditions.

The relationship, $J = d(U - F) / da B$, is the basis of the experimental determination

of J . The distribution of J is assumed to be the constant through the thickness, but according to the finite element analysis J varies along crack front. The distribution of J along the crack front at small scale yielding can be expressed by an equation in the form:

$$J = \frac{K^2}{E} [A_1 - \ln \ln A_2 / (z/t)^{A_3}] \quad (86)$$

where J is a local pointwise energy release rate J , K is the remote stress intensity factor at the boundary, and A_i is constant related to loading. In small scale yielding $A_1 = 4.95K/K_{remote} + 2.8$, $A_2 = 13370K/K_{remote}^2 - 5440K/K_{remote} + 1040$, and $A_3 = 8.51K/K_{remote}$. A comparison of the J distribution with this equation is given in Figure 21.

If the nature of J of the three dimensional field of a thin plate is examined further, the relationship between distribution of J and the plate thickness may be used as an indication of the role of lateral constraint and the influence of the free surface on the stress field. The J distribution (86) has the same quantities as $J(s)da(s)$ in the equation, $\int_{\Gamma} J(s) da(s) ds = -d\Pi$. Using the equation the strain energy release rate $d\Pi$ of whole plate can be obtained.

The free surface has an important influence on the crack tip stress field. An important parameter is the width of the low elastic energy zone at the free surface. Koers, Braam and Bakker (1989) observed in their experimental investigation of the effect of thickness, that there is a low energy zone that was 5.9mm for a thickness of 30mm and 6.5mm for a thickness of 70mm and 110mm. The width of the process zone is a function of loading, area of surface, crack length, thickness and the material behaviour. From Figure 21 it is seen that the low energy zone changes with loading.

The through thickness variation of the strain field is totally different to the stress field. The distribution of strain through the thickness reaches its maximum value near

the free surface. The distribution of J along the crack front does not have the same trend as the strain distribution. This means that J is not a uniquely characteristic quantity of the three dimensional field. In this investigation the dissipation energy was found to develop through the thickness in the same form as the strain distribution.

A thickness reduction due to out of plane displacements is a feature of the three dimensional crack tip stress field. The surface displacements cause a hollow to develop on the free surface near the crack tip due to the strain concentration of ϵ_{33} . Figure 22 shows the distribution of displacement, W , on the free surface of the boundary layer formulation. In the present work the out of plane displacement W has been compared with J using the results of finite element analysis. An equation is obtained from the model to illustrate the distribution of out of plane displacement directly ahead of the crack tip which is the same as the result put forward by Irwin (1989).

$$W = 0.5 J / \sigma_0 \quad (87)$$

W is the displacement on the surface in the thickness direction. J is J_{remote} .

5.1.3 Moderate and Large Scale Yielding for a Non-Hardening Material

With increasing load, the radius of the plastic zone expands, and the von Mises yield criterion can be applied to determine the extent of plastic deformation. The level of deformation is defined by the ratio of radius of plastic zone to the thickness, R_y/t , on the mid-plane. The condition in which R_y is approximately equal to the thickness t is now defined as moderate scale yielding. The condition in which the plastic zone is very much greater than the thickness ($R_y/t = 75$) is defined as large scale yielding.

The distribution of σ_{11} , σ_{22} and σ_{33} in the moderate scale yielding (MSY) condition

is shown in Figure 23. The results display a gradual drop in stress from the mid plane to the free surface. The SSY feature in which the in-plane stress drops sharply near the free surface is lost.

The ratio $(\sigma_{33} / \sigma_{11} + \sigma_{22})$ in MSY is shown in Figure 24(a). It can be seen that the plane strain constraint parameter also decreases from the midplane to the free surface which illustrates the absence of a dominant plane strain zone in the crack front. The distribution of e_{33} is plotted in Figure 24(b). The maximum value is increased markedly and the zone of strain concentration expands compared to small scale yielding.

The crack tip field has also been examined under large scale yielding (LSY). At this deformation level the plastic zone has a constant radius through the thickness. The ratio of radius of plastic zone to the thickness is 75 for the data shown. The σ_{11} , σ_{22} and σ_{33} stresses are shown in Figures 25. These Figures should be compared with these for the small scale and moderate scale yielding stress field. The maximum values of the stresses at the crack tip are $\sigma_{11}/\sigma_0=2.61$, $\sigma_{22}/\sigma_0=3.76$, $\sigma_{33}/\sigma_0=3.17$ which are significantly greater than the stresses at low levels of deformation. The stresses also decline rapidly from the midplane to the free surface.

The distribution of e_{33} under large scale yielding is plotted in Figure 26. The minimum value of e_{33} occurs at the midplane and is about $50\varepsilon_0$. Figure 26(a) shows the distribution of $\sigma_{33}/(\sigma_{22}+\sigma_{11})$. The J distribution along the crack front is shown in Figure 27, in which the strain energy release rate J is normalised by J remote. The variation of loading is expressed by $J/t\sigma_0$. The slope of J distributions are similar to the slope of the stresses. The distribution and variation of the energy release rate still has the same trend as the stress distribution.

In Figures 28 and 29 the radial variation of the opening stress ahead of the crack front is compared with the plane strain HRR field in SSY and MSY condition.

Figure 29 demonstrates that very near the crack tip the opening stress in the interior of the specimen tends towards the plane strain HRR field.

5.1.4 Discussion

The distribution of stresses through the thickness depends on the load level. In SSY the stresses are almost constant through most of the thickness and drop sharply close to the free surface. In MSY the stresses decline throughout most of the thickness in a gradual manner. In LSY the stresses decay from the mid plane and drop quickly to the free surface. The variation in the thickness direction are totally different at these three deformation levels. The distribution of stresses through thickness vary with the increasing load which indicates that the lateral constraint effect reduces with increasing deformation.

The ratio of $\sigma_{33} / (\sigma_{22} + \sigma_{11})$ can be defined as the plane strain constraint parameter. The ratio is uniform through most of the plate thickness in SSY which illustrates that plane strain applies over the most of the thickness. The width of the zone in which the lateral constraint factor $\sigma_{33} / (\sigma_{22} + \sigma_{11})$ is uniform decreases with increasing load. Under LSY the stress state is in transition between plane strain near the mid plane and an unconstrained state close to free surface.

The crack tip strain field also changes with load level. The position of the peak value of the out of plane strain ϵ_{33} moves toward the interior of plate compared to SSY in which the maximum strain occurs at the free surface.

The extent of crack tip triaxial stress field in large scale yielding is not the same as that in the small scale yielding. The distribution of σ_{33} within the plastic zone through thickness (see Fig.26) shows that at a distances, r/t larger than 4, σ_{33} is uniform over the entire thickness. The distance from which this transition occurs is at $r/t = 3$ in small scale yielding. It is also noted that at large scale yielding all the stresses (σ_{11} , σ_{22} and σ_{33}) through the thickness at distances larger than $r/t = 4$ maintain a low and uniform stress level.

J exhibits the same trend as the distribution of stress through the thickness. In Figures 27 J shows the same slope of curve variation as the stress distribution from

mid plane to free surface in the MSY and LSY condition. The variation of J through the thickness reflects the influence of lateral constraint on the crack tip stress field.

5.1.5 Stress Field of a Strain Hardening Materials

The elastic-plastic crack tip field of materials which have strain hardening exponent 6 and 13 were examined at a deformation level corresponding to Ry/t equal to 1.85. The distribution of stresses of the two stress fields were similar. The distribution of σ_{11} , σ_{22} and σ_{33} for the material with hardening exponent 6 are illustrated in Figure 33. The results show a decrease of the stress from the mid-plane to the free surface. The maximum stresses at a distance of $r/t=0.02$ from crack tip on the mid plane are much higher than the non-hardening material at the same load level.

The extent of the plane strain region can be seen in Figure 34(a). The parameter $\sigma_{33}/(\sigma_{11}+\sigma_{22})$ has a value close to 0.5 at the crack front which demonstrates strong plane strain constraint. Plane strain is contained within a depth of $z/t=0.82$, which is larger than the zone for a non-hardening material at the same loading condition. Figure 34(b) shows the distribution of the out-of plane strain.

The distribution of stresses in the crack plane for a material with hardening exponent 13 is shown in Figures 35. The maximum stresses at a distance of $r/t=0.02$ are much lower than the material with a hardening exponent 6.

Figure 36(a) shows the distribution of the lateral constraint parameter $\sigma_{33}/(\sigma_{11}+\sigma_{22})$. The parameter changes from close to 0.5 to nearly 0 which shows the material at the mid plane is subjected to the maximum degree of lateral constraint. The plane strain constraint zone is within $z/t=0.6$

Corresponding to the decrease in lateral constraint from the mid plane to the free surface, the out plane strain e_{33} increases and the maximum value occurs at about $z/t=0.99$. The distribution of e_{33} is displayed in Figure 36(b). A strain concentration is located at intersection of crack plane and free surface, the

maximum value of $\epsilon_{33} / \epsilon_0$ is about 21 which is lower than the value of material with hardening exponent 6.

5.1.6 Discussion

The effect of strain hardening on the crack tip stress field is to cause the stresses within the plastic zone to rise. The lower the hardening exponent, the higher crack tip stress. The opening stress at a distance of $r/t=0.02$ from the crack tip on the mid plane in the case of material with hardening exponent 6 reaches 8 times the yield stress. But the distribution of stress through the thickness is similar to the distribution for a non-hardening material.

Another effect of strain hardening is the change in lateral constraint. Referring to Figures 34 and 36, the extent of the plane strain region is different. The plane strain region of material with exponent 6 is confined to depth of $r/t=0.82$, compared to 0.5 for a non-hardening material. It is apparent the lateral constraint increases with the hardening rate increases.

The third role of strain hardening is to affect the maximum value of the out-plane strain ϵ_{33} . The out of plane constraint increases as the hardening exponent decreases.

5.2 Three Dimensional Modified Boundary Layer Formulations

The three dimensional crack tip stress fields of hardening and non-hardening materials at different load levels have been studied using three dimensional boundary layer formulations. To investigate the effects of in-plane constraint on the three dimensional stress field, the modified boundary layer formulation model has been introduced by adding non-singular T-stress to the K-field on the outer boundary of the boundary layer formulation model. The boundary displacement conditions are given by:

$$\begin{aligned}
 u &= \frac{K_I}{2G} \sqrt{\frac{r}{2\pi}} \cos\left(\frac{\theta}{2}\right) [\kappa - 1 + 2 \sin^2\left(\frac{\theta}{2}\right)] + \frac{rT \cos\theta}{E} \\
 v &= \frac{K_I}{2G} \sqrt{\frac{r}{2\pi}} \sin\left(\frac{\theta}{2}\right) [\kappa + 1 - 2 \cos^2\left(\frac{\theta}{2}\right)] - \frac{rTv \sin\theta}{E}
 \end{aligned} \tag{88}$$

The model adopted is a three dimensional plane stress thin plate subjected to a mode I loading. The displacement W in the thickness direction is allowed to develop freely under the action of in-plane displacement. As the T-stress reflects the constraint effects of the cracked body, the model of modified boundary layer formulation can be regarded as a simulating crack tip conditions in an arbitrary geometry under contained yielding. The distribution of the remote T-stress through thickness is supposed to be uniform for a thin plate with a through crack reference to Nakamura and Parks (1992). Negative, and positive T-stresses at a level of $0.6 \sigma_0$ have been imposed on the outer boundary.

The boundary conditions were applied in two steps. Initially the displacements corresponding to the T-stress were imposed, then the displacement corresponding to an increasing stress intensity factor were applied while T-stress maintaining a constant. The method of two-steps ensures a constant T stress at all levels of deformation.

5.2.1 Effects of T-Stress on Three Dimensional Stress Field for a Non-Hardening Material

Figures 37 and Figure 38 show the distribution of opening stress through the thickness directly ahead of the crack with $T=0$. The stresses are normalised by the yield stress σ_0 , while z is normalised by the thickness t . The radial distance r is normalised by J/σ_0 . The stress profiles are shown for two different deformation levels.

One is small scale yielding (SSY) and another moderate scale yielding (MSY). In small scale yielding the radius of the plastic zone is very much less than the plate thickness, while in MSY the plastic zone radius and the plate thickness are comparable.

A negative T stress reduced the stress level ahead of crack. The stress profiles for two different deformation levels with a negative T are plotted in Figures 39 and 40. Figure 41 and Figure 42 display the opening stress profile under a positive T -stress at two deformation levels.

The variation of the plastic zone radius directly ahead of the crack through the thickness with different stress levels are shown in Figures 43, 44 and Figure 45. A compressive T -stress enlarged the maximum radius of plastic zone. However the effect of the negative T -stress on the plastic zone through the thickness is not uniform. The radius of the plastic zone near the mid plane is larger than the parts close to the free surface. In contrast tensile, or positive, T -stresses caused the plastic zone to decrease in size and shape, the maximum radius of plastic zone through the thickness occurred close to the free surface rather than near the mid plane. In large scale yielding the radius of plastic zone through the thickness developed into a uniform state with either positive or negative T -stresses and zero T .

5.2.2 Discussion

The effect of the T stress on the plastic zone shape and size in two dimensional stress fields has been studied by Larsson and Carlsson (1973). Du and Hancock (1991) also described the variation of the size and shape of a plastic zone as a function of the T -stress in two dimensions. The effects of T -stresses on a three-dimensional plastic zone is similar to the two dimensional field. That is a negative T -stress makes the plastic zone enlarge while positive T -stresses cause the plastic zone to diminish. Nevertheless the effect of T -stress on the each part of the thickness is apparently different. A negative T makes the radius of plastic zone advance near

the midplane. In contrast a positive T-stress makes the plastic zone near the midplane reduce more than the region close to the free surface. The variation of the plastic zone size is also influenced by the deformation level. In small scale yielding the crack front is in plane strain state, the distribution of plastic zone radius is essentially uniform. In large scale yielding the plastic zone is in a state of plane stress, the distribution of plasticity through thickness is also uniform. It is evident that the T-stress affects the stress field in plane strain state. Due to the absence of studies of effect of T-stress on the plane stress crack tip fields, the action of T-stresses on plane stress is not understood. It seems the effects of T-stress on the plane stress field are not very strong which may cause the radius of plastic zone through thickness to develop in a non-uniform manner.

From Figures 39 and 41 the distribution of opening stress σ_{22} in small scale yielding shows that a negative T-stress reduces the stress level in the same way as in the two dimensional stress field, while the positive T-stress does not affect the crack tip stresses at all. As the stress state in most parts of crack tip front is in plane strain, the distribution of stress through the thickness are uniform except in the region very near the free surface.

The influence of T-stress on the lateral constraint is shown in Figures 38, 40 and 42. At similar deformation levels, the distribution of opening stress through the thickness with positive T-stress shows that plane strain state exists throughout most of the thickness. In the case of negative T-stress, the distribution curve from midplane to the free surface shows the plane strain region is more limited. The width of the plane strain zone at the zero T stresses is intermediate between these two cases.

6. Conclusions

- (1) The crack tip stress field of a thin plate shows a strong stress triaxiality in the crack front .
- (2) The plane strain condition in the mid-plane declines through the thickness. The variation of stress distribution from mid-plane to free surface depends on the level of loading..
- (3) The pointwise energy release rate J characterises the amplitude of the local stress field. The through thickness variation of J follows the variation in the local stresses in the crack front at different load levels. The variation of J along the thickness reflects the variation of lateral constraint.
- (4) The distribution of J along the thickness can be expressed by the equation:

$$J = \frac{K^2}{E} [A_1 - \ln \ln A_2 / (z/t)^{A_3}]$$

The equation can be used to calculate the energy release rate of the whole of plate

- (5) The distribution of out of plane displacement near the crack tip on the free surface in small scale yielding can be expressed in a simple form:

$$w = 0.5J / \sigma_0$$

- (6) The effect of the hardening exponent is to increase the stresses in the crack tip plastic zone and enhance the lateral constraint.
- (7) The T-stress affects the plastic zone size and shape of the three dimensional field. As the effects of T-stress on the plane strain and plane stress are different, the distribution of plastic zone through thickness is not uniform.

7 Reference

- ABAQUS, Version 5.3, 1993, Hibbit, Karlsson and Sorensen, Inc. Providence, R.I.
- Al-Ani and Hancock, J. W., 1991, *J. Mech. Phys. Solids*, V.39, No.1, 23-43
- Anderson, T.L. and Dodds, R.H., 1991, *J of Testing and Evaluation*, V.19, No.2, 123-134
- Anderson, T.L., Vanaparthi, N.M.R., 1993, in *Constraint Effects in Fracture*, ASTM STP 1171, Philadelphia, 473-491
- Anderston, W.E., 1969, Battelle Northwest Rept. SA-2290
- Begley, C. and Landes, J., 1972, ASTM STP 514, 1-20
- Begley, C. and Landes, J., 1974, ASTM STP 560, 170-186
- Benthem, J.P., 1975, Report WTHD Nr.74, Dept. of Mechanical Engrg, Delft University of Technology.
- Benthem, J. P., 1977, *Int. J. of Solids and Struct.*, V.13, 479-492
- Betegon, C. & Hancock, J., 1991, *J of Applied Mechanics*, V.58, 104-110
- Bilby, B.A., Cardew, G. E., Goldthorpe, M.R, and Howard, I.C., 1986, " in *Size Effects in Fracture*", Mechanical Engineering, Publications Limited, London, 37-46
- Broek, D., 1974, *Fail safe design procedures*, Agard Fracture Mechanics Survey, Allen, F.C., Chapter II
- Broek, D., 1986, 'Elementary Engineering Fracture Mechanics ' 3rd, pp109
- Brocks, W. and Olschewski, J., 1986, *Int. J. of Solids and Struc.*, V.22, 693-708
- Cause, T.A., 1970, *Int. J. Fract.*, V.6, 326-328
- Cause, T.A. and Vanburen, W., 1971, *Int. J. Fract.*, V.7, 1-15
- Chao, Y.J., Yang, S., and Sutton, M.A., 1993, *Engineering Fracture Mechanics*, V.45, 1-20
- Cherepanov, G. P., 1967, *Crack propagation in Continuous Media*, USSR
- Dixon, J.R., 1965, *Int. J. of Fract. Mech.*, V.1, pp224-243
- Dodds, R. & Anderson, T. L., 1991, *Int. J. Fract.*, V.48, 1-29
- Dodds, R., Shih, C. F., and Anderson, T. L., 1993, *Int. J. of Fracture*, V.64, 101-103

- Du, Z.Z. and Hancock, J.W.,1991, *J of Mech. Phys Solids*, V.39, 555-567
- Eshelby, J.D. 1956, 'The Continuum Theory of Lattice Defects', *Solid State Physics*, V.3, Academic Press, 79-114
- Faleskog, J., 1994, *Int. J. of Solids and Struct.*, V.31, 1-26
- Folias, J.,1975, *J Applied Mechanics*, V.42, 663-677
- Griffith, A.A., 1921, *Phil. Trans. R. Soc.* 163-198
- Hutchinson, J., 1968, *J. of Mech. Phys.Solids*,V.16, 13-21
- Hartranft, R.J. and Sih, G. C., 1968, *J. of Math. Phys.* , V.47, 276-291
- Hartranft, R. J. and Sih, G. C., 1970, *Int. J. Engrg Sci.* , V.8, 711-729
- Irwin, G.R., 1960, In 'Proc. 7th Sagamore Ordnance Materal Research Conference', V.5, 63-78
- Koers, R.W.J. Braam,H. and Bakker,A.,1989, *Proceeding of the 7th Int. Conf. of Fract.*, Houston, Texas.
- Koppenhoefer, K.C. and Dodds, R.H.,1994, ' Size and deformation limits to maintain constraint in K and J testing of bending specimens ', report in University of Illinois at Urbana- Champaign
- Larsson, S.G.,& Carlsson, A.J., 1973, *J. of Mech. and Phys. Solids*, V.21, 263-278
- Levers, P.S., and Radon, J.C.,1982, *Int. J. Fract.*, V.19, 331-325.
- Li, Shih, C.F. and Needleman, J 1985, *Engineering Fracture Mechanics*, V.21, No.2, 405-421
- Levy, N., Marcal, P.V. and Rice, J.R.,1971, *J. of Engrg and Design*, V.17, 64-75
- McClintock, F.A., 1971, *Fracture*, Eds., H.Liebowitz, vol.3, Academic Press. London, 47-225
- McMeeking, R.A and Parks, C.M., 1979, *ASTM STP668*, Eds., J.D.Landes et al, ASTM, Philadelphia. 175-194
- Nakamura,T. and Parks, D.M., 1988, *J of Applied Mechanics*, V.55, 806-813
- Nakamura,T. and Parks, D.M., 1990, *J of Mech. Phys. Solids*, V.38, No.6, 787-812
- Narasimhan, R. and Rosakis, A. J., 1988, *AMD-V.91*, ASME, 239-254
- Navalainen and Dodds, R.H., 1995, *UIIU-ENG-94-2001*, Univ. of Illinois at Urbana-

Champaign, Illinois 61801

- O'Dowd, N.P. and Shih, C.F., 1991, *J. Mech. Phys. Solids*, V.39, 989-1015
- O'Dowd, N.P. and Shih, C.F., 1992, *J. Mech. Phys. Solids*, V.40, 939-1011
- Orowan, E., 1948, *Report Program Physics*, V.12, 185-230
- Rice, J.R., 1968, *J. Appl. Mech.*, V.35, 379-386
- Rice, J.R. and Tracey, 1973, *Eng. Fract. Mech.*, V.3, 255-265
- Rice, J.R., 1974, *J. of Mech. and Phys. Solids*, V.22, 17-26
- Rice, J.R. and Rosengren, G.F., 1968, *J. of Mech. Phys. Solids*, V.16, 1-12
- Rooke, D.P. & Cartwright, D.J., 1976, *Compendium of stress intensity factors*, Her Majesty's Stationary Office, London
- Sham, T.L., 1991, *Int. J. Fract.*, V.48, 81-102.
- Shi, G.C. and Hartranft, R.J., 1973, *Int. J. of Fract.*, V.9, 75-85
- Shih, C.F. and German, M.D., 1981, *Int. J. of Fract.*, V.17, 27-43
- Sorensen, W., and Dodds, R.H., 1991, *Int. J. of Fract.*, V.47, pp105-126
- Timoshenko, S., and Goodier, J.N., 1970, 'Theory of Elasticity', McGraw-Hill, New York.
- Underwood, J., Freiman, S., and Barratta, F., 1984, STP855, ASTM, Philadelphia, USA
- Wallin, K., 1993, STP1171, ASTM, Philadelphia, USA
- Williams, M.L., 1957, *J. of Applied Mechanics*, V.24, 111-114
- Williams, M.L., 1961, *J. of Applied Mechanics*, V.28, 79-119
- Westergaard, H.M., 1939, *J. of Applied Mechanics*, V.6, A49-53
- Xia, L., Wang T.C. and Shih, C.F., 1993, *J. Mech. Phys. Solids*, V.41, 665
- Yang, W., and Freund, L. B., 1985, *Int. J. of Solids and Struct.*, V.21, 977-994

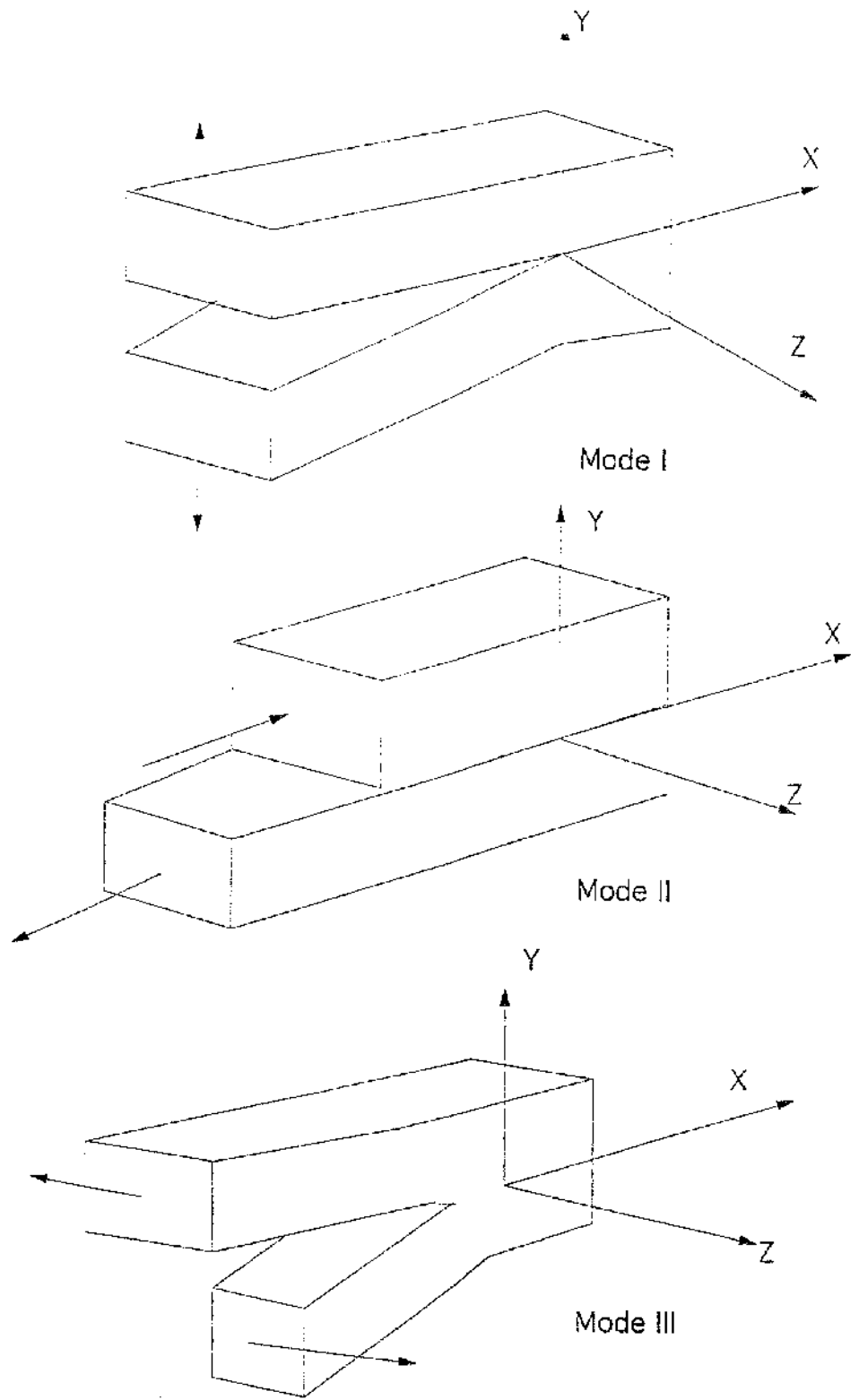


Figure 1 Fracture modes

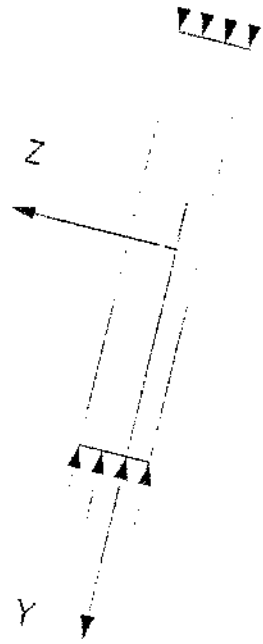
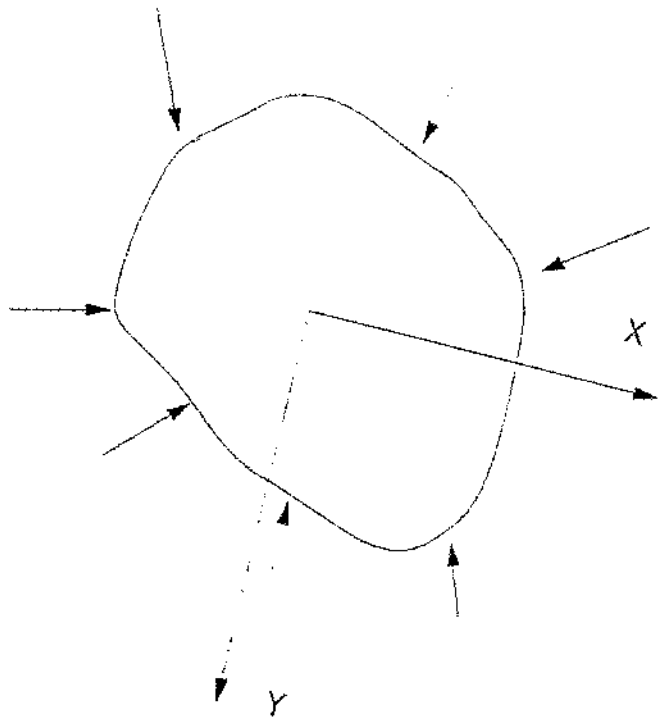


Figure 2
Plane stress

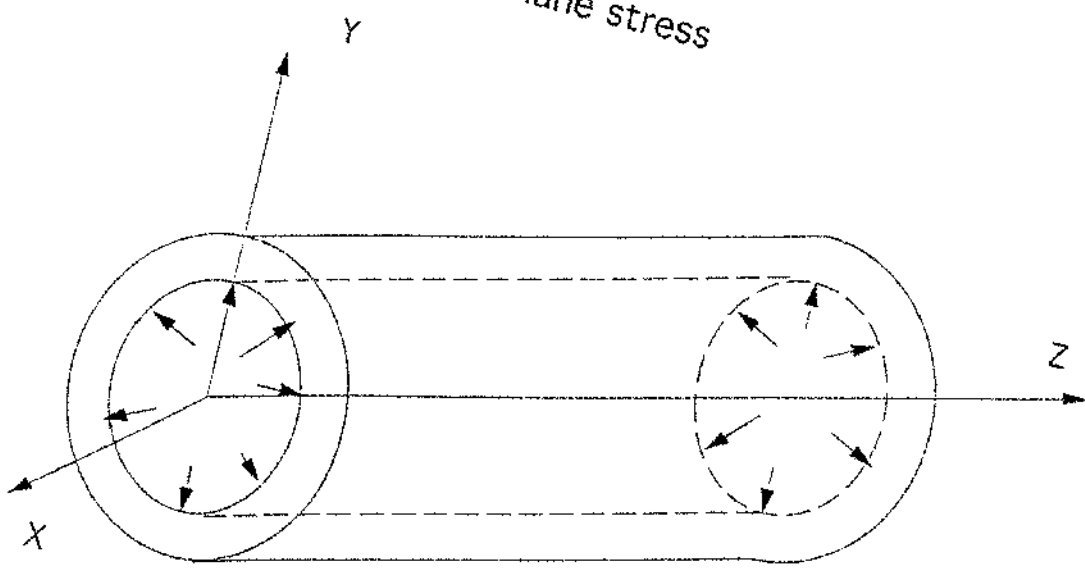


Figure 3
Plane strain

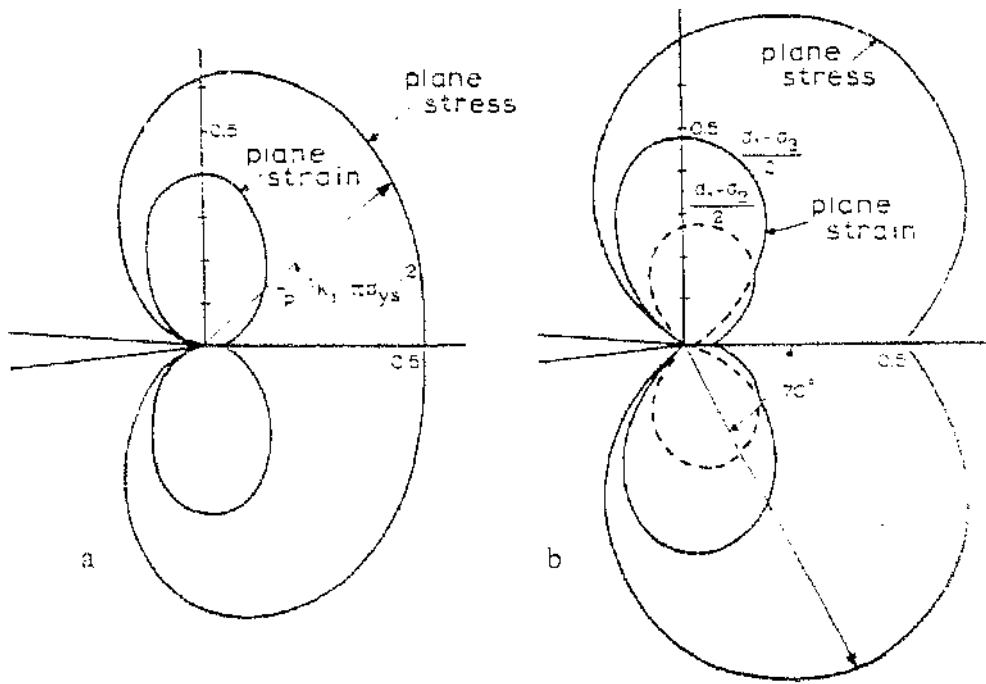


Figure 4 Plastic zone shapes according to Von Mises and Tresca yield criteria
 a. Von Mises criterion; b. Tresca criterion

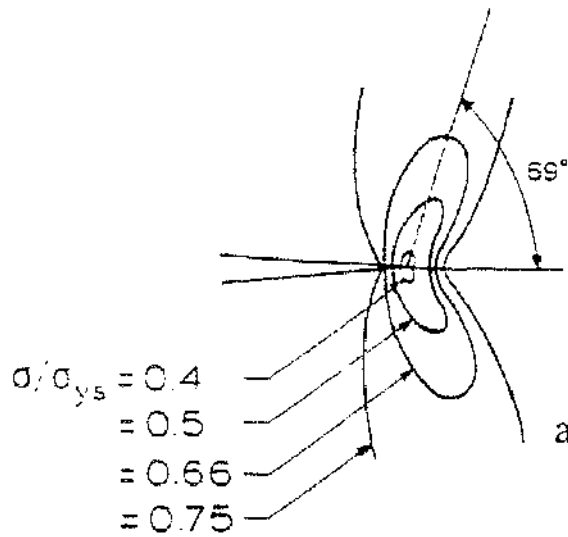


Fig. 5 More accurate plastic zone shape according to Tuba (1975)

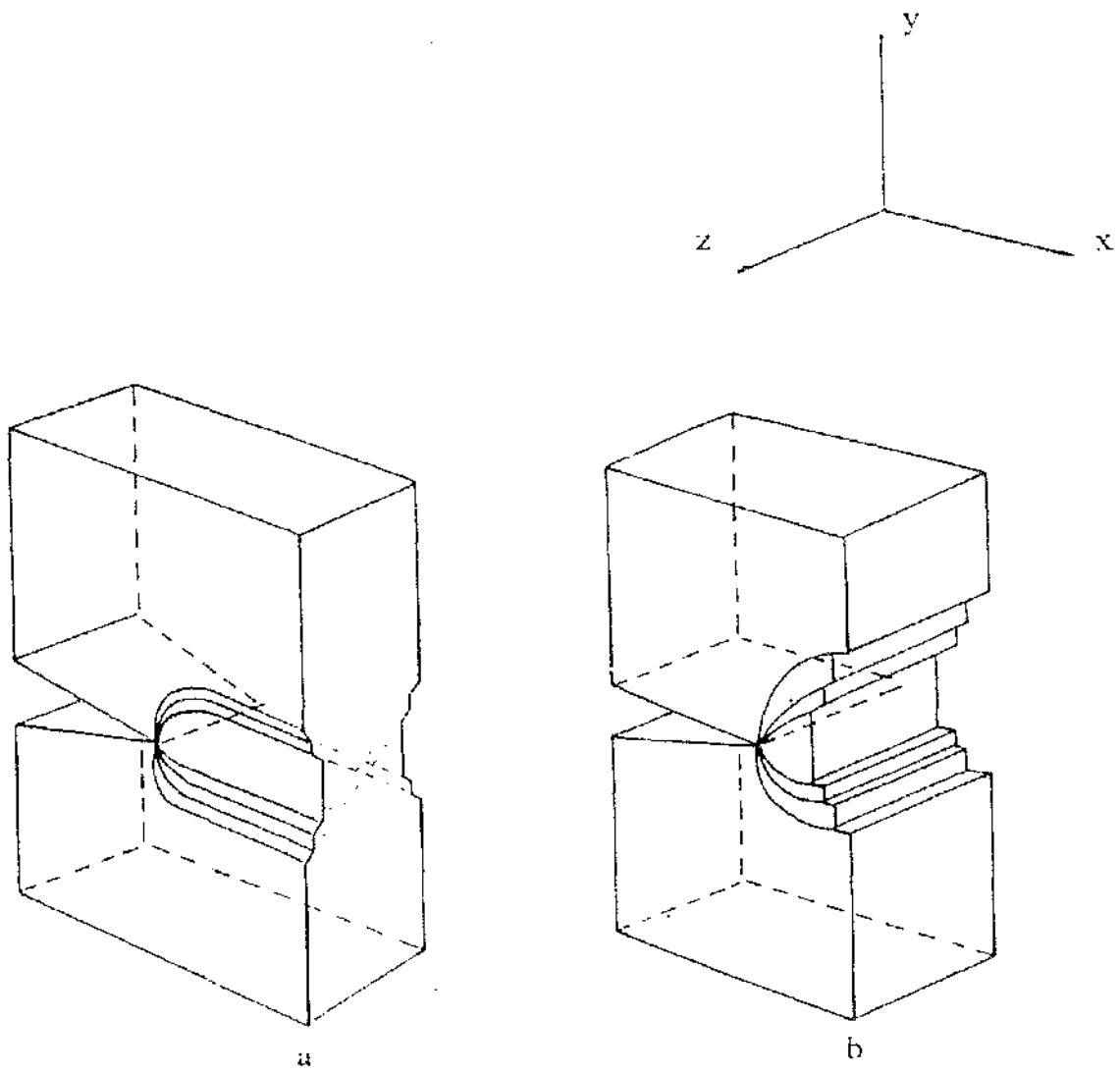


Figure 6 Deformation patterns

a. 45° degree shear deformation in plane stress; b. Hinge type deformation in plane strain

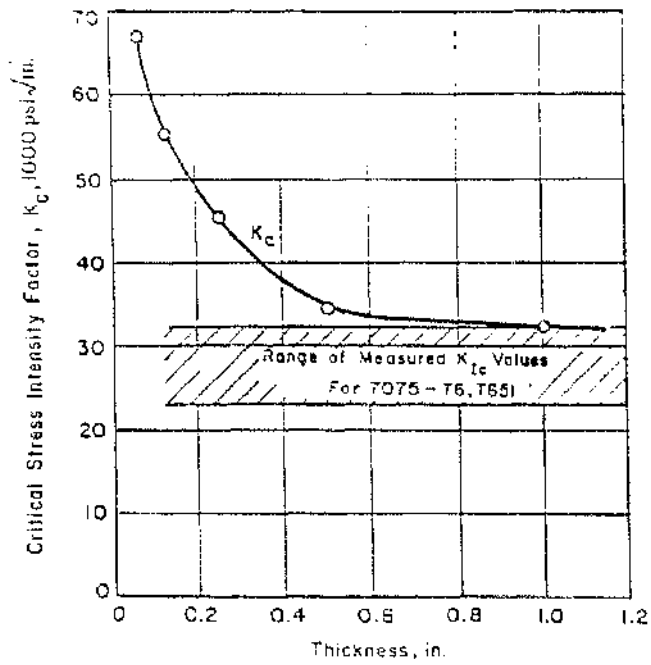


Figure 7 Fracture toughness of 7075-T6, T651 sheet and plate from tests of fatigue-cracked edge notched specimen according to Kaufman(1970)

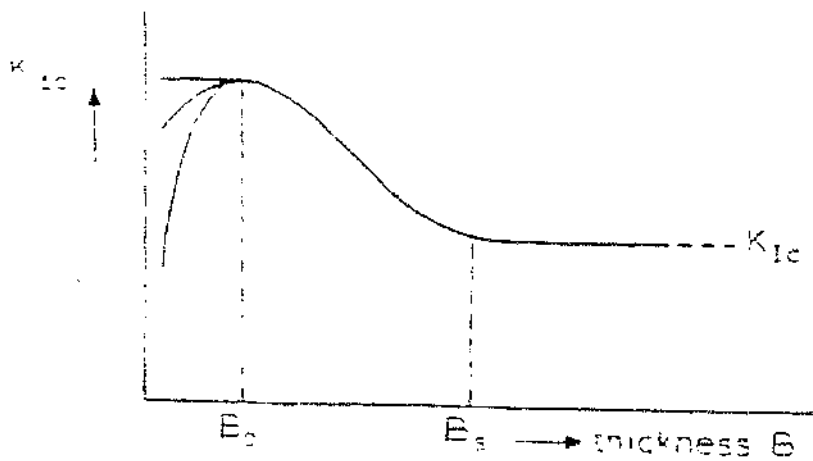


Figure 8 Toughness as a function of thickness according to Broek (1986)

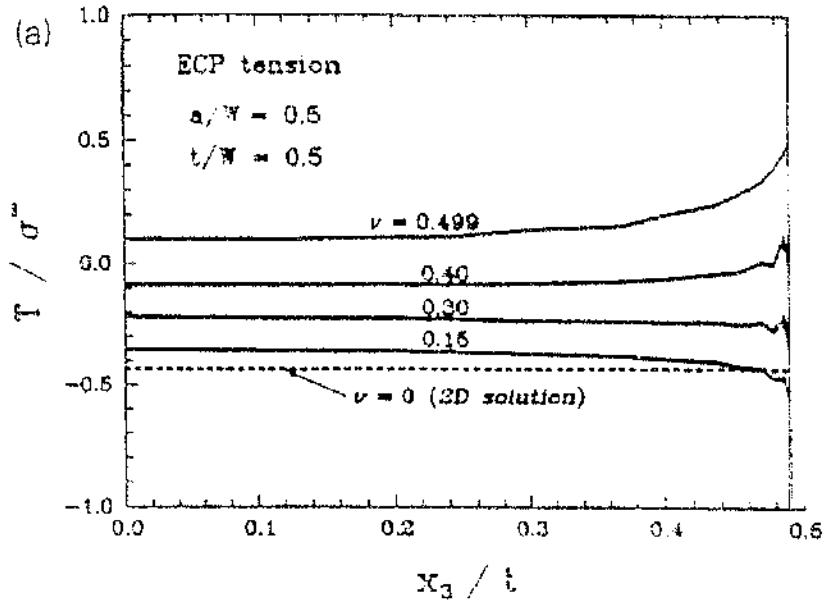


Figure 9 Variation of normalized T-stress along the crack front in a thin elastic plate according to Nakamura & Parks(1992)

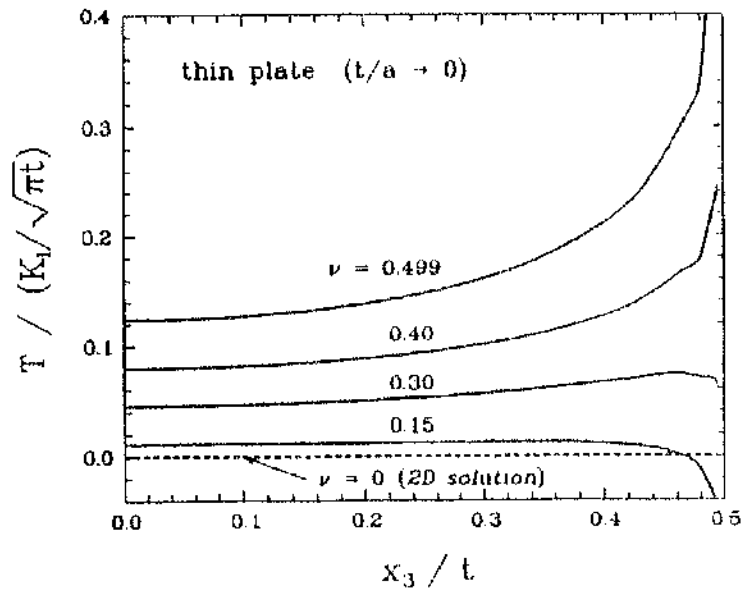


Figure 10 Variation of normalized inherent T-stress along the crack front of an edge cracked plate as a function of Poisson's ratio according to Nakamura and Parks (1992)

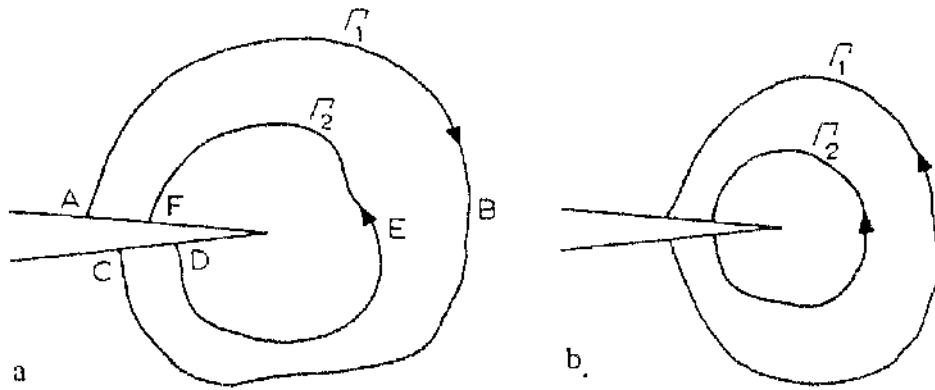


Figure 11 The contour around a crack tip

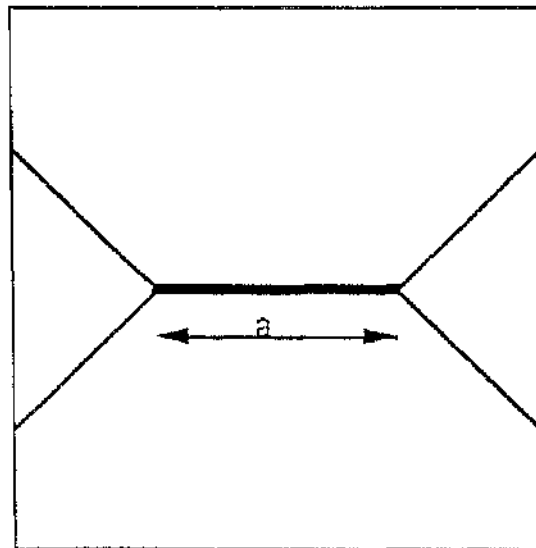


Figure 12 (a) The plane strain slip line field for a centre cracked plate in tension

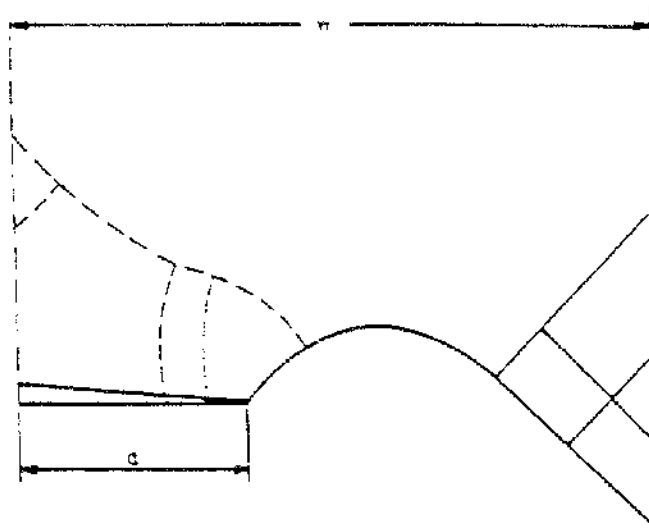


Figure 12 (b) The plane strain slip line field for a deep cracked bend bar is indicated by the thick lines, while the thin lines indicate the extension to the slip line field for short cracks

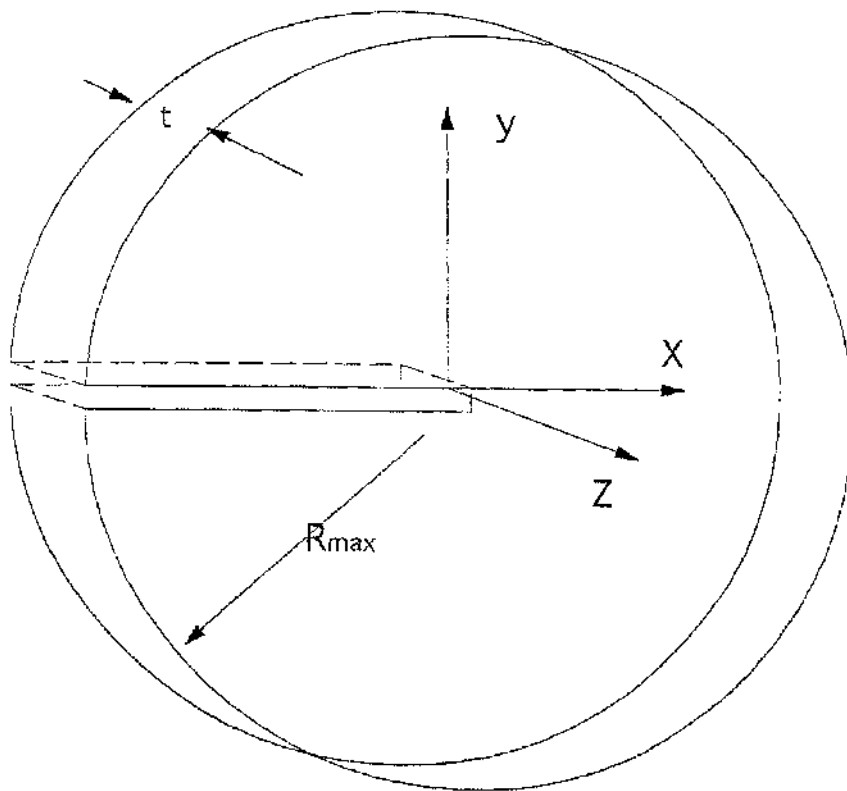


Figure 13 A cracked circular disk representing a near crack front region of a thin plate

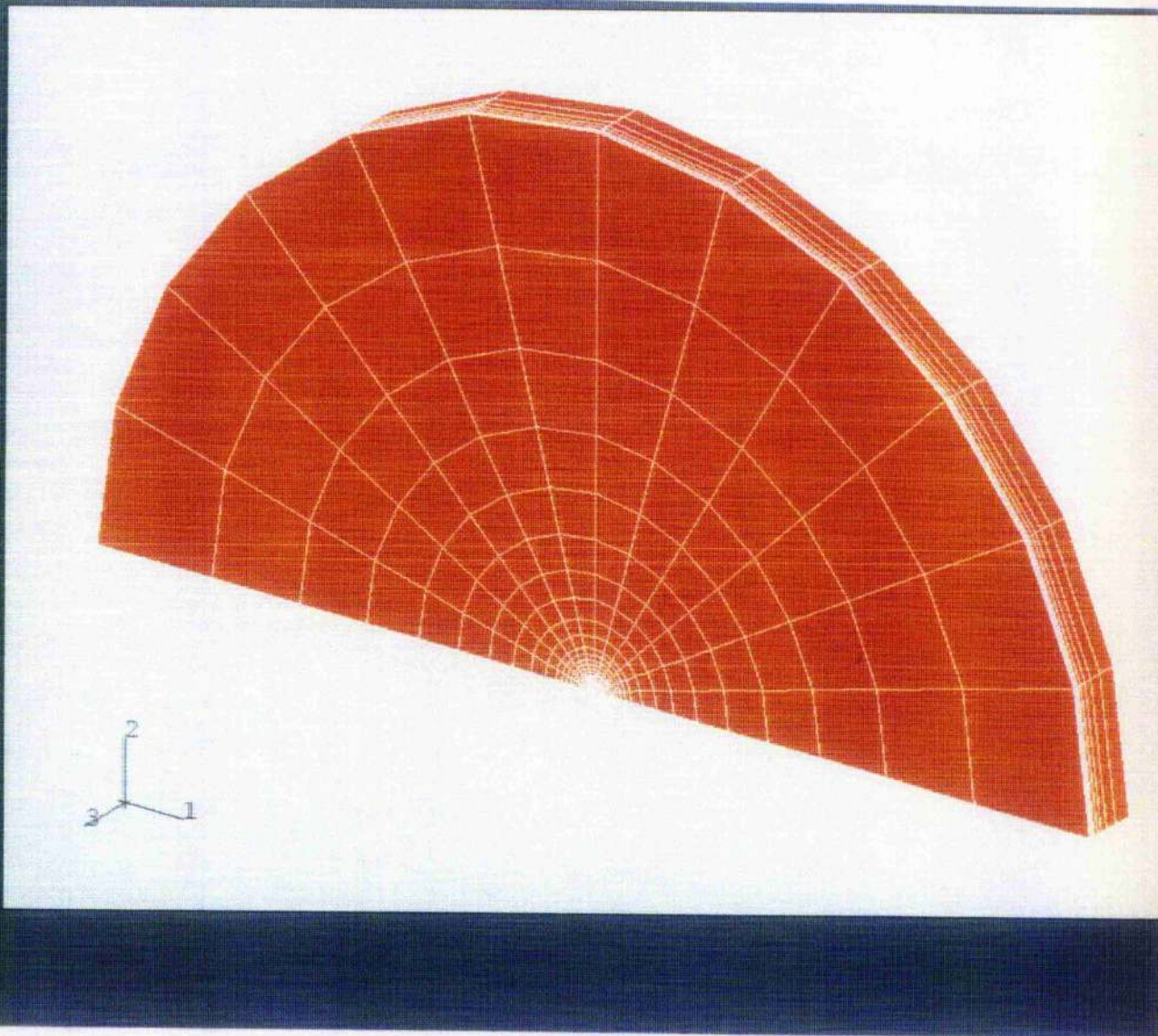


Figure 14 Three dimensional model of boundary layer fomulation

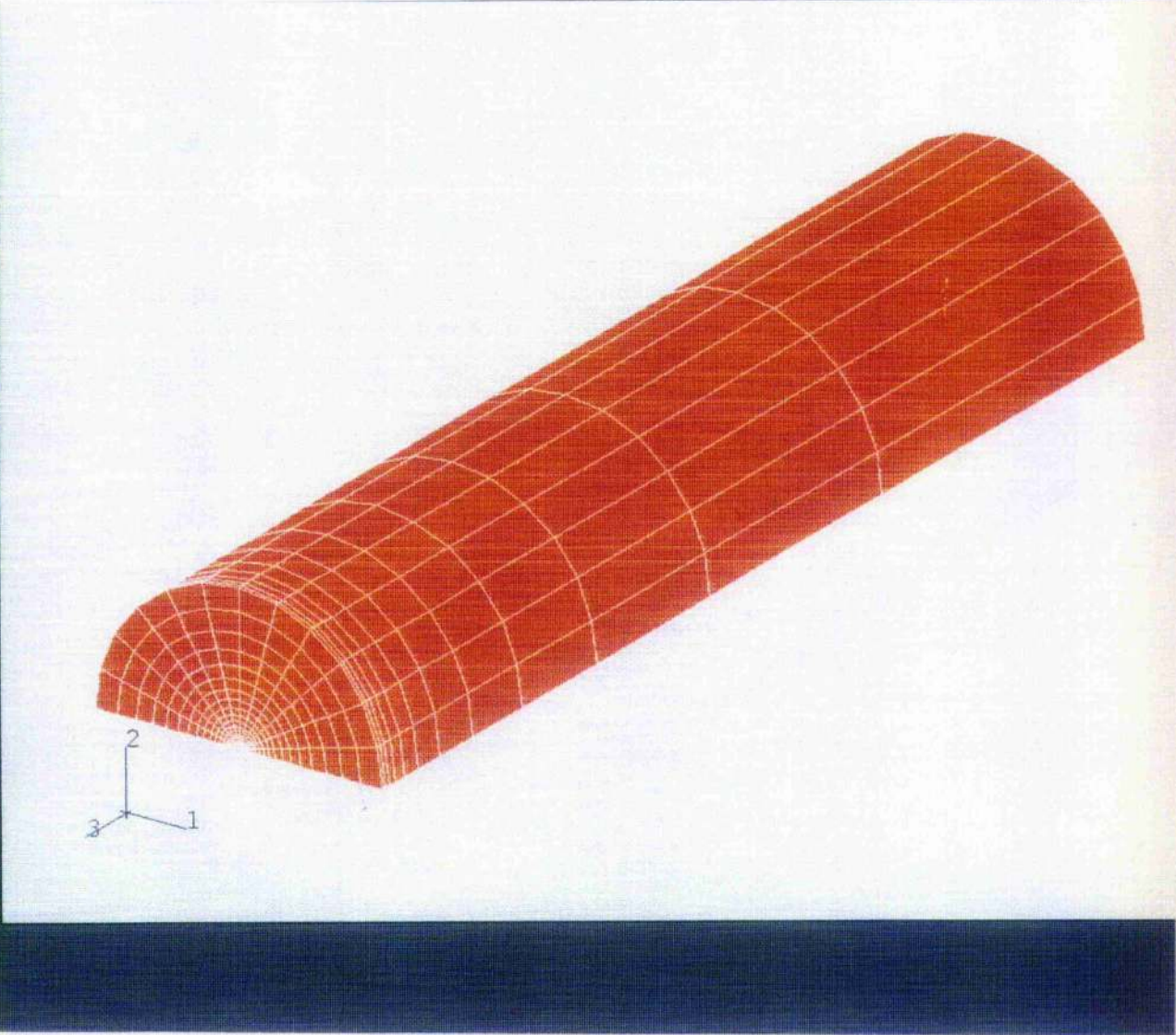


Figure 15 The mesh of substructure model

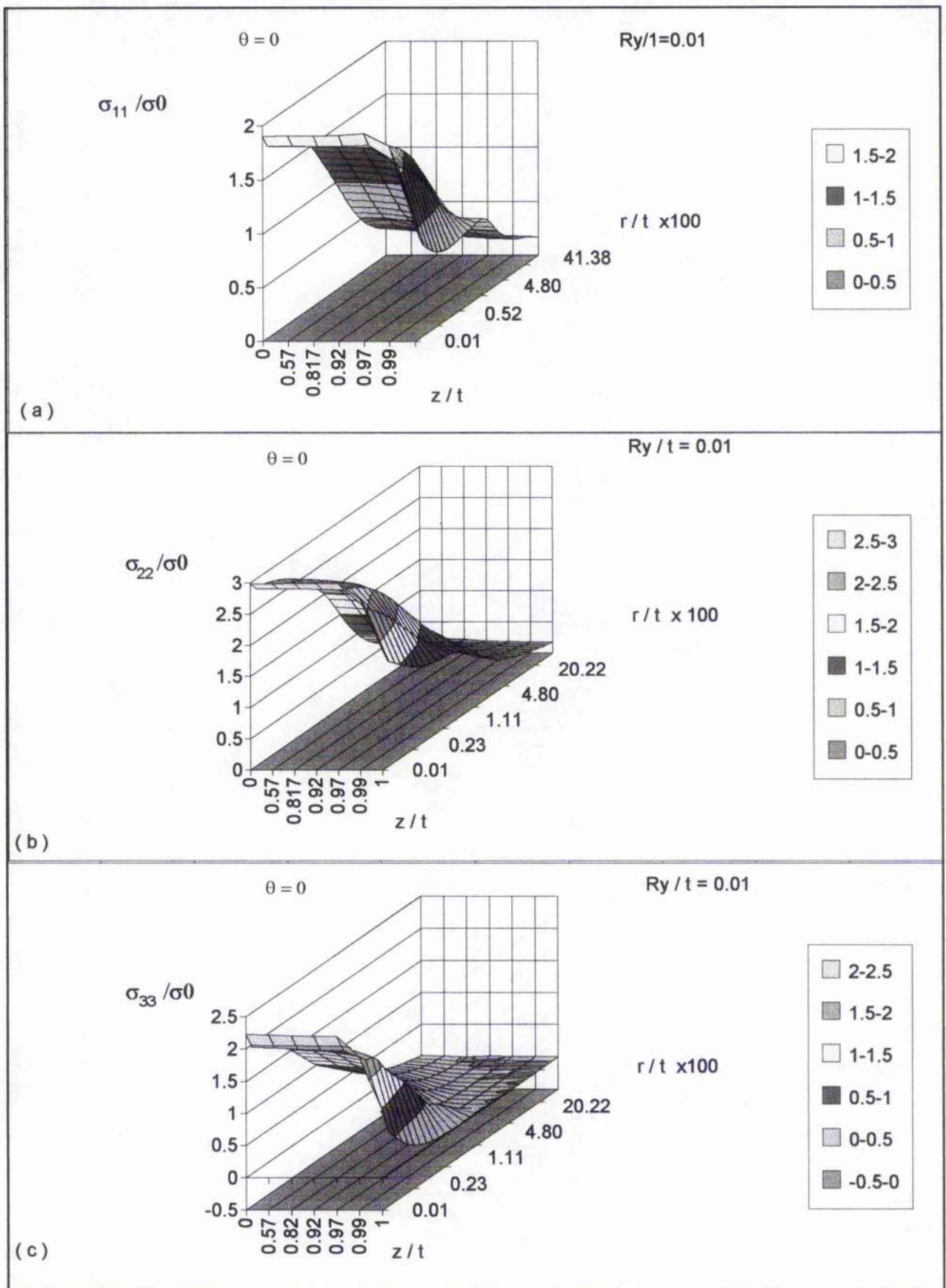


Figure 16 The stress distribution through the thickness in SSY

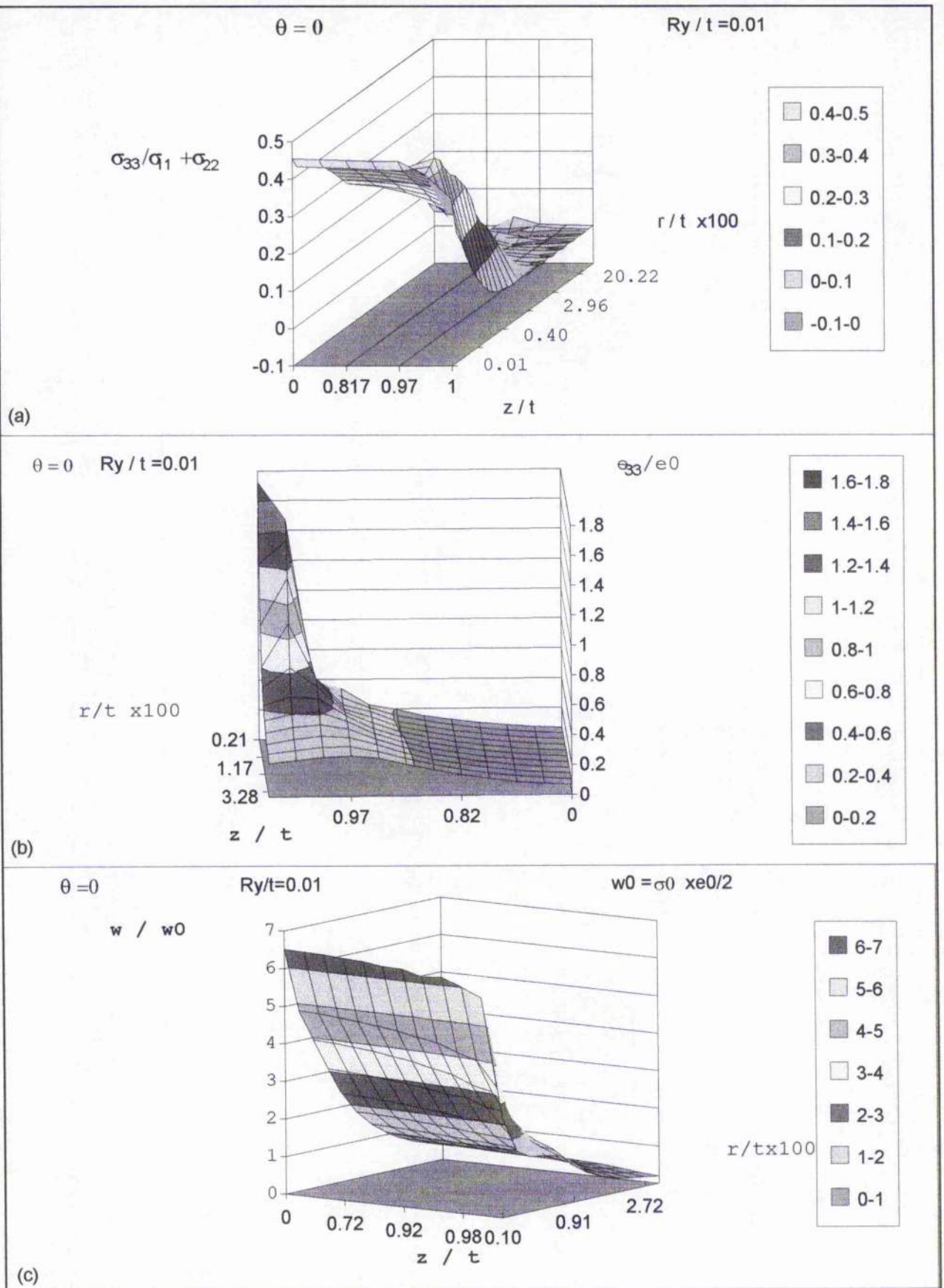


Figure 17 (a) Distribution of $\sigma_{33}/(\sigma_{11} + \sigma_{22})$ (b) Distribution of out plane strain (c) Distribution of elastic strain energy density through the thickness

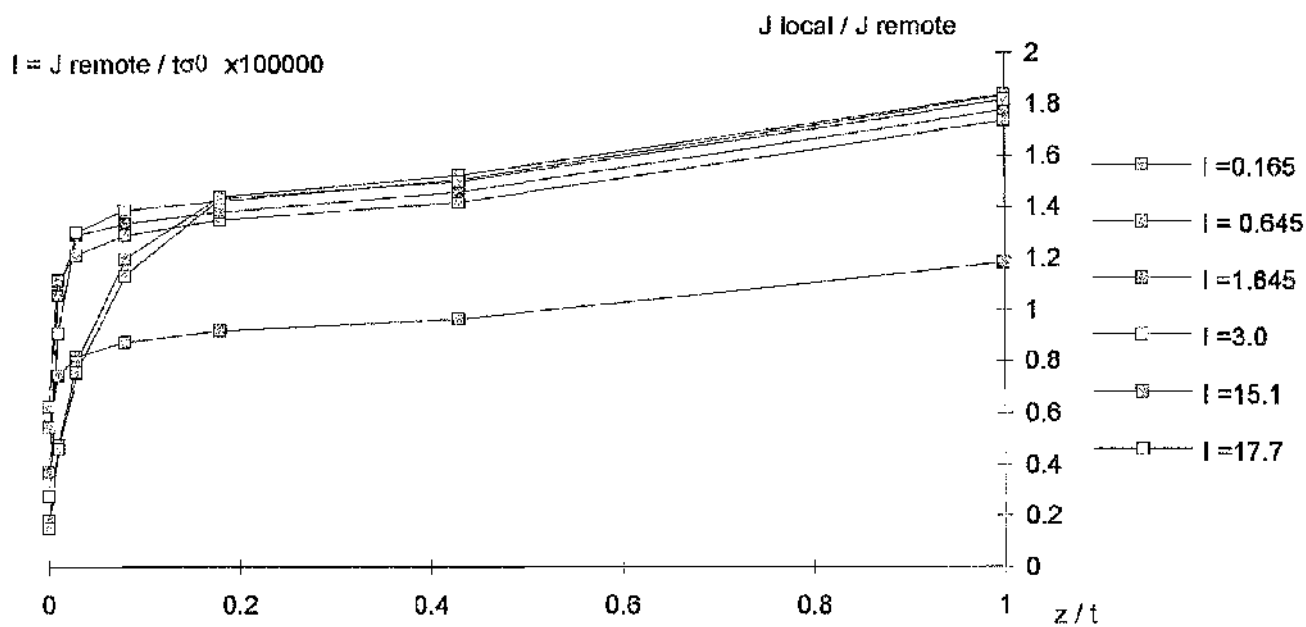


Figure 18 J distribution through the thickness as a function of loading in SSY

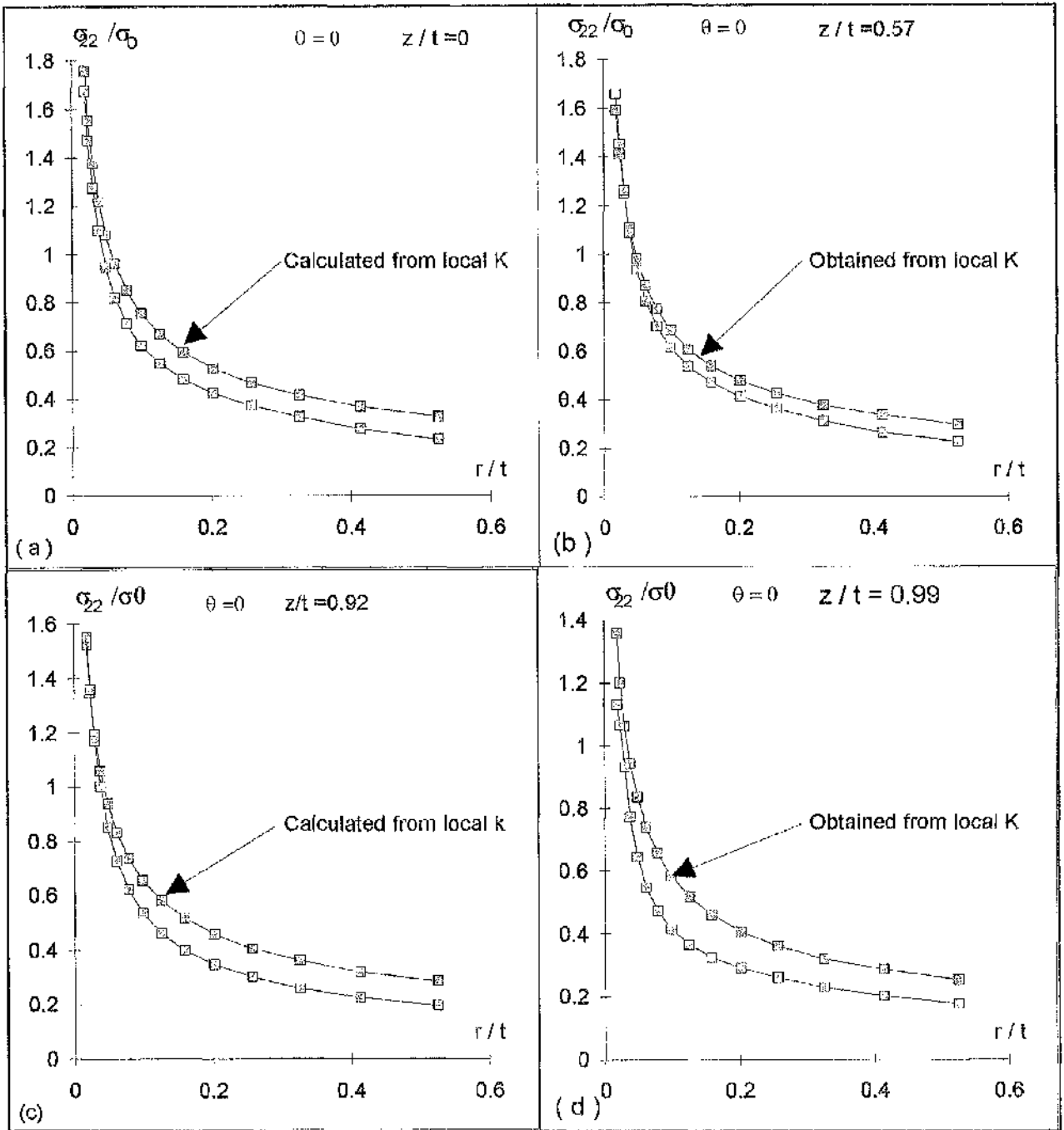


Figure 19 Comparison of the stress σ_{22} distribution at section $z/t=0$, $z/t=0.57$, $z/t=0.92$, and $z/t=0.99$ with the stresses determined from the local K

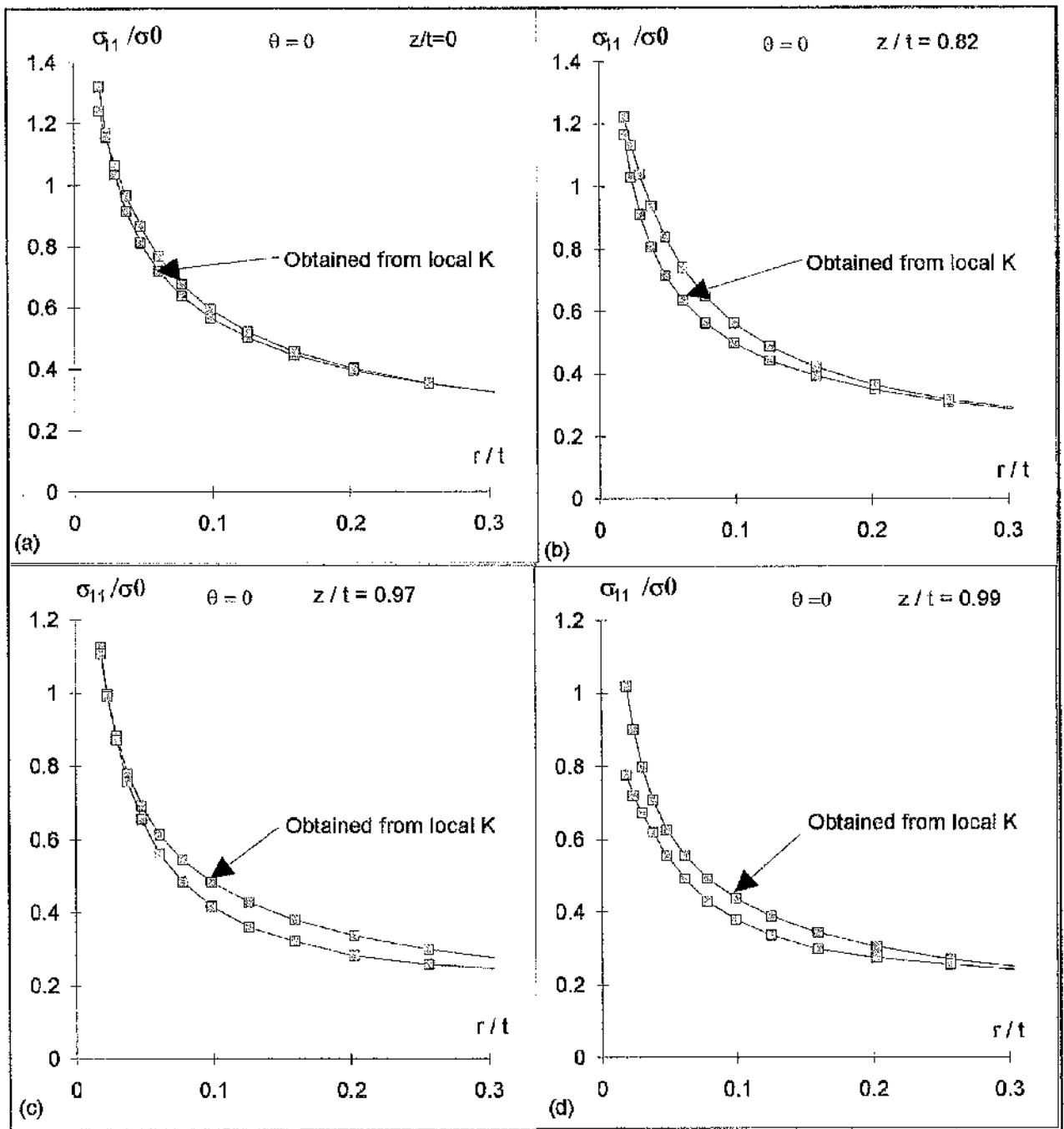


Figure 20 A comparison of stress σ_{11} distribution at section $z/t=0$, $z/t=0.82$, $z/t=0.92$, and $z/t=0.99$ with the stresses determined from the local K

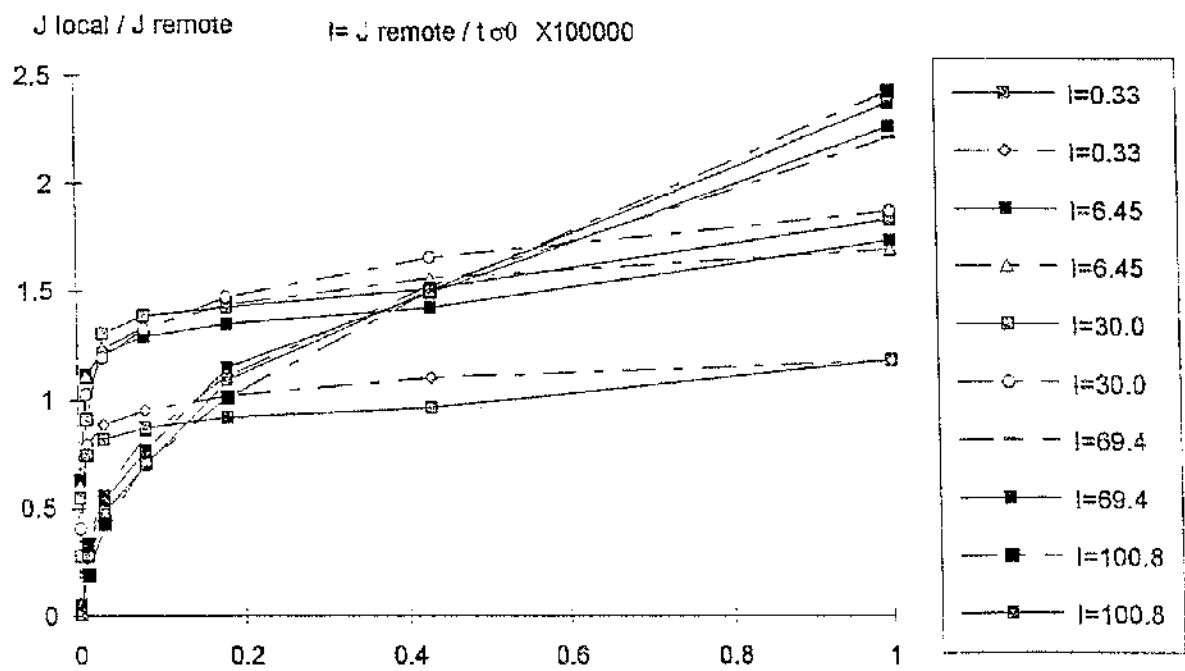


Figure 21 A comparison of the J distribution through the thickness with J from Eqn.86 as a function of loading

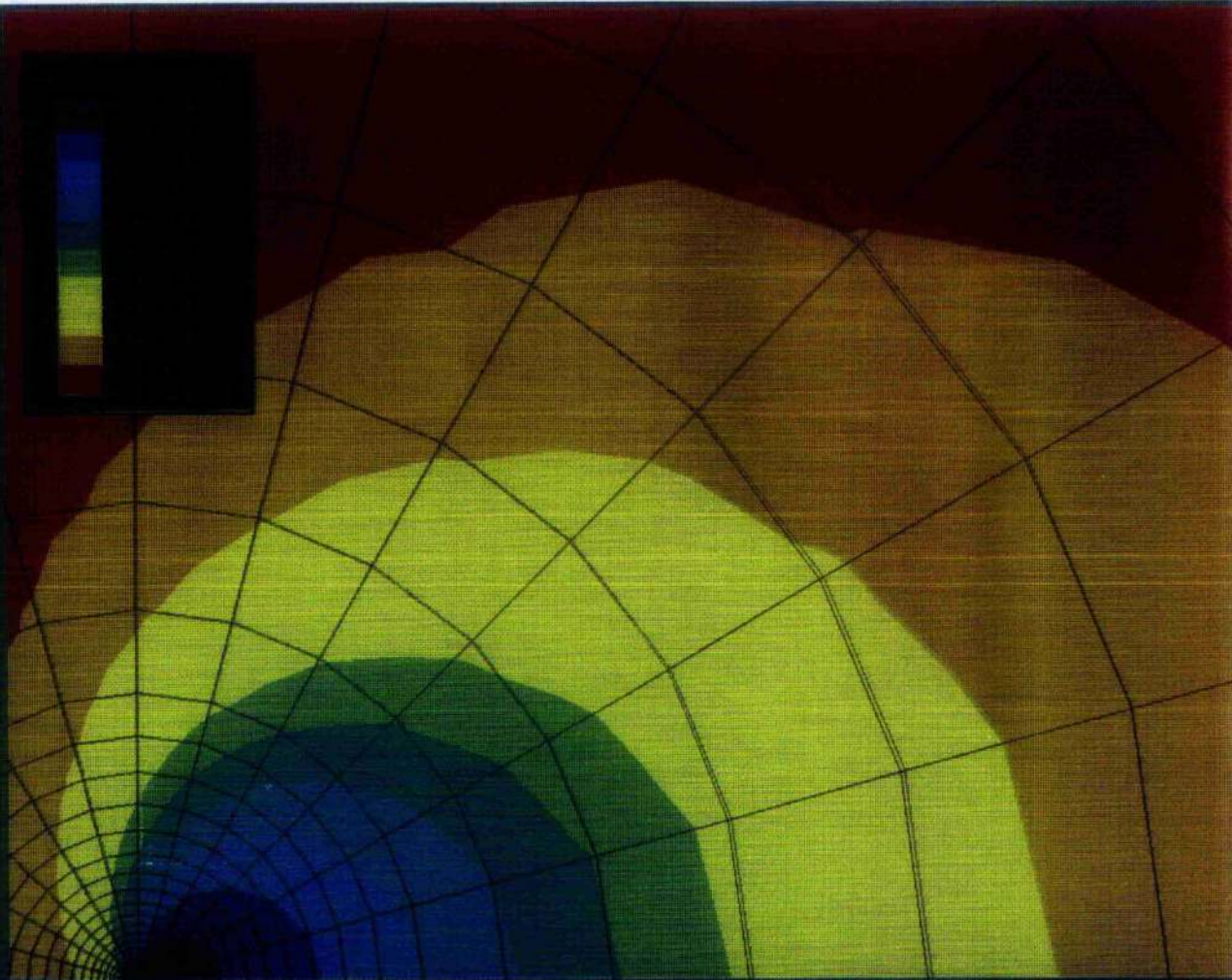


Figure 22 The distribution of out of plane displacement W on the free surface with $J= 6.05E08$

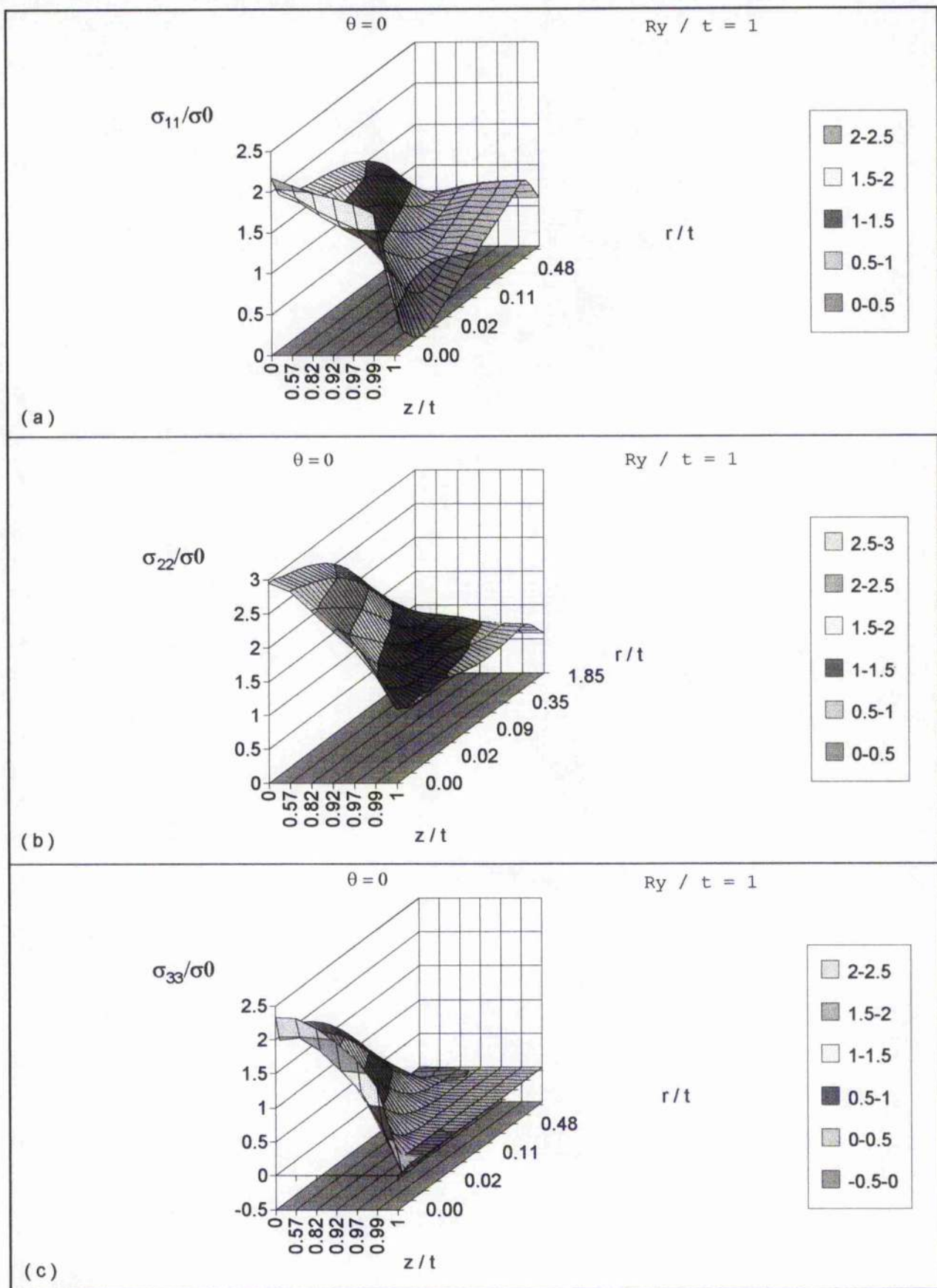


Figure 23 The stress distribution through the thickness in MSY

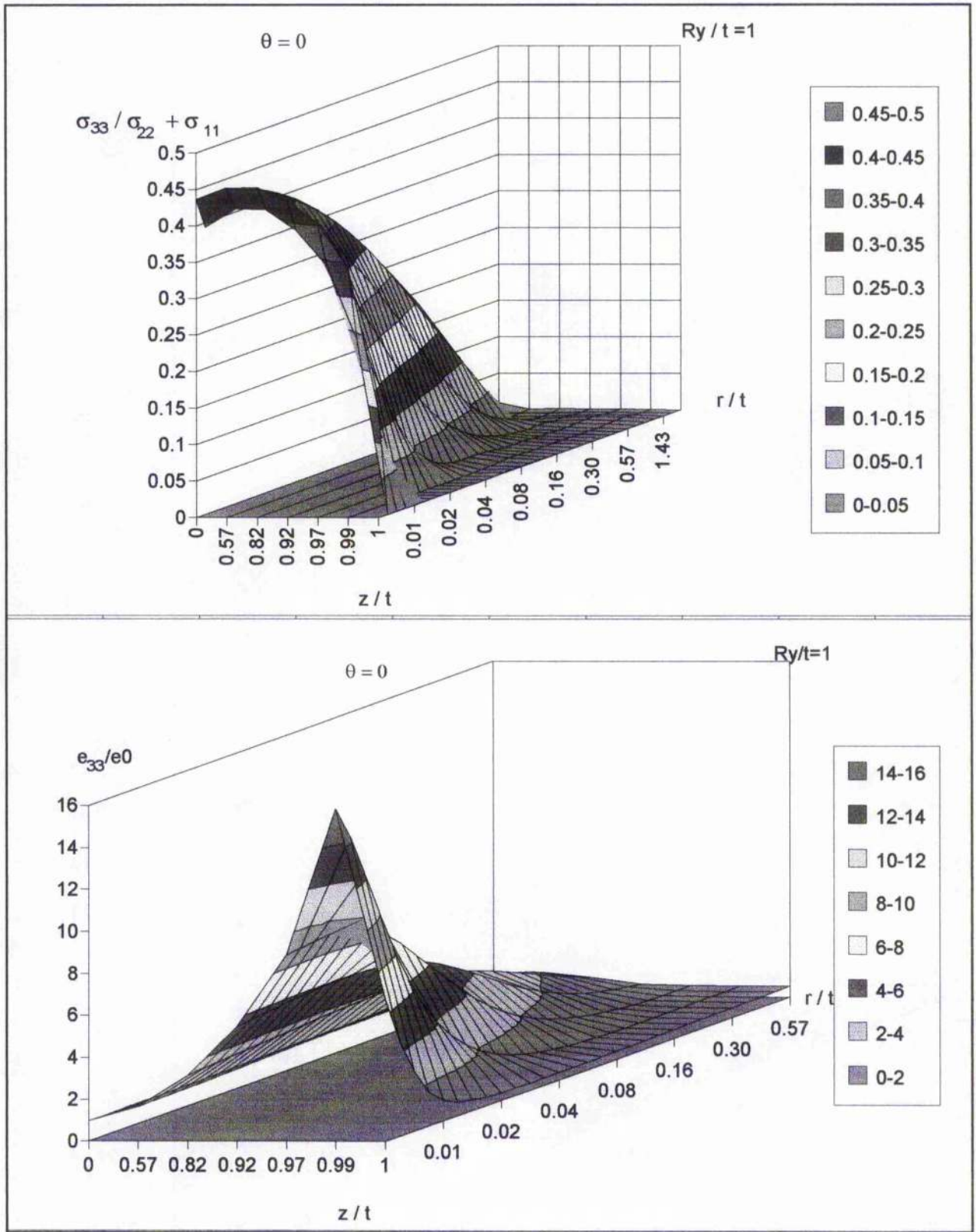


Figure 24 (a) Distribution of $\sigma_{33}/(\sigma_{22}+\sigma_{11})$ (b) The distribution of the out plane strain e_{33} through the thickness in MSY

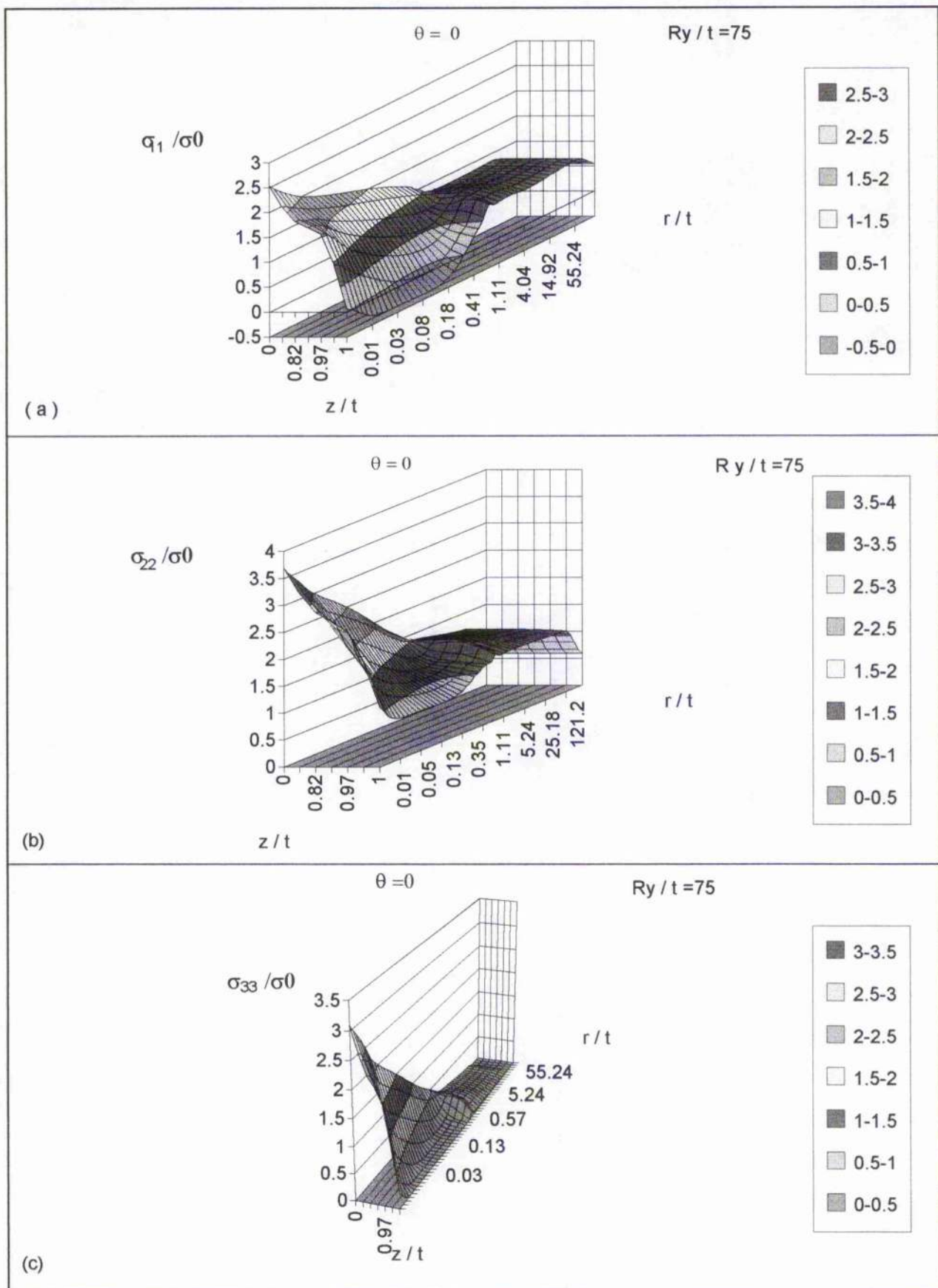


Figure 25 The distribution through the thickness in LSY

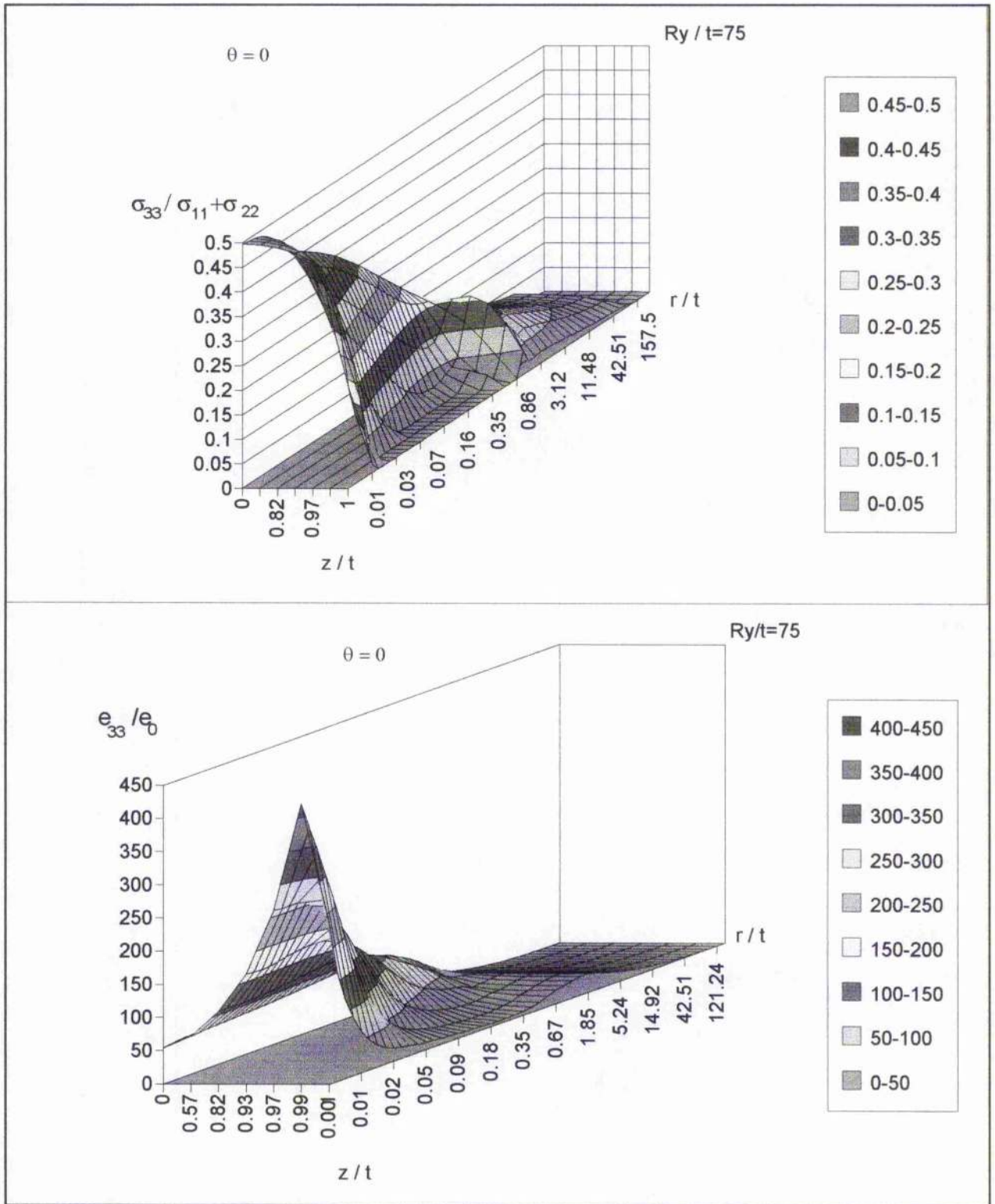


Figure 26(a) The distribution of $\sigma_{33}/(\sigma_{11} + \sigma_{22})$ (b) The distribution of the out plane strain through the thickness in LSY

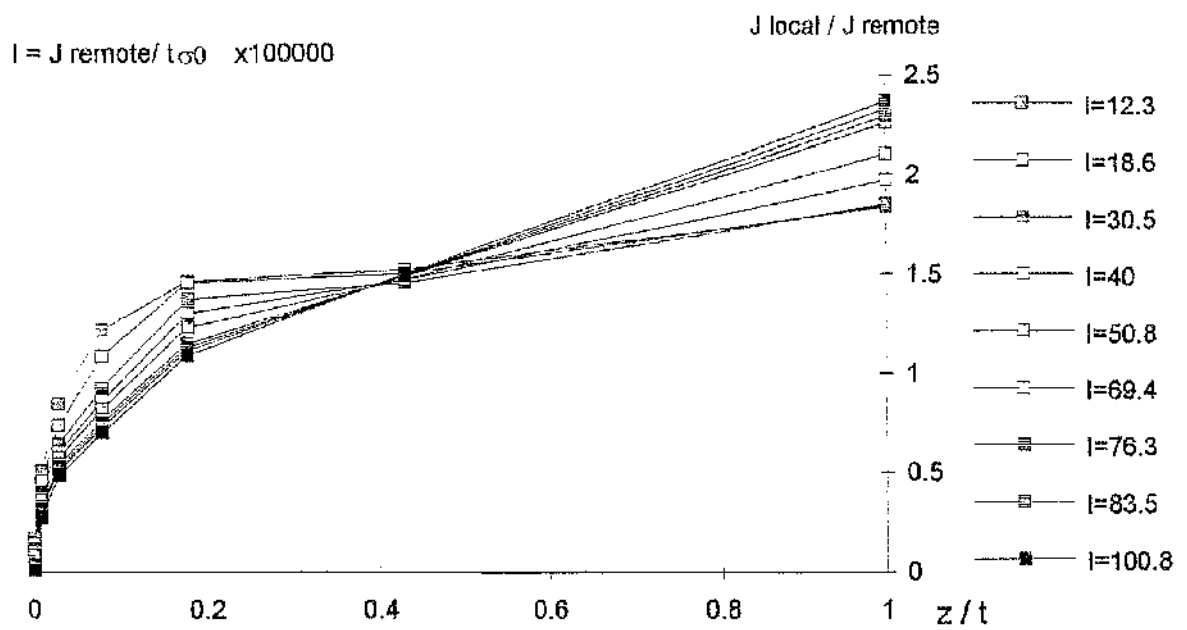


Figure 27 J distribution through the thickness as a function of loading in MSY

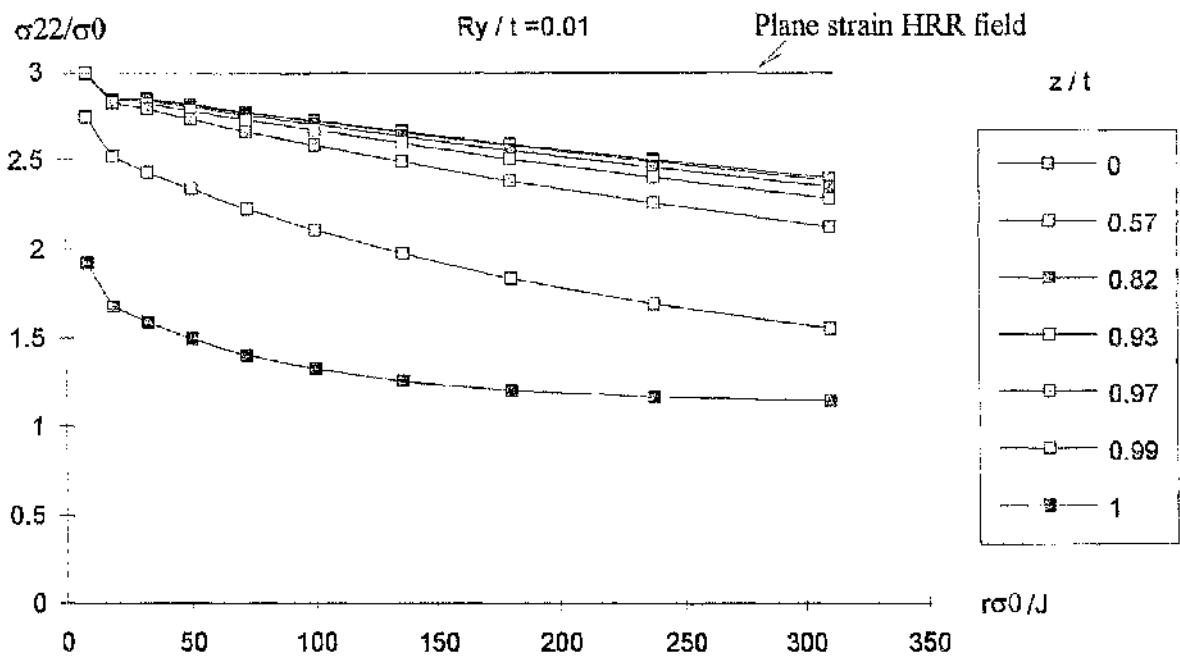


Figure 28 Stress distribution ahead of the crack tip at different section through the thickness

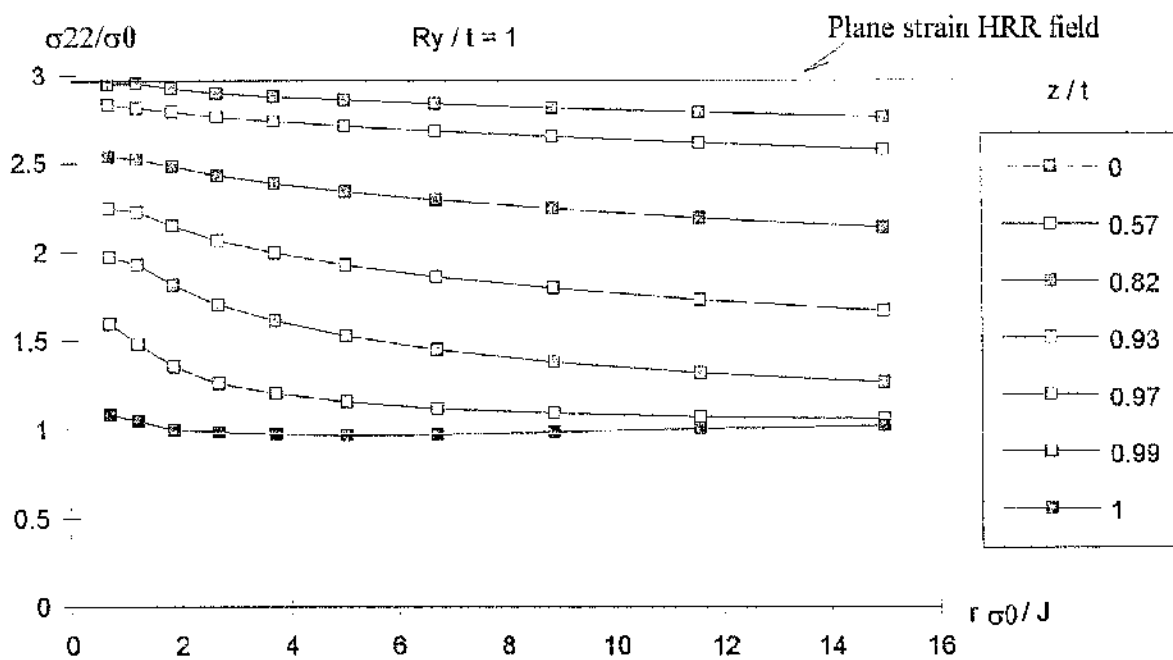


Figure 29 Stress distribution ahead of the crack tip at different sections through the thickness

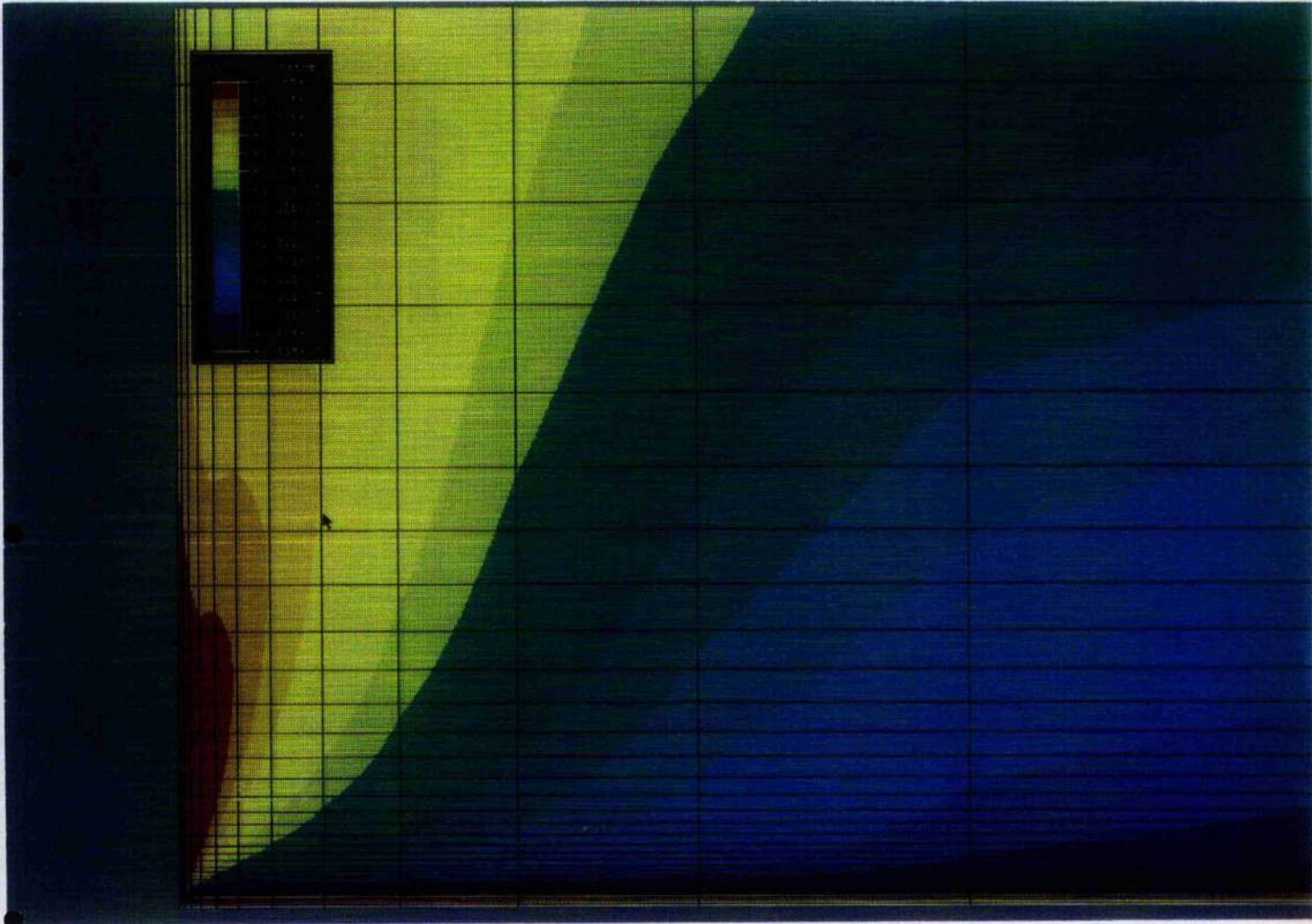


Figure 30 The distribution of stress σ_{11} through the thickness with
 $J = 6.05E08$

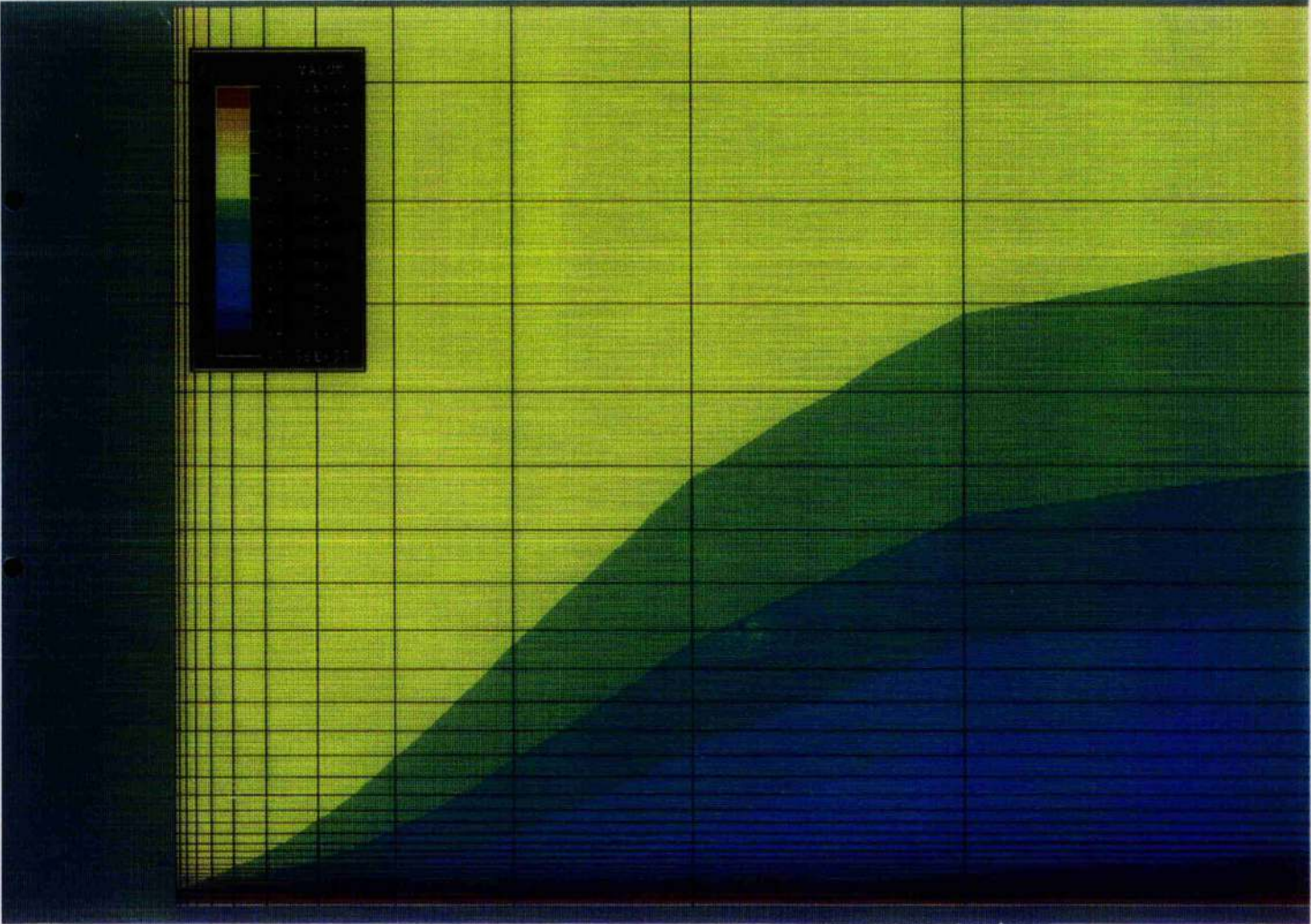


Figure 31 The distribution of stress σ_{22} through the thickness with

$$J = 6.05E08$$

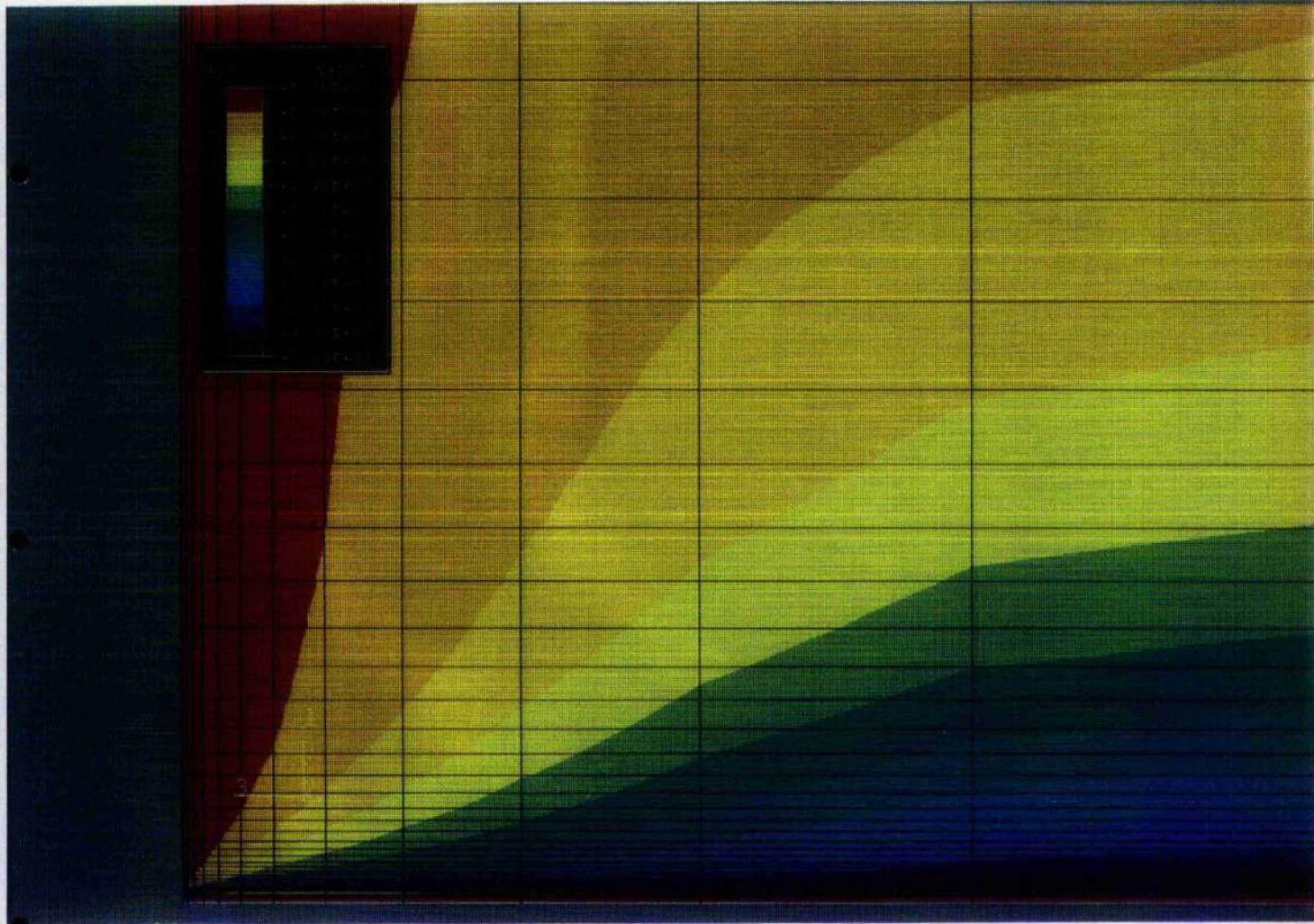


Figure 32 The distribution of stress σ_{33} through the thickness with

$$J = 6.05E08$$

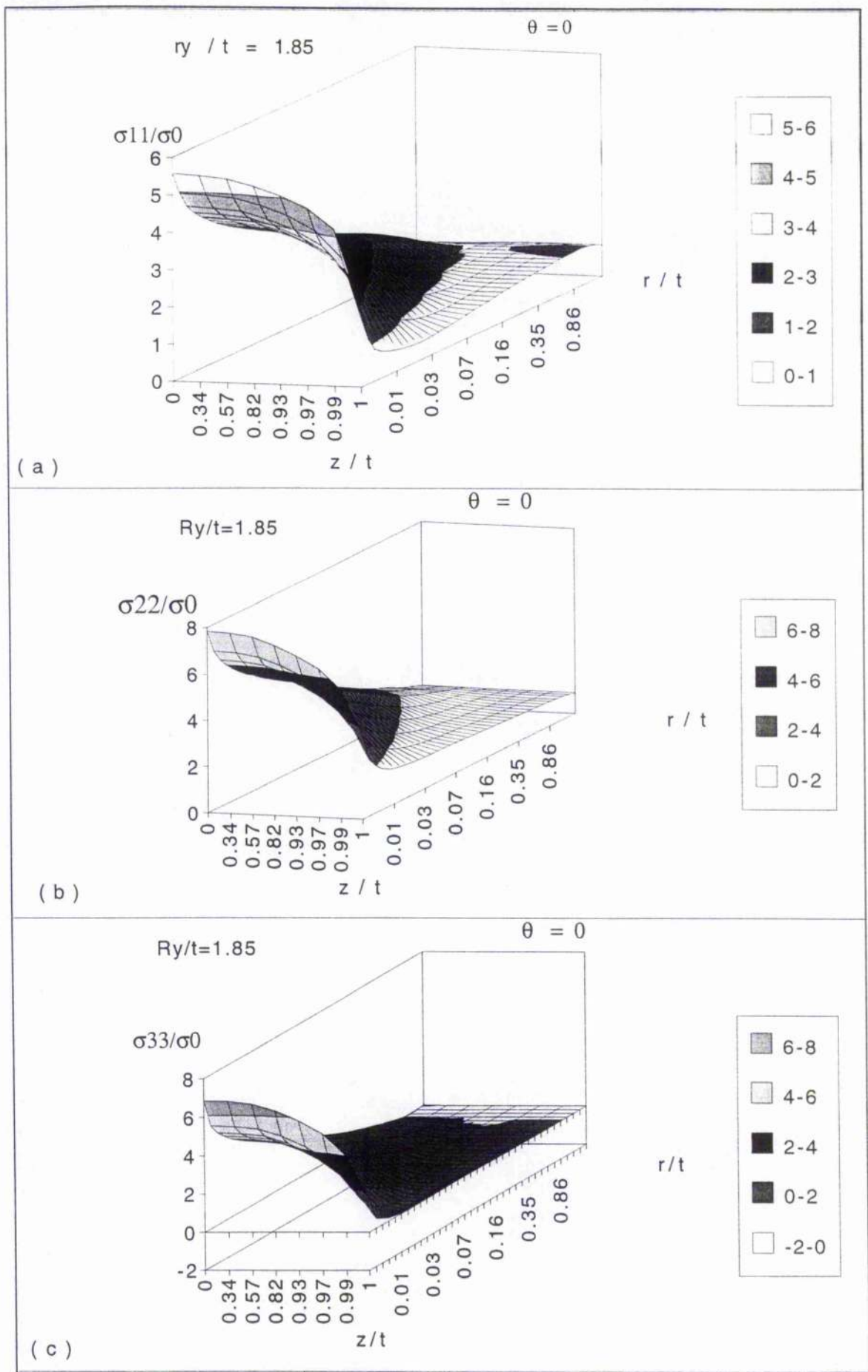


Figure 33(a)(b)(c) The distribution of stresses through the thickness of material with hardening exponent 6

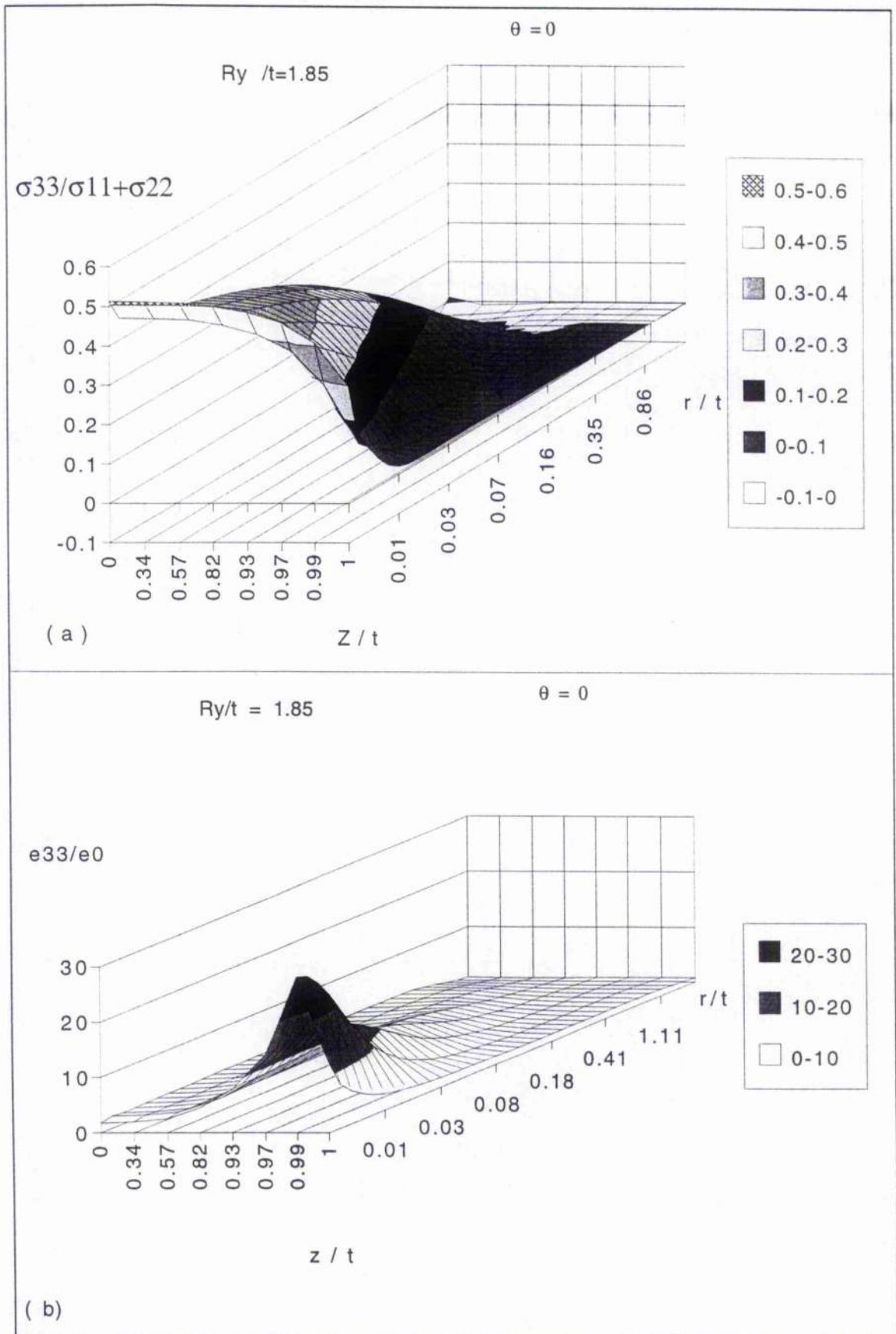


Figure 34(a) Distribution of $\sigma_{33} / \sigma_{22} + \sigma_{11}$ (b) Distribution of out -plane strain e_{33} through the thickness of the material with hardening exponent 6

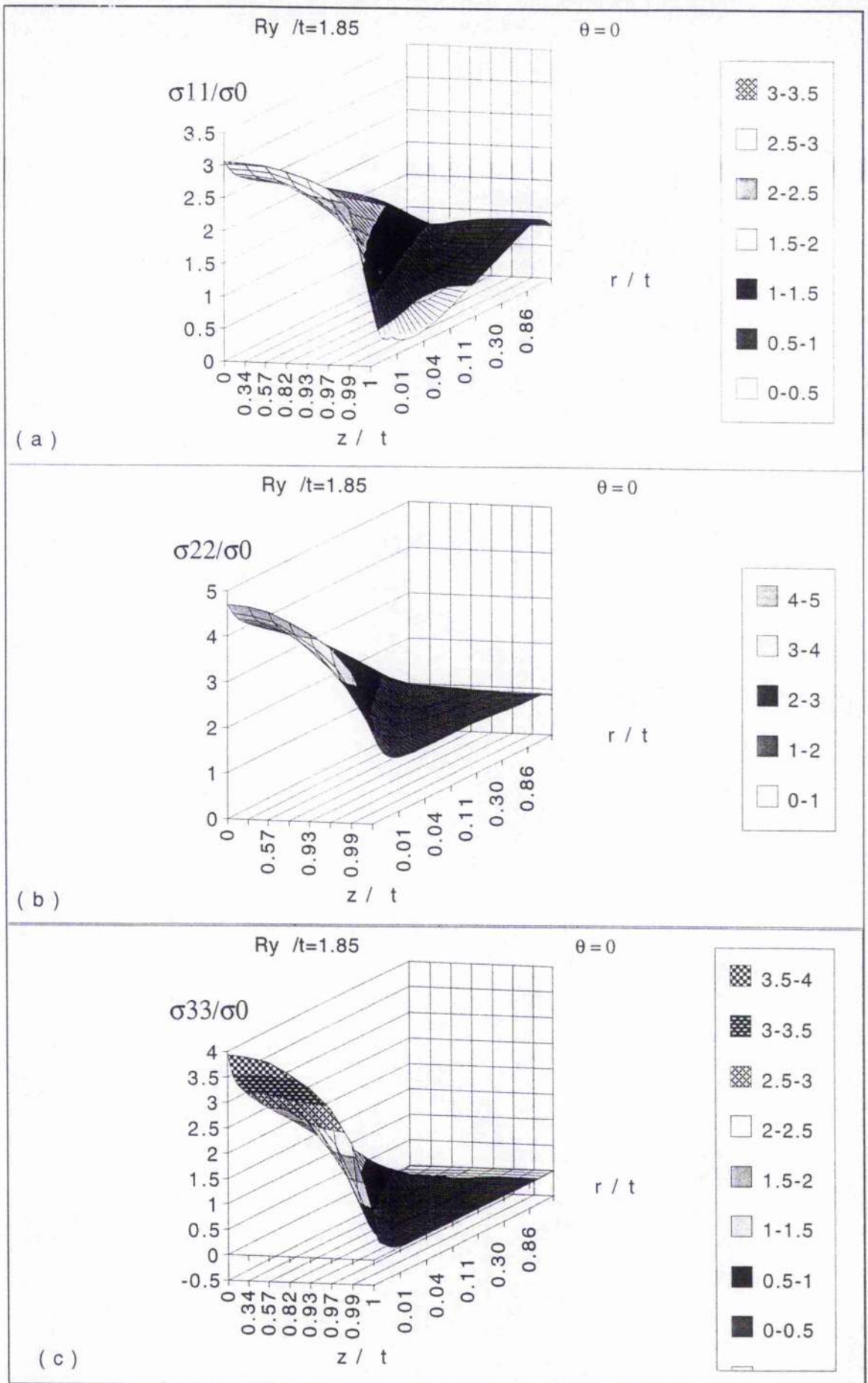


Figure 35 (a)(b)(c) The distribution of stresses through the thickness of material with hardening exponent 13

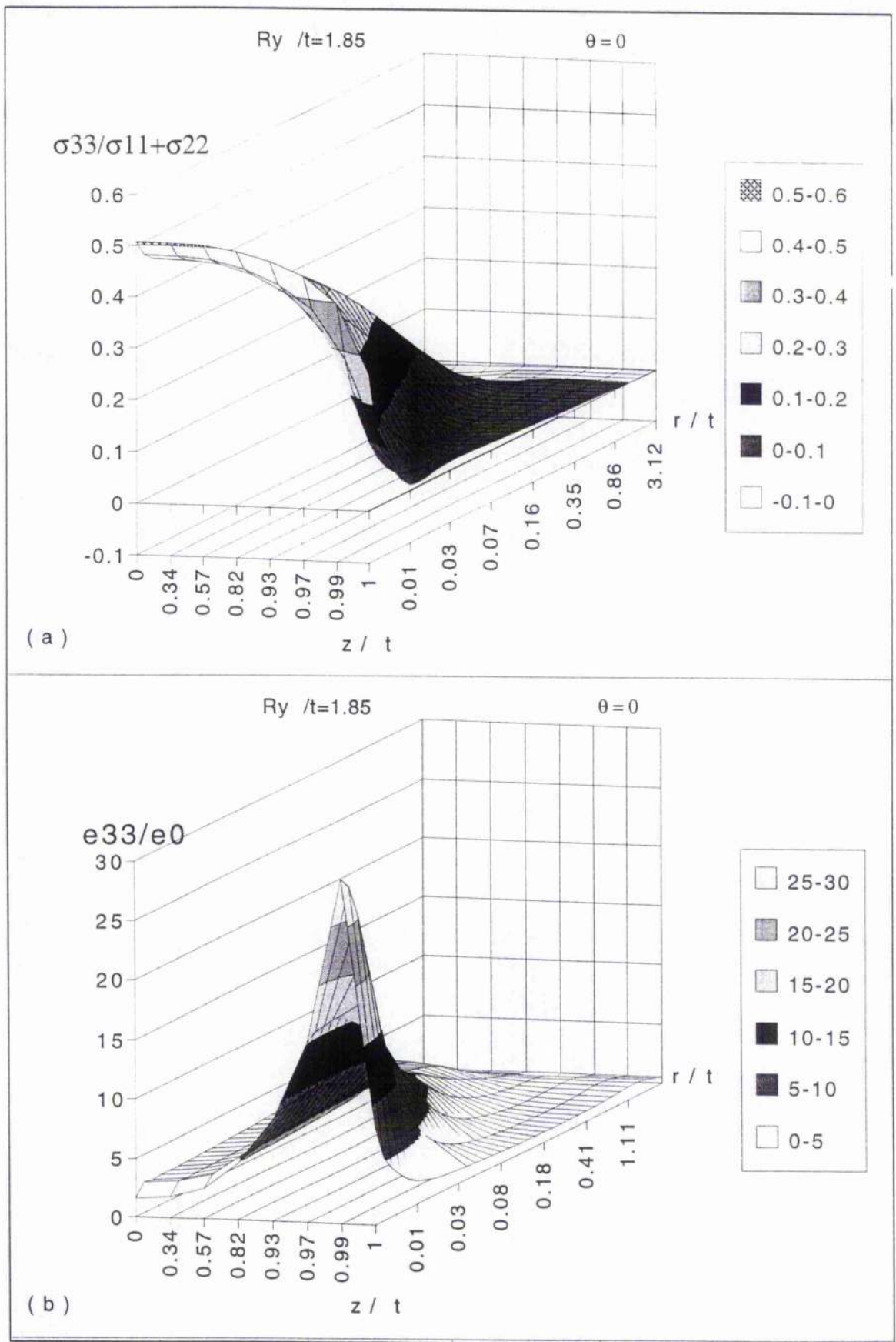


Figure 36 (a) Distribution of $\sigma_{33} / (\sigma_{22} + \sigma_{11})$ (b) Distribution of out-Plane strain e_{33} through the thickness of the material with hardening exponent 6

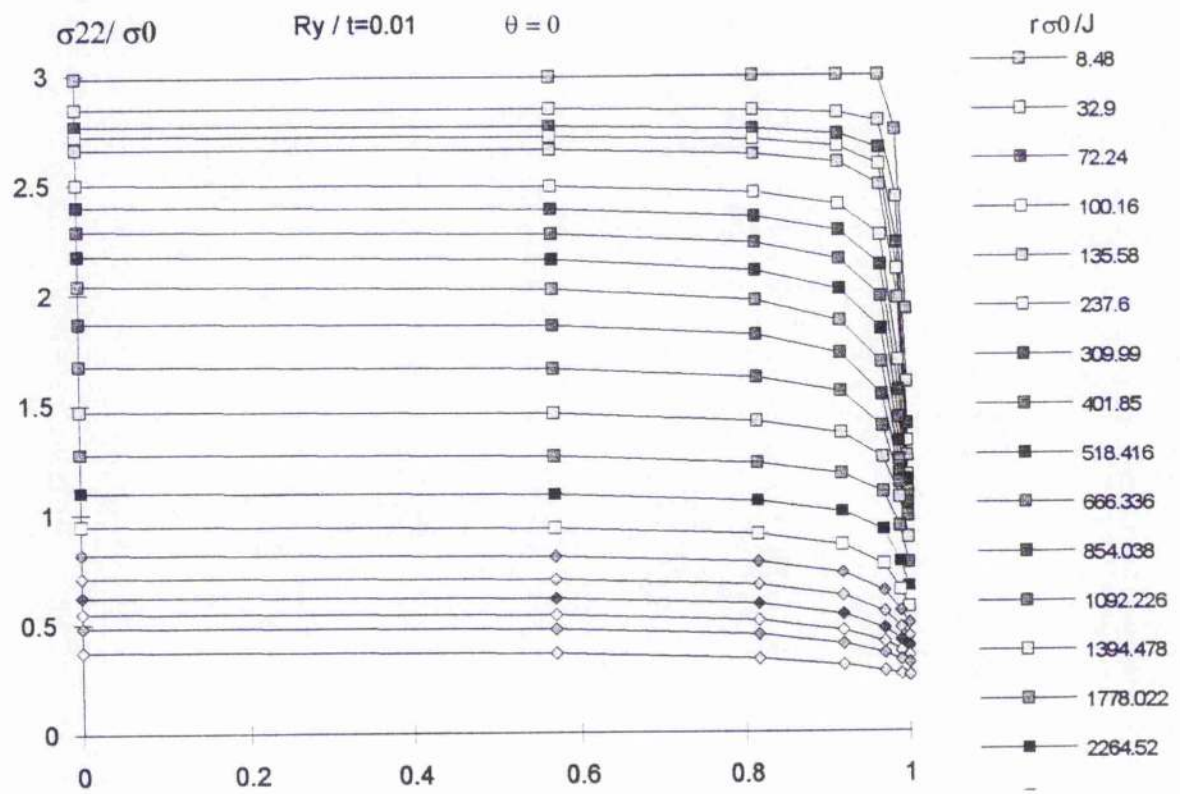


Figure 37 The opening stress through the thickness in SSY
 with $T = 0$

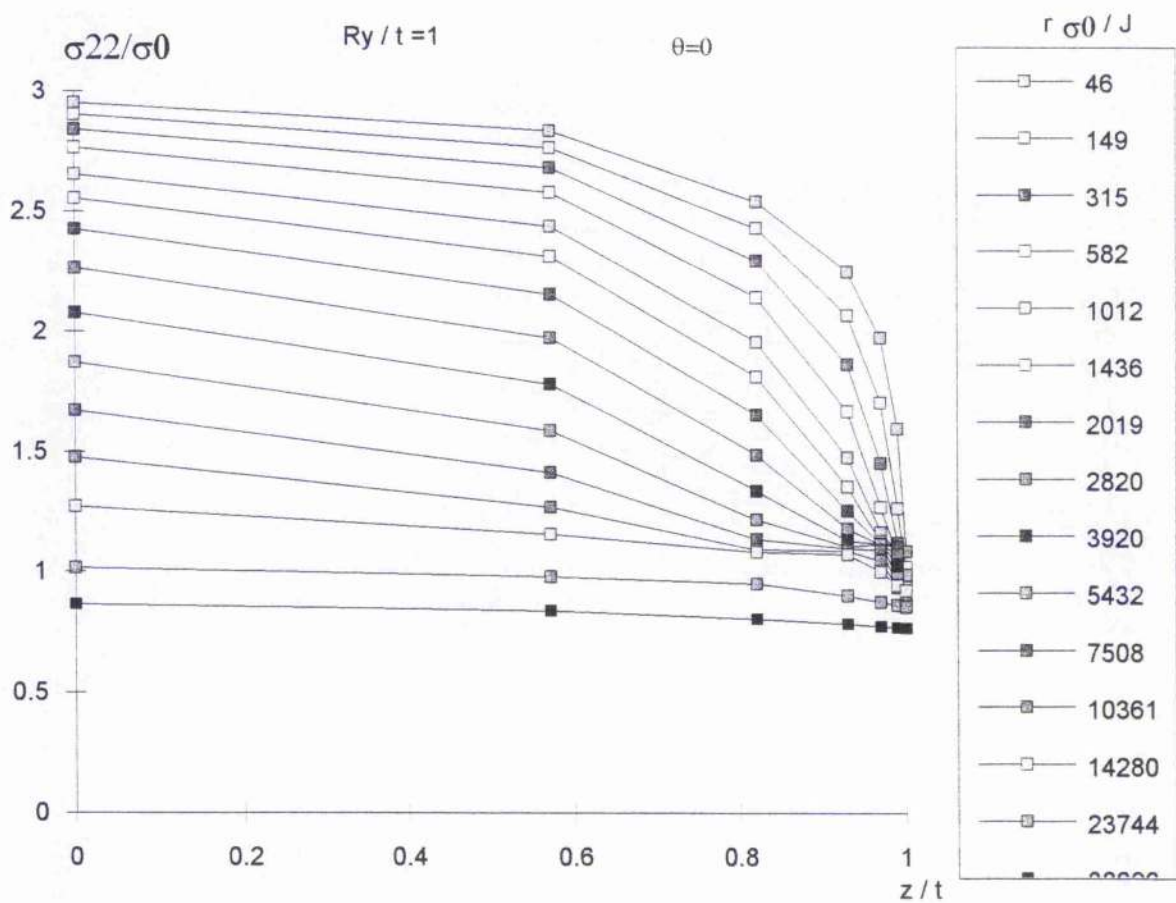


Figure 38 The opening stress through the thickness in MSY with $T=0$

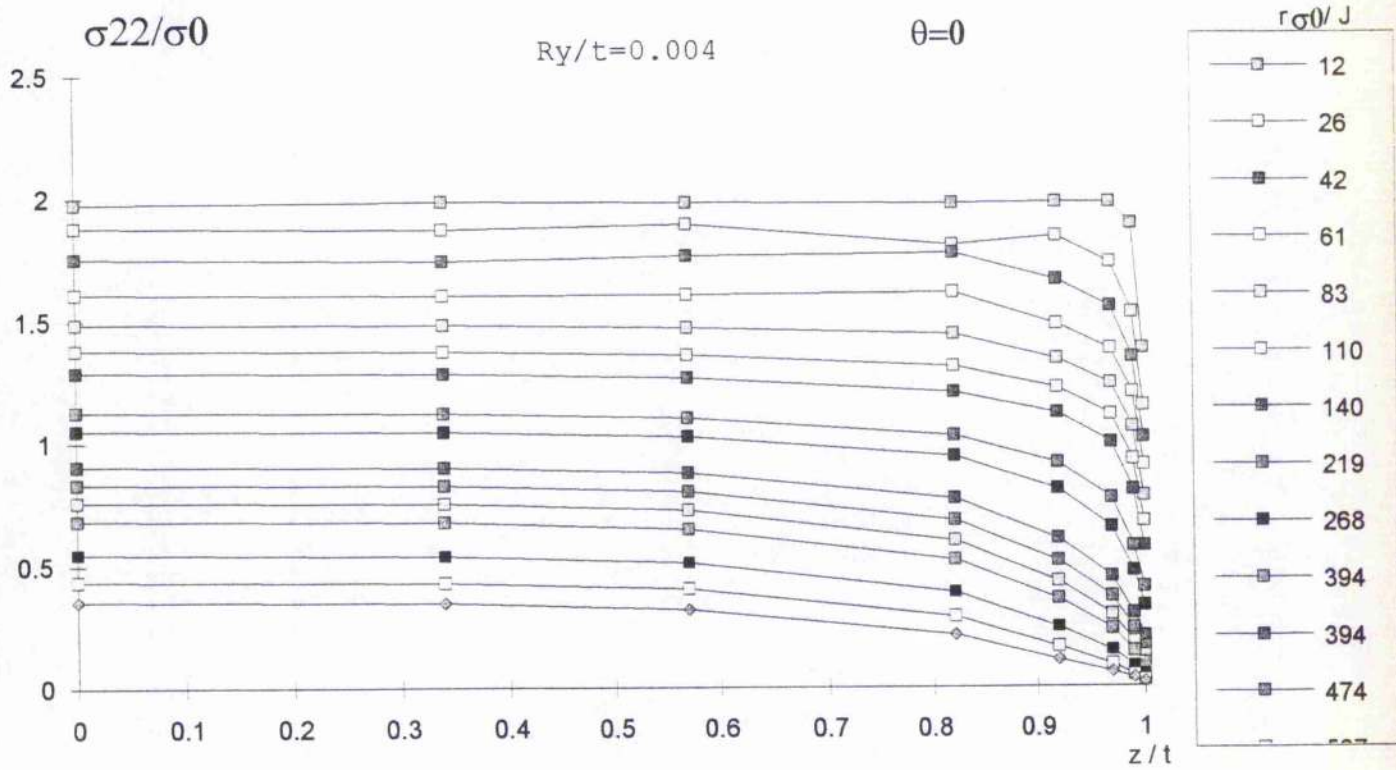


Figure 39 The distribution of σ_{22} through the thickness in the small scale yielding with $T=-0.6\sigma_0$

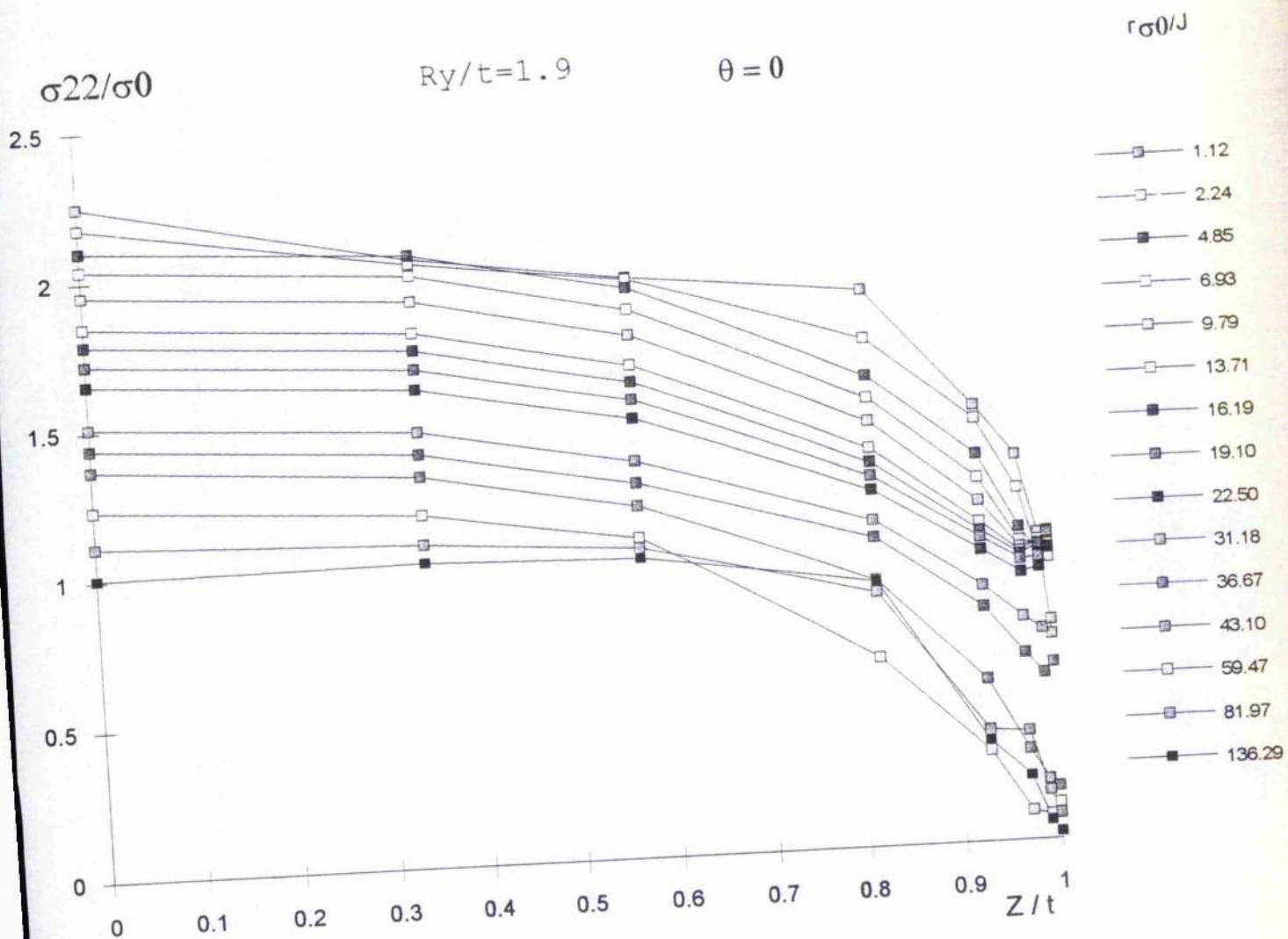


Figure 40 Distribution of opening stress through the thickness in the moderate scale yielding with $T = -0.6\sigma_0$

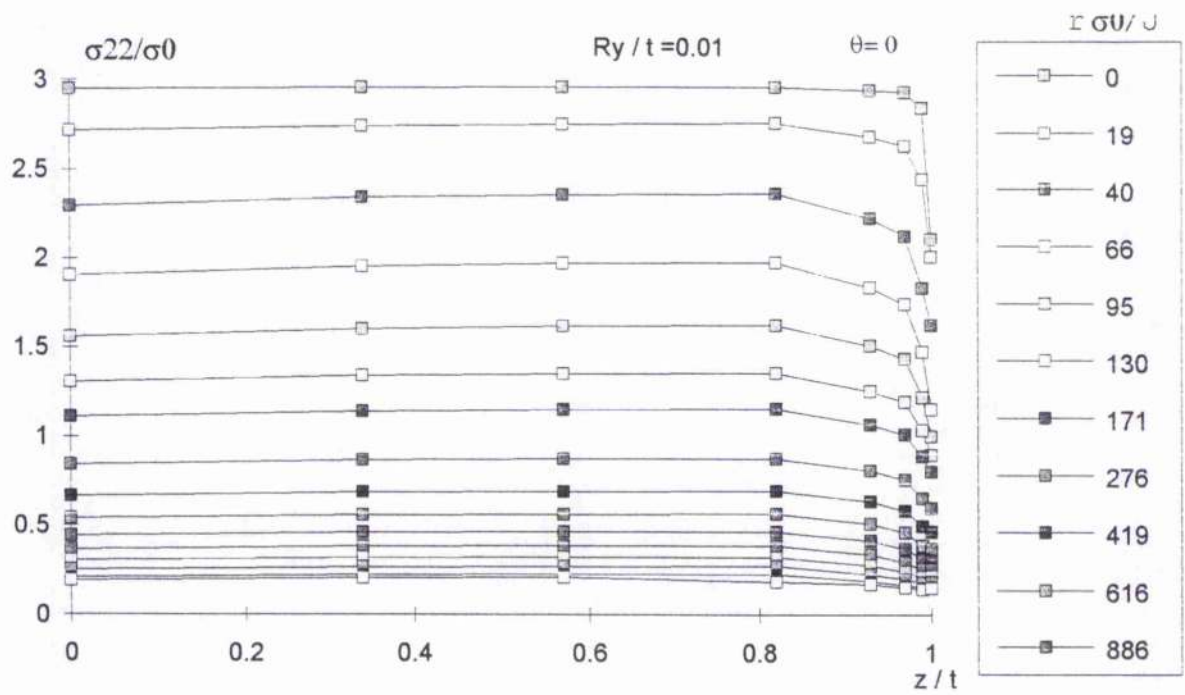


Figure 41 Distribution of opening stress in SSY
with $T=0.6\sigma_0$

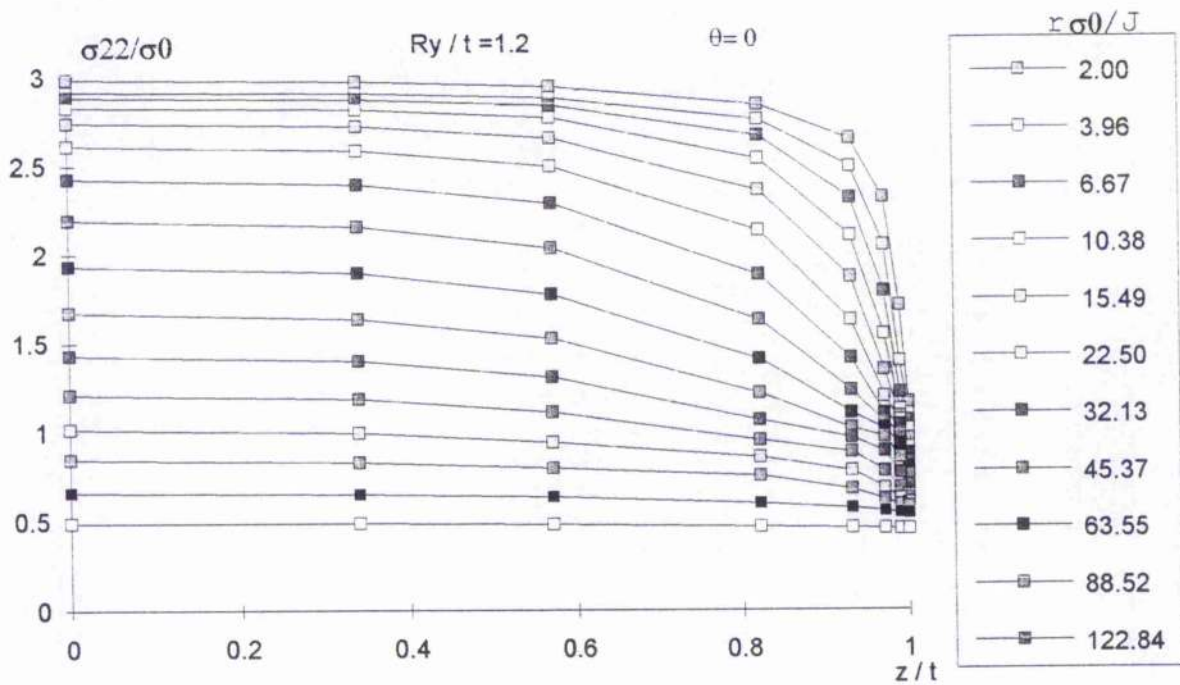


Figure 42 Distribution of opening stress in MSY condition with $T=0.6\sigma_0$

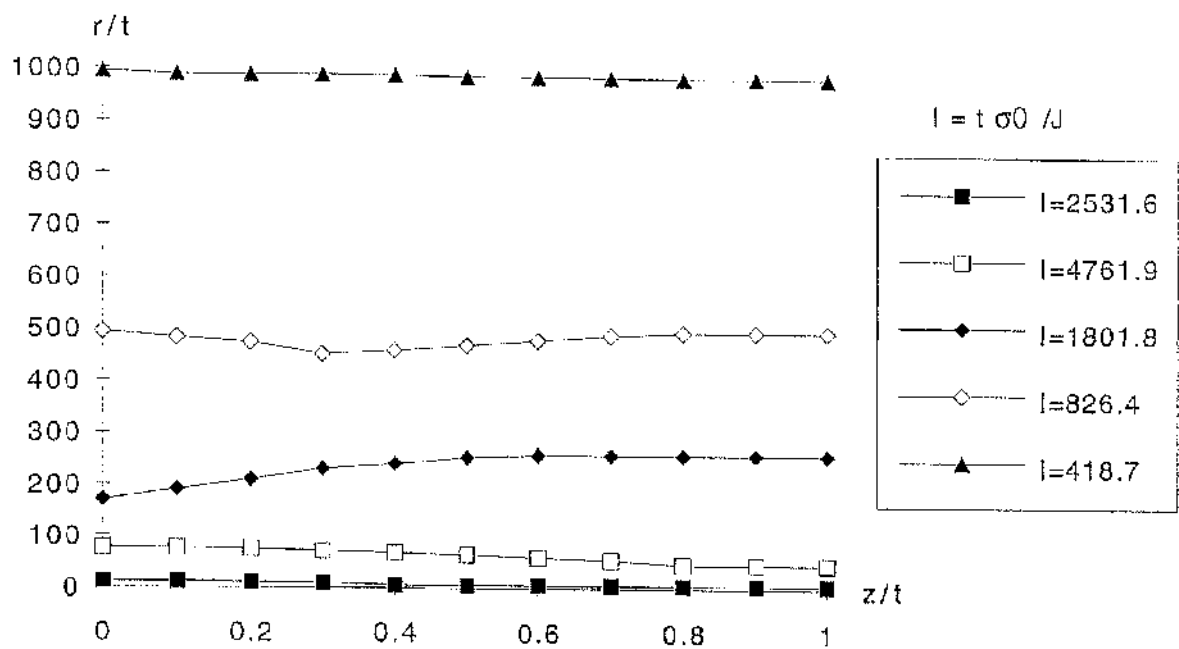


Figure 43 Variation of plastic zone radius on the crack plane at varied loading with $T=0$

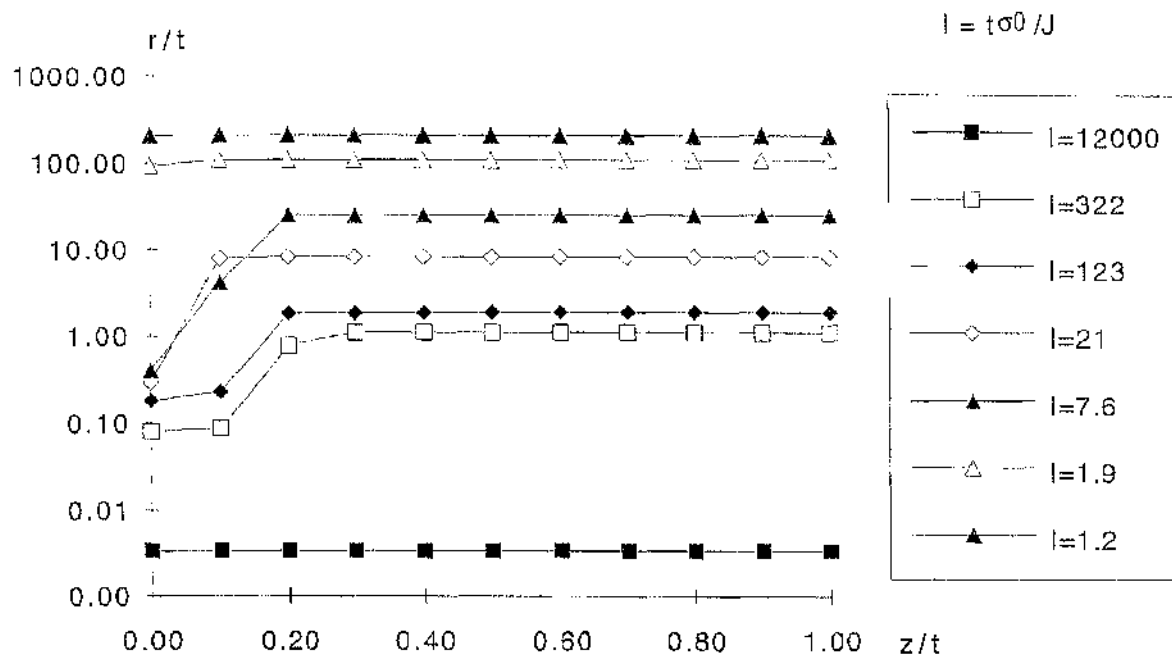


Figure 44 Variation of plastic zone radius on the crack plane at varied loading with $T=0.6\sigma_0$

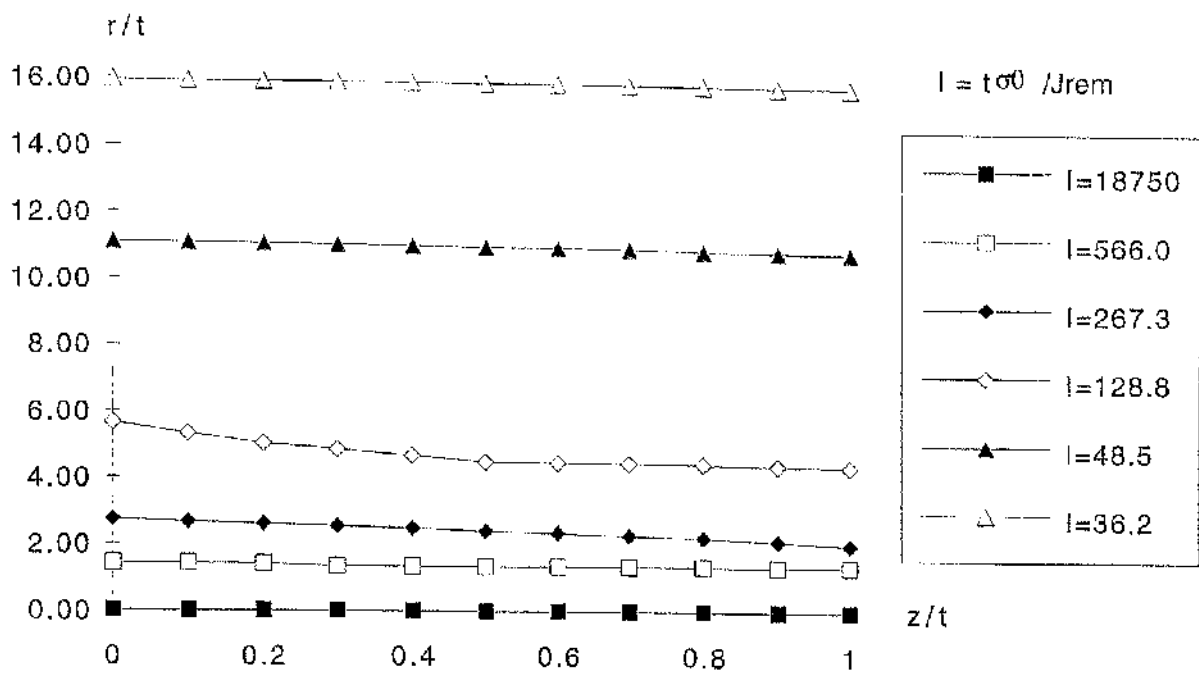


Figure 45 Variation of plastic zone radius on the crack plane at varied loading with $T=+0.6\sigma_0$